



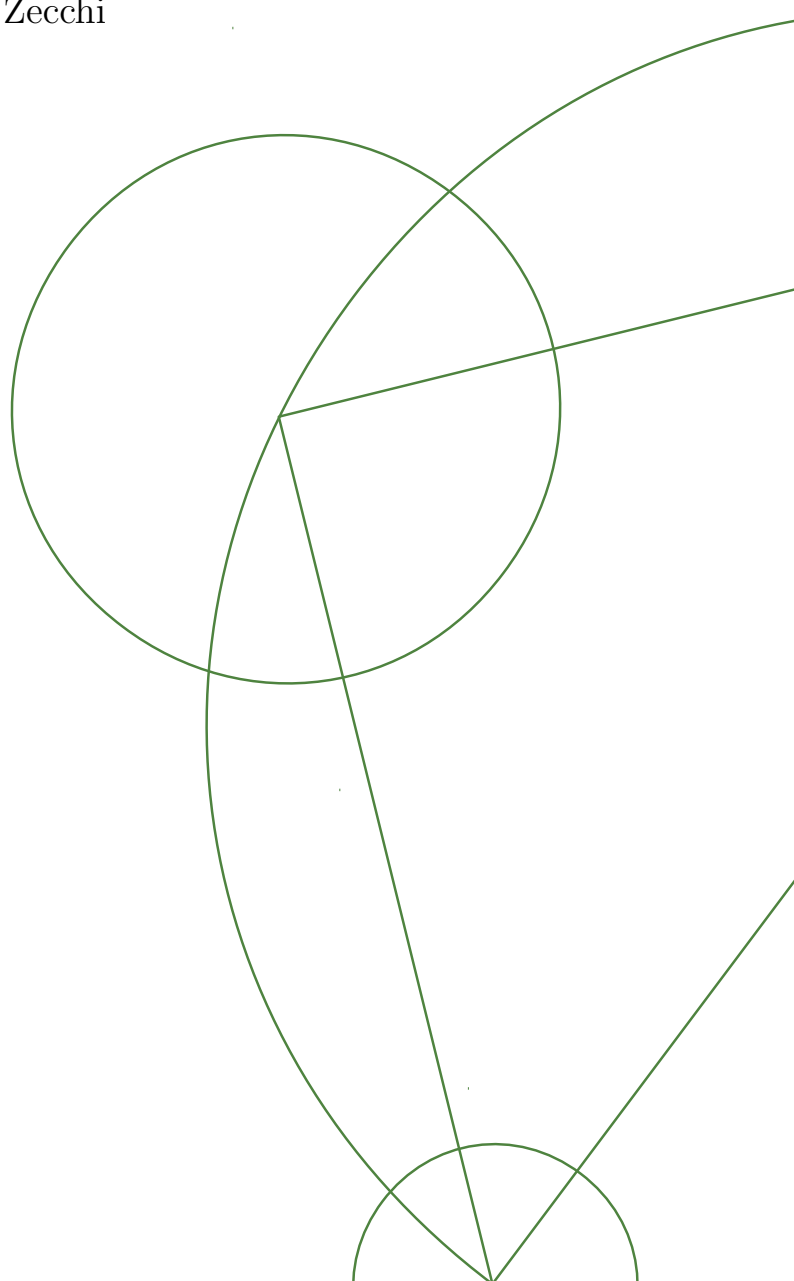
PhD Thesis  
On polarization in biomembranes

Karis Amata Zecchi

Supervisor:  
Thomas Heimburg

Niels Bohr Institute  
University of Copenhagen

Submitted: October 31, 2016





*Ai miei nonni*



# Acknowledgments

*Caminante, no hay camino. Se hace camino al andar.  
(Walker, there is no path. The path is made by walking.)*

– Antonio Machado,

First of all I would like to thank my supervisor, Thomas Heimburg, for introducing me to this fascinating research field. For always encouraging critical and independent thinking, through (challenging) freedom and trust.

A great thank goes to Lars D. Mosgaard with whom I collaborated in the theoretical part of my thesis, for sure the most stimulating and enjoyable time of my PhD. A special thanks goes to the electrical workshop and to Axel Boisen in particular, for his constant and extremely precious help in any problem with the electrical setup, and for always bringing a laughter. The NBI library, for their fast and incredibly valuable help (especially with the *lost* literature).

All the past and present members of the Membrane Biophysics Group for great support and environment. The biocomplexity group and all its member, present and past.

Ulrich Keyser and his group, for welcoming me as a member of the during my stay abroad in Cambridge and for the lively and stimulating environment. I learned a lot. A special thank Kerstin Gopfrich, for guiding me into the world of DNA origami. And Alex, for showing me how to fold an origami with DNA.

Finally, I would like to thank all the people I'm grateful to be surrounded by, both here and at home.

H. and A. for being in my life. Fabio, and Jerney, (for taking care of me when I forget to). Raffa, Marco, Virgy, Fede, Greg, Sara, Bellone, Lille, Lilla, , Monica, Nkero, David, Emily, Rocky and whoever is reading this (because this is why you are reading it).

Last, I would like to thank my family, for always being there no matter which distance.



## Abstract

In the electrical representation of biological membranes, the lipid bilayer is often considered as a simple insulator mostly impermeable to the passage of ions or small molecules. This view is included in the electrical equivalent of the membrane of excitable cells, that models the bilayer as a planar capacitor whose capacitance is independent of the applied electric field. This has been shown not to be true, especially close to the lipid phase transition, where the compressibility of the membrane is maxima and electrostrictive forces can change the membrane dimensions significantly. Moreover, membrane dimensions change significantly at the transition, and this, in turn, can change the value of the capacitance. Furthermore, lipid bilayers show finite permeability to ions, which is also maxima at the transition due to the enhanced area fluctuation. Biological membranes display lipid melting close to physiological conditions, making these effects biologically relevant.

In this work, we consider the case of asymmetric membranes which can display spontaneous polarization in the absence of a field. We describe their behaviour in an electric field in a thermodynamical framework, writing their Gibbs Free Energy as a quadratic function of voltage with a linear term proportional to the spontaneous polarization. Close to the phase transition, we find that the membrane displays piezoelectric, flexoelectric and thermoelectric behaviour. In particular, the membrane capacitance is a nonlinear function of the applied voltage. Furthermore, in the presence of spontaneous polarization, our thermodynamical description is able to explain the outward rectified current-voltage relationship measured on synthetic lipid bilayers.

Due to the nonlinear dependence of the membrane capacitance and conductance on voltage and the presence of spontaneous polarization, the traditional equivalent circuit of the membrane is not an accurate description in physiological conditions. An updated equivalent circuit of the lipid bilayer is here proposed, which takes into account the nonlinearities of the membrane and their time dependence. Using our updated equivalent model, we predict the response of the bilayer to common voltage experiments, e.g. voltage jumps and impedance spectroscopy. Our results show that the lipid bilayer alone can display several electrical behaviours similar to those measured for biological membranes and considered to be distinctive features of protein channels, like outward rectification and gating currents. Moreover, the dynamics of the nonlinearities can account for the inductive impedance at low frequencies. Finally, our proposed equivalent model is suggested by the structure and physical properties of the system, and not from empirical analysis of the data. Therefore, it has predictive power.

In the experimental part of this work, we find qualitative similarities between the melting enthalpy and the temperature dependence of the membrane capacitance, as expected from our theory. Measurements of I-V on different geometries, point in the direction of a flexoelectric mechanism behind current rectification in lipid bilayers. Finally, we suggest that our updated equivalent circuit should be included in the interpretation of electrophysiological data.

---

---

## Publication List

The work of this thesis has led to the following publications:

- Karis A. Zecchi, Lars D. Mosgaard and Thomas Heimburg. Mechano-capacitive properties of polarized membranes and the application to conductance measurements of lipid membrane patches. *Journal of Physics: Conference Series*, in print .
- Lars D. Mosgaard\* , Karis A. Zecchi\*, Thomas Heimburg and Rima Budvytyte. The Effect of the Nonlinearity of the Response of Lipid Membranes to Voltage Perturbations on the Interpretation of Their Electrical Properties. A New Theoretical Description. *Membranes*, 5:495-512, 2015
- Lars D. Mosgaard\* , Karis A. Zecchi\* , Thomas Heimburg. Mechano-capacitive properties of polarized membranes. *Soft Matter*. 11(40):7899-7910
- Thomas Heimburg, Andreas Blicher, Lars D Mosgaard and Karis A. Zecchi. Electromechanical properties of biomembranes and nerves. *Journal of Physics: Conference Series*. 558(1). 2014

---

# Contents

<b>I</b>	<b>Introduction</b>	<b>1</b>
<b>1</b>	<b>Introduction</b>	<b>3</b>
1.1	Biological membranes . . . . .	3
1.2	Lipids . . . . .	5
1.2.1	Lipid melting . . . . .	6
1.3	Equivalent circuit of the membrane . . . . .	7
1.4	Objective and outline . . . . .	10
<b>2</b>	<b>Thermodynamics</b>	<b>11</b>
2.1	Phase Transitions . . . . .	15
<b>II</b>	<b>Theory</b>	<b>19</b>
<b>3</b>	<b>Polarization effects</b>	<b>21</b>
3.1	Membrane capacitor . . . . .	21
3.2	Thermodynamics of membranes in electric fields . . . . .	27
3.2.1	Electrostriction . . . . .	30
3.2.2	Phase transition in the presence of an electric field . . . . .	32
3.2.3	Charge on the membrane capacitor . . . . .	34
3.3	Discussion . . . . .	40
<b>4</b>	<b>Nonlinear dynamic behaviour in common experiments</b>	<b>45</b>
4.1	Nonlinearities . . . . .	47
4.1.1	Conduction through the membrane . . . . .	47
4.1.2	Charge on the membrane capacitor . . . . .	50
4.2	Voltage jumps . . . . .	52
4.2.1	Ionic currents . . . . .	52
4.2.2	Capacitive current . . . . .	53
4.3	Impedance spectroscopy . . . . .	55
4.3.1	Linearized equilibrium response . . . . .	56
4.4	Discussion . . . . .	58
4.4.1	Lipid channels and rectification . . . . .	59
4.4.2	Gating Currents . . . . .	60

4.4.3	Membrane Inductance . . . . .	61
<b>III Experiments</b>		<b>65</b>
<b>5</b>	<b>Materials and Methods</b>	<b>67</b>
5.1	Materials . . . . .	67
5.1.1	Sample preparation . . . . .	67
5.2	Methods . . . . .	68
5.2.1	Calorimetry . . . . .	68
5.2.2	Patch Clamp Setup . . . . .	69
5.3	BLM setup . . . . .	70
<b>6</b>	<b>Results</b>	<b>73</b>
6.1	Temperature dependence of the membrane capacitance . . . . .	73
6.2	Lipid ion channels and rectification . . . . .	78
6.2.1	BLM . . . . .	79
6.2.2	Patch pipette . . . . .	82
6.3	Discussion . . . . .	84
6.3.1	Capacitance measurements . . . . .	84
6.3.2	Lipid Ion channels and rectification . . . . .	88
<b>7</b>	<b>Conclusions</b>	<b>91</b>

Part I  
Introduction



# 1

## Introduction

Biological membranes are one of the most fundamental units in biology. Surrounding every living cell, they basically define the cell from the surrounding environment. Furthermore, the different organelles inside the cell are also enclosed in biological membranes. They therefore provide structure and organization to the cell. In addition to this, they regulate transport processes acting as a semipermeable wall and enable communication with the environment [1]. They are mainly constituted by a bimolecular lipid matrix (with a thickness of about 5-8nm [2]) and proteins which are embedded or attached to it. In the following we will provide a brief overview on the history of membranes models and then we will mainly focus on the lipid portion of the membrane, which is the main subject of the theoretical and experimental part of this thesis.

### 1.1 Biological membranes

The first hint of the existence of some sort of envelope surrounding cells dates back to the end of the 18th century, when in 1773 William Hewson observed red globules (as the red blood cells were called at the time) under a microscope and found that they were not globular but rather flat [3], thus rejecting the idea that they were liquid droplets. It was not until one century later, however, that a membrane theory started developing. One of the milestones of this development is the experiment made by Gorter and Grendel in 1925 [4], by which the bimolecular structure of the lipid bilayer was postulated for the first time. With the aid of a Langmuir trough, they spread lipids extracted from red blood cells on a water surface and found that the surface area of the resulting monolayer was double the area of the intact cells, within their experimental error. The presence of proteins was suggested by Danielli and Davson in 1935 based on the observation that the surface tension of biological membranes was significantly lower than that expected for the lipid bilayer [5]. They proposed that the lipid bilayer was sandwiched

between two layers of adsorbed proteins. The first direct evidence of the presence of double layer in the membrane, however, arrived only in 1958 thanks to Robertson and the advent of electron microscopy [6].

The most accepted membrane model originates from the so called *fluid mosaic model*, proposed by Singer and Nicolson in 1972 [7]. Their model describes the membrane as essentially a bimolecular fluid made from the lipid bilayer where integral proteins are immersed and free to diffuse while peripheral proteins are adsorbed to the surface. While considering in their model the possibility for lipid-protein interaction, their action was limited to the very short range and longer range interactions were disregarded, leaving the membrane as a substantially homogeneous fluid. Protein-lipid interaction (on a longer range) and lateral heterogeneity have been addressed in the *mattress model* by Mouritsen and Bloom [8], in which inhomogeneity results from the mismatch between the hydrophobic regions of proteins and lipids.

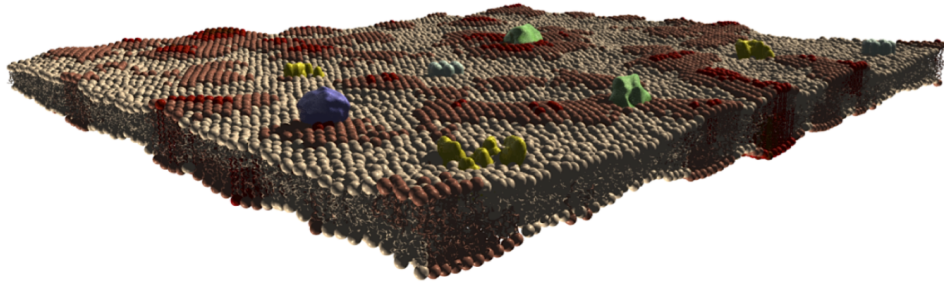


Figure 1.1: Modern view of biological membranes, showing heterogeneous organization of proteins, lipid of different species and states organized in domains. Picture taken from [9]

Nowadays biomembranes are believed to be highly heterogeneous and dynamic structures, where domains enriched in sphingolipids and cholesterol can be found (*rafts*) and where lipids and protein interact dynamically [10] (see Fig. (1.1)).

Lipid composition in membranes can vary greatly depending on the organism, the tissue and the physiological or growth conditions [11]. Interestingly membrane composition seems to be fairly conserved through same organs of different species, suggesting a functional role [11]. It has further been shown that several organisms are able to modify their lipid composition when their growth conditions (e.g. temperature, pressure) are changed [12].

## 1.2 Lipids

Lipids are the main component of biological membranes<sup>1</sup>. They are amphiphilic molecules, made of a hydrophobic and a hydrophilic part.

In the case of phospholipids (the most abundant lipid species in biological membranes [11]), the hydrophobic part is constituted by two hydrocarbon chains which can differ mainly in length (ranging between 12 and 24 carbons) and saturation [2]. The hydrophilic part is made of a negatively charged phosphate group which is linked to an organic compound. Ester bonds link the two hydrocarbon chains and the phosphate group to a glycerol backbone. The polar headgroup can differ in size, polarity and charge of the compound that is linked to the phosphate group. The most common are the positively charged choline and ethanolamine and the neutral serine and glycerol. The corresponding headgroups are indicated as PC (phosphatidylcholine), PE (phosphatidylethanolamine) - both zwitterionic, PS (phosphatidylserine) and PG (phosphatidylglycerol) - both negatively charged.

Zwitterionic headgroups carry no net charge but they have a net dipole moment pointing out of the membrane. Due mainly to the inclination of the headgroup with respect to the plane of the membrane and the presence of oriented water surrounding the membrane, the net dipole moment of lipids point towards the interior of the membrane, as confirmed from the measured surface potential of lipid monolayers of about 300-500 mV [13]. In a planar symmetric membrane made of zwitterionic lipids, however, the net dipole moment of the two monolayers cancel each other and the membrane has no net dipole. Between 10% and 20% of lipids of biological membranes are charged [2], and charges are often distributed asymmetrically between the two monolayers [14]. In charged and asymmetric membranes, the membrane can show a net polarization. The implications of such a polarization will be investigated in chapter 3.

Due to their amphiphilic nature, lipid molecules display interesting self-assembling behaviour when placed in solvents. In particular, in polar solvents like water, they tend to assemble in structures which minimize the contact of the hydrophobic part with water. Depending on the lipid concentration and external parameters like pressure, pH, ion concentration, one can find them organized in different phases: lamellar, (bilayers, unilamellar vesicles), micelles, inverse micelles, cubic phase, ... [2]. In the following we will mainly deal with lipid bilayers.

---

<sup>1</sup>The mass ratio between proteins and lipids varies from 0.25 to 4, with a typical value of 1 [2]. This include the transmembrane domain as well as the extra-membrane domain of the proteins.

### 1.2.1 Lipid melting

Lipid molecules can be found in different states, which differ mainly on the configuration of their hydrocarbon chains. The lowest energy state for the lipid tail is the *all trans* configuration, where the chains are fully stretched. Through rotation around the carbon-carbon bond, the hydrocarbon chains can be found in more convoluted conformations.

Lipid bilayers as a result can exist in different phases, depending on their lateral and transverse order. At low temperature, for example, one finds lipids organized in a solid-ordered phase ( $S_o$ , or gel phase). This is characterized by the lipid chains being in an ordered, all-trans configuration, and the headgroups organized in a triangular lattice (Fig. (1.2),left). At higher temperatures, the chain order is lost (as also the higher energy configurations of the hydrocarbon chains become accessible) and the lipids move in the bilayer like a two-dimensional liquid (Fig. (1.2),right). This phase is called liquid-disordered ( $L_d$ , or fluid phase). Lipids can be found in other phases, like the liquid-ordered phase ( $L_o$ ) where the headgroups have no lateral order (liquid) while the chains are all stretched (ordered), which is observed for example in the presence of cholesterol [15], or the ripple phase ( $P_{\beta'}$ ).

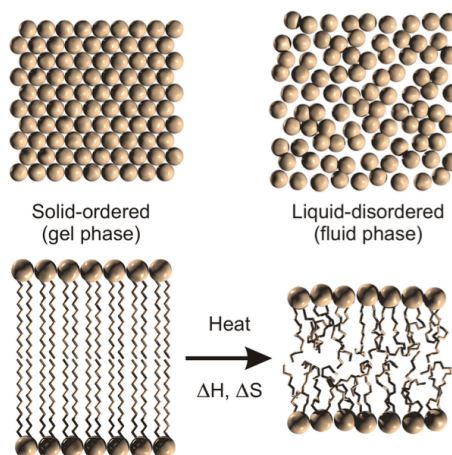


Figure 1.2: Lipid melting transition between a solid-ordered (gel) phase, **left**, and a liquid-disordered (fluid) phase, **right**. Upon melting, both chains and headgroups lose their order. The fluid phase corresponds to a higher enthalpy and entropy state. The membrane area increases by about 25%(**top**) while the thickness decreases by 16%(**bottom**) [16]. Picture taken from [9]

The transition from the gel phase to the fluid phase occurs over a wide temperature range (from  $-20^{\circ}\text{C}$  to up to  $60^{\circ}\text{C}$  [2]) depending on the lipid species (in particular, it depends on chain length and saturation, and on headgroup type [17]). It is accompanied by an increase in enthalpy and entropy, due mainly to the increase in the number of accessible chain config-

### 1.3. Equivalent circuit of the membrane

---

urations at higher temperature [2].

As illustrated in Fig. (1.2), the lipid phase transition results in a macroscopic change in the membrane dimensions. In particular, the thickness is larger in the gel phase, where the chains are fully stretched, while the area is minimum (due to the tight packing of the headgroups). For DPPC bilayers this corresponds to a change in area of 25% and a change in thickness of  $-16\%$  from the gel to the fluid phase [16]. The phase transition in lipids is characterized by other interesting macroscopic properties, which will be described in the next chapter.

One of the striking properties of biological membrane is that they display lipid melting a few degrees physiological temperature [18]. This is shown in Fig. (1.3) for an intact membrane of *E.Coli*. The heat capacity profile, measured with differential scanning calorimetry, has a maximum few degrees below growth temperature, which indicates the presence of a melting transition. Interestingly, the relative position of the lipid melting with respect to physiological temperature is conserved in several different organisms [18] and despite changes in the growth or physiological conditions [2].

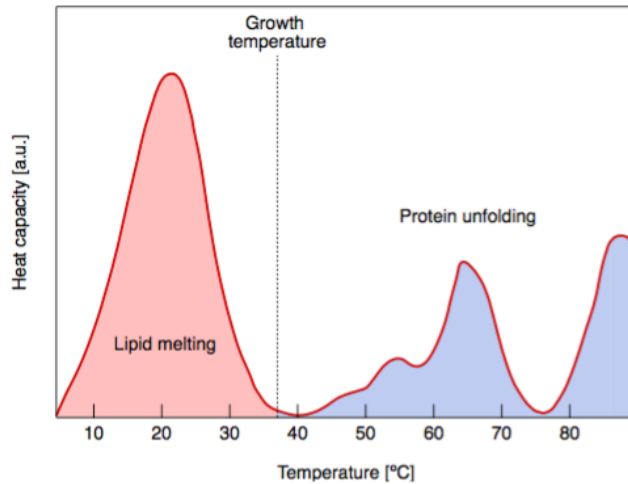


Figure 1.3: Heat capacity profile of a native *E.Coli* membrane. The pink area shows the lipid melting, as indicated by the heat capacity reaching a maximum few degrees below body temperature. The blue area shows protein unfolding. Picture taken from [9], adapted from [18]

### 1.3 Equivalent circuit of the membrane

Many physiological cell functions are regulated by electric potentials across the plasma membrane. The most notable of these is probably the initiation

and propagation of the nerve pulse in neurons. Nerve signals are transient voltage changes (action potentials) traveling along the axons [19]. In general, the electrical properties of the membrane are studied and understood with the aid of equivalent circuits. An equivalent circuit is an electrical circuit whose response to certain electrical perturbation is the same measured for the membrane.

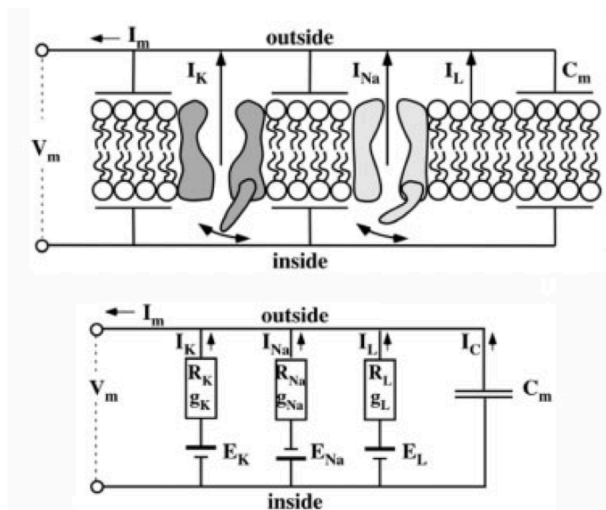


Figure 1.4: Equivalent circuit of the axon membrane, according to the Hodgkin and Huxley model [20]. **Top:** Transmembrane proteins selective for sodium and potassium open and close allowing the flow on ionic currents. The lipid bilayers is represented as an inert capacitor. **Bottom:** The equivalent circuit is a combination of time and voltage dependent resistors and the constant membrane capacitance.

The most widely accepted equivalent circuit of the membrane of excitable cells is the one proposed by Hodgkin and Huxley in 1952 to describe the propagation of the action potential in the membrane of the giant squid axon (measured in 1939 by Cole and Curtis [19]). It is shown in Fig. (1.4) (bottom). In order to describe the current measured across the membrane in response to voltage perturbations, they considered that the membrane is selectively permeable to sodium and potassium ions and that the permeability to the two ions have a different voltage and time dependence. At the time of their model little was known on the structure and composition of the membrane, and the lipid bilayer was mainly viewed an impermeable insulator. For this reason they assumed the bilayer to behave like a constant capacitor and ascribed the role of conduction through the membrane to transmembrane proteins that can open and close in response to changes in voltage. According to the circuit of Fig. (1.4) (bottom), the current response,  $I_m$ , of the membrane to an applied voltage  $\Psi$ , is the sum of the ionic currents

### 1.3. Equivalent circuit of the membrane

---

through the resistors and a capacitive current:

$$I_m = C_m \frac{d\Psi}{dt} + g_K(\Psi, t)(\Psi - E_K) + g_{Na}(\Psi, t)(\Psi - E_{Na}) \quad (1.1)$$

where the first term is the capacitive current in the assumption of constant capacitance<sup>2</sup>.  $E_K$  and  $E_{Na}$  are the resting potentials for potassium and sodium and  $g_K(\Psi, t)$  and  $g_{Na}(\Psi, t)$  are the time and voltage dependent conductances of the potassium and sodium channel<sup>3</sup>. The explicit dependence of the conductances on time and voltage is the core of the Hodgkin and Huxley model. It is an empirical mathematical model based solely on the inspection of the electrical data for the squid axon and as such unlikely to give information on the molecular mechanism behind the changes in permeability (as pointed out by the authors in the original paper [20]). Using the cable equation and , their model describes the propagation of the pulse along the axon.

Relying on the flow of ions through channels (*i.e.* currents through resistors) the Hodgkin-Huxley (HH) model is dissipative in nature. This is in contrast to the experimental finding that no net heat is produced in conjunction with the pulse [21], which instead is a distinctive feature of an adiabatic process. Furthermore, being a pure electrical model it cannot explain the mechanical changes in the axon membranes measured during nerve activity [22, 23]. These observations led to the proposal of the soliton model by Heimburg and Jackson [18]. They suggested that the propagation of the action potential can be explained in terms of a density wave propagating along the nerve. In particular, they suggested that the membrane undergoes a phase transition from fluid to gel and back to fluid during the nerve pulse. Thus, it is an adiabatic process which naturally includes mechanical changes in the membrane.

In conclusion, the equivalent model of the membrane proposed by Hodgkin and Huxley assumes that the lipid portion of the membrane behaves as an inert insulator of constant capacitance and impermeable to the passage of ions. This is based on the few information available in 1952 on the physical properties of the lipid bilayer. We note that the assumption of constant capacitance already breaks down few degrees below physiological temperature, where lipid melting occurs and the dimensions of the membrane change significantly. Moreover, voltage differences of the order of 100 mV across the membrane are expected to affect the structure of the bilayer and hence its electrical properties [24]. Despite its clear biological relevance, the behaviour of lipid bilayers in the presence of voltage is not fully understood.

---

<sup>2</sup>It comes from:

$$I_c = \frac{d(C_m \Psi)}{dt} = C_m \frac{d\Psi}{dt} + \Psi \frac{dC_m}{dt}$$

<sup>3</sup>we have omitted the contribution to the leak current  $I_L$

## 1.4 Objective and outline

The aim of this work is to advance our understanding of the physical properties of lipid bilayers in the presence of voltage and in proximity of the phase transition. This is motivated by the observation that lipid melting occurs close to physiological condition and by the importance (and omnipresence) of voltage differences across the membrane of many cells. In particular, we will check (and eventually revise) the assumption of constant capacitance in the equivalent circuit of the membrane.

We will start by briefly introducing the thermodynamical tools that will be used throughout the thesis in chapter 2, where the thermodynamical properties of the phase transition will be introduced. Part I and II are the theoretical and experimental parts of the works done during my PhD.

In Part I we will study the properties of the membrane in an electric field in a thermodynamical framework in chapter 3. We will use the finding of chapter 3 in order to inspect and eventually update the equivalent circuit of the membrane. It will be discussed in the context of common electrophysiological experiment. This will be done in chapter 4.

Part II is the experimental part of this work. Chapter 5 introduces the methodology used and in chapter 6 we will test some of the predictions made on the theoretical part of this thesis. Finally some concluding remarks and further perspective are outlined in chapter 7

## 2

# Thermodynamics

In this chapter we will introduce the thermodynamical "tools" which will be used in the theoretical part of the thesis. Since we are interested in studying couplings between thermal, electrical and mechanical properties, thermodynamics provides a general framework which naturally include them all. In section 2.1 we will introduce the reader to the main features of phase transitions in lipid membranes.<sup>1</sup>

The first postulate of the axiomatic foundation of thermodynamics states the existence of the equilibrium state for a system. An equilibrium state is a state in which the system is macroscopically completely (and uniquely) characterized by its extensive variables, e.g. internal energy  $U$ , volume  $v$ , and mole numbers of chemical components  $n_i$ . They are the thermodynamical coordinates of the system. The minimum number of coordinates needed to describe the equilibrium state depends on the degrees of freedom of the system. So, if electrical properties are studied, an extra variable is needed<sup>2</sup>. If the state can be described *uniquely* by its minimum set of thermodynamical coordinates and it is time independent, that is called an equilibrium state.

The basic problem of thermodynamics is to determine the new equilibrium state of the system that eventually results after removing one (or some) internal constraint in a closed system. Any other thermodynamical problem can be considered as a branch of this. It can be solved by assuming the existence of a function of the extensive variables of the system  $(U, v, n_i, \dots)$  which is defined for all the equilibrium states. Such a function is called the entropy,  $S$ , and has the property that, in the absence of internal constraints, the values taken by the extensive variables are those that maximise the entropy (over all the accessible equilibrium states). The entropy function must further be continuous, differentiable, additive and monotonically increasing

---

<sup>1</sup> We will here follow the axiomatic development of thermodynamics following the treatment of Callen [25], rather than the chronological one. The two developments are equivalent.

<sup>2</sup> This particular case will be considered in chapter 3

with the internal energy<sup>3</sup>. It turns out that if one knows the expression of the entropy in terms of the thermodynamical coordinates of the system, the problem of thermodynamics can be solved by only using the extremum principle. For this reason, the relation between the entropy and the extensive variables is called the *fundamental equation* and it contains all the thermodynamical information of the system:

$$S = S(U, v, n_i, \dots) \quad (2.1)$$

Where the dots stand for any thermodynamic variable needed to characterize the system. If we think of equilibrium states as points in the thermodynamic configuration space whose coordinates are the extensive variable of the system, the fundamental equation defines a surface in the configuration space<sup>4</sup>. A curve on that surface defines a quasi static process between two equilibrium states. If internal constraints are changed, a system will move to the newly accessible point of the surface which have have a highest entropy and not inversely, in this sense the process is irreversible. Analogously, reversible processes are those between points on the intersection between the fundamental equation an the isoentropic plane.

The monotonic dependence of the entropy on the internal energy makes it always possible to invert the fundamental equation and express it in terms of the internal energy without losing thermodynamical information:

$$U = U(S, v, n_i, \dots) \quad (2.2)$$

Equation 2.1 and 2.2 are thermodynamically equivalent, thus the latter is also called fundamental equation and it can also be seen as a surface in the configuration space. As a result, the maximum principle for the entropy is translated in a minimum principle for the internal energy. The infinitesimal change in internal energy is given by the differential form of 2.2, which, for a single component system is given by:

$$dU = \underbrace{\left(\frac{\partial U}{\partial S}\right)_{v, n_i, \dots}}_{\equiv T} dS + \underbrace{\left(\frac{\partial U}{\partial v}\right)_{S, n_i, \dots}}_{\equiv -p} dv + \underbrace{\left(\frac{\partial U}{\partial n}\right)_{S, v, \dots}}_{\equiv \mu} dn + \dots \quad (2.3)$$

where the partial derivative of the internal energy with respect to entropy, volume, and mole number are called temperature, negative of the pressure

<sup>3</sup>For completeness, the entropy function here defined must have one more property in order to coincide with the traditional formulation, namely that it vanishes in the states for which  $(\partial U/\partial S)_{v, n_i, \dots} = 0$  (at the the zero of temperature). Moreover, the additivity property implies that the entropy of a simple system is homogenous first order function of the extensive parameters.

<sup>4</sup>More correctly, it defines an hyperspace, since the coordinates can, and usually are, more than two. Note that the thermodynamical coordinates, also called natural variables of the system or generalized coordinates, constitute a set of independent (or orthogonal) variables.

---

and chemical potential. They are intensive quantities, as a consequence of the energy being an homogeneous first order function and they all depend on the extensive coordinates of the system:

$$\begin{aligned}
 T &= T(S, v, n, \dots) \\
 p &= p(S, v, n, \dots) \\
 \mu &= \mu(S, v, n, \dots) \\
 &\dots
 \end{aligned}
 \tag{2.4}$$

Eq. (2.4) are the equations of state of the system. From their definition, it follows that they define a conservative vector field with corresponding potential given by the internal energy, and are thus sometimes called thermodynamic forces. In other words, they are the components of the gradient of the internal energy with respect to the extensive coordinates,  $\nabla U(S, v, n, \dots) = (T, -p, \mu, \dots)$ .<sup>5</sup> As such, knowledge of all the equations of state is equivalent to knowledge of the fundamental equation. The intensive variables just introduced are thermodynamically conjugated to the correspondent extensive variables. From the above considerations it follows that the product of an extensive coordinates and its conjugated intensive one constitutes a function of state. Finally, the differential of the intensive variables with respect to the extensive ones, constitute the Hessian matrix of the internal energy. From the symmetry of the Hessian, one can determine the Maxwell relations between coupling coefficients of the intensive variables and the non conjugated extensive ones<sup>6</sup>. Using the definition of the thermodynamic forces, the differential of the internal energy can be written in the more familiar way:

$$dU = TdS - pdv + \mu dn + \dots \tag{2.5}$$

Note that Eq. (2.5) formally contains the first and the second law of thermodynamics by recognizing in the first term the reversible heat change (*i.e.*  $\delta Q = TdS$ ) and in the other terms the work done on the system ( $\delta W = -pdV + \mu dn + \dots$ ). In this way it can be expressed as  $dU = \delta Q + \delta W$ .

The fundamental equation introduced so far is defined over its natural variables, that are the extensive variables. They represent an independent set of coordinates for the internal energy, which can be changed independently from outside. The internal constraints of the system, which determine its

---

<sup>5</sup>In a more familiar analogy, the intensive thermodynamical variables play to the internal energy a role that is somewhat analogous to role played by electric field to electric potential in electrostatics (or forces and mechanical potential in mechanics). The analogy sounds more familiar because the electric potential is defined on the physical space, while the internal energy is defined on the more abstract configuration space.

<sup>6</sup> The number of Maxwell equations is equal the number of coordinates. Considering only S,v,n one has:  $\partial T/\partial v = -\partial p/\partial S$ ,  $\partial T/\partial n = \partial \mu/\partial S$  and  $\partial p/\partial n = -\partial \mu/\partial v$

evolution to new equilibrium states, are also defined on the extensive variables. If, for instance, one has control on the pressure instead of the volume, minimizing the internal energy with respect to the volume would not give information on the new equilibrium state if a change in pressure is applied. In this example, the energy formulation  $U(S, v, n, \dots)$  would be inappropriate for the type of problem. A solution could still be found (because the complete thermodynamical information is included in the fundamental equation) but it would turn out to be considerably more complicated than simple application of the extremum principle<sup>7</sup>. The power and simplicity of thermodynamics relies on describing the real system with the appropriate formalism. In other words, one would need to have an equivalent formulation of the fundamental equation for each combination of independent variables controlled in experiments. This can be achieved with aid of Legendre transforms. In the example above, the new equilibrium state could be determined by having a function with natural variables  $(S, p, n)$  which contains the same thermodynamical content of the internal energy. That function is one of the thermodynamical potentials, and is called the enthalpy. The minimum of the enthalpy defines the equilibrium of the systems where  $(S, p, n)$  are independently controlled. The most common thermodynamical potentials are:<sup>8</sup>

$$H(S, p, n) = U + pv \quad \text{Enthalpy} \quad (2.6)$$

$$F(T, v, n) = U - TS \quad \text{Helmholtz Free Energy} \quad (2.7)$$

$$G(T, p, n) = H - TS = U - pv + TS \quad \text{Gibbs Free Energy} \quad (2.8)$$

In the most common experimental situation of constant temperature and pressure, the appropriate thermodynamical formulation is represented by the Gibbs Free Energy. In this formulation, the minimum of the Gibbs free energy with respect to its coordinates, defines the equilibrium system.

<sup>7</sup>In other words, one cannot just write the energy as a function of pressure  $U(S, p, n, \dots)$ , instead of volume, because the extremum principle works only on the natural variables.

<sup>8</sup>In general, for a system with internal energy  $dU = TdS + \sum_i x_i dX_i$  (with  $x_i dX_i$  being any of the  $k$  conjugated pair of intensive and extensive variable that describes the system) instead of the two functions  $U$  and  $H$ , one will have  $2^k$  functions of state in the form:

$$U + \sum' x_i X_i$$

where the summation is taken over any set of the coordinates and forces.

Equivalently, instead of only the two free energy functions  $F$  and  $G$  there will be  $2^k$  functions in the form:

$$U - TS + \sum' x_i X_i$$

## 2.1 Phase Transitions

As introduced before, lipid melting in biological membranes occurs few degrees below physiological temperature. Interesting macroscopic changes are related to the lipid transition and will be the main subject of this thesis.

In the following we treat the lipid melting as a two state transition between a solid-ordered (gel) and a liquid-disordered (fluid) state. The melting temperature,  $T_m$  is defined as the temperature at which the two states are found with the same probability:

$$\frac{P_{fluid}(T_m)}{P_{gel}(T_m)} = \exp\left(-\frac{\Delta G}{RT_m}\right) = 1 \quad (2.9)$$

where  $R = 8.314J/molK$  is the molar gas constant and  $\Delta G$  is the difference in the Gibbs free energy of the two states, which is zero at the transition:

$$\Delta G = G_{fluid} - G_{gel} = \Delta H_0 - T_m \Delta S_0 = 0 \quad \text{or} \quad T_m = \frac{\Delta H_0}{\Delta S_0} \quad (2.10)$$

Here  $\Delta H_0$  and  $\Delta S_0$  are the enthalpy and the entropy difference between the fluid and the gel phase. They can be measured using differential scanning calorimetry (DSC), a technique that allows measurement of the heat capacity at constant pressure of a sample as a function temperature. Heat capacity is defined as:

$$c_p \equiv \left(\frac{\partial Q}{\partial T}\right)_p = \left(\frac{\partial H}{\partial T}\right)_p = T \left(\frac{\partial S}{\partial T}\right)_p \quad (2.11)$$

The heat capacity quantifies the amount of heat required to change the temperature of a mole of substance by a certain amount and therefore shows a peak at the temperature at which the system undergoes a phase transition. By integrating the heat capacity over the temperature one can determine the melting enthalpy and entropy. Literature values for DPPC vesicles are  $\Delta H_0 = 39kJ/mol$  and  $\Delta S_0 = 124.14J/mol$ , with a melting temperature  $T_m = 314.15K$  [16]. Calorimetric data give information on the melting properties in conditions of constant pressure. However, the melting transition is known to be affected by changes in several parameters like lateral pressure, hydrostatic pressure [2], voltage [26], lipid composition (e.g. presence of cholesterol), pH [27, 28], ionic environment [27] and the presence of proteins, peptides [29], and other chemicals like anesthetics [30] and neurotransmitters [31]. In other words, anything that affects the free energy difference of the system is expected to influence the melting transition. In chapter 3 we will work out the effect of an electric field on the lipid transition.

Treating the lipid melting as a two state transition from a gel to a fluid state governed by a van't Hoff law we can write the equilibrium constant between the two states:

$$K(T) = \exp\left(-n\frac{\Delta G}{RT}\right) \quad (2.12)$$

where  $n$  is the cooperative unit size which describes the number of lipids that melt in a cooperative way (for a DPPC membrane it is about 170). From the equilibrium constant we can derive the probability to find a lipid in the fluid state as:

$$P_{fluid}(T) = \frac{K(T)}{1 + K(T)} \quad (2.13)$$

$P_{fluid}(T)$  also indicates the molar fraction of lipids in the fluid phase. According to this, the mean enthalpy is given  $\langle \Delta H(T) \rangle = \Delta H_0 P_{fluid}(T)$ . In a similar way one can express the statistical average of the other extensive variables (e.g. area and volume).

**Susceptibilities and fluctuations** According to the definition of the heat capacity (Eq. (2.11)), and using the expression of the mean enthalpy, it can be proved that the heat capacity is proportional to the fluctuations in the enthalpy:

$$c_p = \left( \frac{\partial \langle H \rangle}{\partial T} \right)_p = \frac{\langle H^2 \rangle - \langle H \rangle^2}{RT} \quad (2.14)$$

This means that at the transition, where the heat capacity is at a maximum, the fluctuations in the enthalpy are also maxima. This does not hold only for the heat capacity but it is a general result of thermodynamics<sup>9</sup>, according to which the thermodynamical susceptibilities of the system are proportional to the fluctuations of the correspondent extensive variables. A thermodynamic susceptibility is defined as the derivative of an extensive variable with respect to the conjugated intensive variables. In the case of volume  $v$  and area  $A$ , for example, the thermodynamic susceptibilities are the isothermal volume and area compressibilities. They are proportional to the fluctuations in volume and area:

$$\begin{aligned} \kappa_T^V &= -\frac{1}{\langle v \rangle} \left( \frac{\partial \langle v \rangle}{\partial p} \right)_T = \frac{\langle v^2 \rangle - \langle v \rangle^2}{\langle v \rangle RT} \\ \kappa_T^A &= -\frac{1}{\langle A \rangle} \left( \frac{\partial \langle A \rangle}{\partial \pi} \right)_T = \frac{\langle A^2 \rangle - \langle A \rangle^2}{\langle A \rangle RT} \end{aligned} \quad (2.15)$$

where  $\pi$  is the lateral pressure (the intensive variable conjugated to the area  $A$ ).

Lipid membranes undergo significant changes in their dimensions upon melting. In particular, going from the gel to the fluid phase the volume changes of about 4%, the area of 24% and the thickness of  $-16\%$  [16]. Changes in volume in lipid bilayers have been found to be proportional to the changes in enthalpy [16]:

$$\Delta v(T) = \gamma_v \Delta H(T) \quad (2.16)$$

---

<sup>9</sup>This result can be proved in an equivalent way in the entropy representation, assuming the entropy is an harmonic function of its extensive coordinates for small fluctuations around the equilibrium state. For a full derivation see [32]

where  $\gamma_v = 7.8 \cdot 10^{-10} m^3/J$  is the proportionality coefficient which is practically the same for different lipid species and composition, including biological membranes [33]. By using more indirect methods, the same relation has been found to hold for changes in the area:

$$\Delta A(T) = \gamma_A \Delta H(T) \quad (2.17)$$

with proportionality constant  $\gamma_A = 0.89 m^2/J$  [16]. Due to the small relative changes in volume, a similar relation can be assumed for the changes in thickness.

In a system where area and volume change proportionally to the enthalpy, the correspondent susceptibility are also expected to be proportional. This means that the area and volume compressibility are proportional to the heat capacity.

$$\begin{aligned} \Delta \kappa_T^v &= \frac{\gamma_v^2 T}{\langle v \rangle} \Delta c_p \\ \Delta \kappa_T^A &= \frac{\gamma_A^2 T}{\langle A \rangle} \Delta c_p \end{aligned} \quad (2.18)$$

The most striking consequence of Eq. (2.18) is that the elastic constant, being proportional to the heat capacity, will also exhibit a peak at the phase transition. This means that at the transition the membrane is more compressible and small changes in hydrostatic and lateral pressure result in big changes in volume and area. Another more practical consequence of Eq. (2.18) is that information of the elastic constant and the geometry of the system can be inferred from calorimetric experiments.



**Part II**  
**Theory**



# 3

## Polarization effects

In the previous chapters we have seen how the the mechanical properties of membranes change in proximity of their phase transition and how this, in turn, can be affected by changes in the intensive thermodynamical variables. We have also briefly introduced the behaviour of membranes in the presence of electric fields, though far for the transition. In this chapter we investigate how the electrical and mechanical properties are coupled in a thermodynamical framework and discuss them in proximity of the phase transition. <sup>1</sup>

### 3.1 Membrane capacitor

Different ions are present at difference concentrations on the two sides of biological membrane. For instance, the concentration of potassium ions inside the squid axon is 400 mM and only 20 mM outside. If the membrane is only permeable for potassium, this results in a voltage difference of about -75 mV between the inside and the outside of the cell once the electrochemical equilibrium has been reached. In general, most of the cells sustain voltage differences across their plasma membrane of about  $\pm 100$  mV. For a membrane which is about 5 nm thick, this would result in an electric field of about  $2 \cdot 10^7$  V/m.

Because of their bimolecular thickness and low dielectric constant compared to that of the surrounding water ( $\epsilon \simeq 4\epsilon_0$  for lipids while  $\simeq 80\epsilon_0$  for water), lipid membranes are usually represented as planar capacitors filled with a dielectric when describing their response to electric fields. The value of the capacitance is determined by the dielectric constant of the membrane  $\epsilon$ , along with its geometry, according to the familiar formula:

$$C_m = \epsilon \frac{A}{d}, \quad (3.1)$$

---

<sup>1</sup>The theoretical development presented in this chapter has been made in collaboration with Lars D. Mosgaard

where the dielectric constant is  $\epsilon = \epsilon_0 \epsilon_r$  (with  $\epsilon_0 = 8.854 \cdot 10^{-12} F/m$  the vacuum permittivity and  $\epsilon_r = 2 - 4$  the relative permittivity of the membrane),  $A$  is the area of the membrane and  $d$  is the membrane thickness. This model implies that the dielectric properties of the lipid membrane are uniform over the membrane thickness  $d$ , or, in other words, that the membrane is an homogeneous and isotropic dielectric and the dielectric constant  $\epsilon$  is indeed constant. This is, however, not the case in practice, since the dielectric constant changes significantly between the hydrocarbon interior of the membrane, the polar head group region and the adjacent aqueous phase (i.e. the diffuse double layer region made by oriented water molecules). Each of these regions has further a different thickness, and therefore its own capacitance and conductance value. The equivalent electrical representation of the membrane would then contain a series of capacitors normal to the membrane plane (one for each region). The total capacitance of a series combination of capacitors cannot be larger than the smallest contribution. Since the smallest capacitor is the one representing the hydrocarbon interior [34, 35], this means that practically the entire membrane capacitance arises from the hydrocarbon interior, over which the entire voltage drop is assumed to happen. We will in the following embrace this view, and consider the contribution to the capacitance from the polar headgroup and the aqueous medium to be negligible, which is supported by experimental and theoretical evidence and treat the membrane as an homogeneous dielectric <sup>23</sup>.

The membrane capacitance is often quantified by the specific capacitance (capacitance per unit area), which has the advantage of being fairly constant for different membrane systems and has a value of about  $c_m = \epsilon/d \simeq 1 \mu F/cm^2$ <sup>4</sup> for membranes of different compositions and geometries<sup>5</sup>. So much so, that capacitance measurements are often used to make estimations of membrane area, e.g. in experiments on membrane patches.

In this capacitor model the role of the conducting plates is played by the electrolyte surrounding the membrane (which is assumed to be a perfect conductor) and the geometry of the capacitor is considered to be constant. Both are rough approximations, but while the former has been addressed and

---

<sup>2</sup>Note, however, that when using the values of the membrane thickness in 3.1 instead of just the hydrocarbon interior, we are underestimating the membrane capacitance by a factor of  $\simeq 0.8$  (assuming a thickness of the hydrocarbon region of  $\simeq 3nm$  [35] and a thickness in the fluid phase of  $3.9nm$  [16])

<sup>3</sup>Among the observations on support of this hypothesis there is the experimental agreement between the value of thickness of the hydrocarbon core estimated from 3.1 using the dielectric constant of bulk hydrocarbons and the one directly measured with X-ray diffraction. Furthermore, it is supported by the observation that bilayer capacitance is inversely proportional to the number of carbon in the hydrocarbon chain, and that for a given hydrocarbon chain the value of the capacitance seems independent on the type of polar head [36]

<sup>4</sup>assuming  $\epsilon_r = 4$  and  $d = 3.9nm$  [16]

<sup>5</sup>In the case of artificial membranes containing solvent the value is usually lower  $\simeq 0.5 \mu F/cm^2$ .

### 3.1. Membrane capacitor

refined in models that study of electrical properties of the membrane [37], the latter is often considered to be a fairly good description and offhandedly accepted. According to Eq. (3.1), any change in the dimensions of the membrane can potentially affect its capacitance. We discussed in chapter 2 how the area and the thickness of lipid bilayers are significantly different in the gel and in the fluid phase. Considering a 24.6% increase in the area and a 16.3% decrease in thickness from the gel to the fluid phase of DDPC vesicles [16], one expects an increase in the membrane capacitance of about 50% from the gel to the fluid state. The state of the membrane is not the only parameter that can influence the value of the capacitance. In the following we will discuss the validity of the assumption of constant capacitance, in particular with respect to its dependence on voltage.

When a voltage difference,  $\Psi^6$ , is present between the two plates of the membrane capacitor, the ions in solution accumulate on the surface of the membrane and charge the capacitor. The amount of charge,  $q$ , on the membrane surface for a given voltage depends on the value of the capacitance of the membrane, according to:

$$q = C_m \cdot \Psi. \quad (3.2)$$

The electric field inside and outside a charged capacitor can be calculated using the superposition principle (see Fig. (3.1))<sup>7</sup> The electric field produced by an homogeneous planar charge distribution (with charge density,  $\sigma = q/A$ ) is uniform, orthogonal to the charged plane (outward for positive charge, and inward for negative charge) and has a magnitude  $|E| = q/2A\epsilon$ , where  $\epsilon$  is the permittivity of the surrounding medium. We see from Fig. (3.1) that the resulting field for a charged membrane is zero outside and has a magnitude  $|E| = \sigma/\epsilon$  inside.

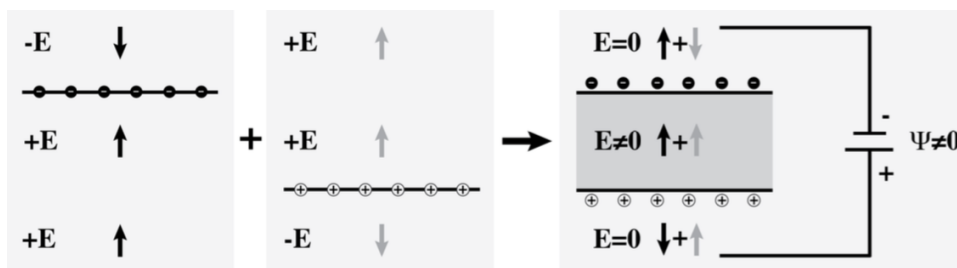


Figure 3.1: Electric field of a charged capacitor. Outside the capacitor the field is zero, while inside is non zero. As a result a voltage difference is present across it. Picture taken from [38]

<sup>6</sup>In the following we consider  $\Psi \equiv -\Delta V$ , with  $\Delta V_{(b-a)} = -\int_a^b \vec{E} \cdot d\vec{l}$ ,  $\vec{E}$  being the electric field.

<sup>7</sup>Here and in the following, we choose a coordinate system where the  $z$  axis has the direction of the normal vector of the membrane.

The presence of a dielectric between the plates of the capacitor results in an electric field which is lower than the one in the case of vacuum by a factor equal to the relative dielectric constant of the dielectric. The reason for the decrease lies in the polarization of the dielectric. Once a dielectric is polarized by an externally applied field, induced or oriented dipoles in the dielectric create an electric field in the opposite direction which tends to minimize the free energy, and thus the total field. The extent to which the applied field is counteracted is an indication of whether a material is a good or bad insulator. In the case of conductors, the counterbalance is exact and therefore the total field inside a good conductor is zero. If the dielectric is homogeneous and isotropic, the field inside the charged capacitor is uniform and the voltage difference between its plates is given by  $\Psi = E \cdot d$ .

**Electrostriction** When the membrane capacitor is charged, the opposite charges on its plates will attract each other exerting a mechanical force on the capacitor, which tends to compress the membrane. This effect is called electrostriction, and is shown in Fig. (3.2).

The extent to which the membrane is compressed depends on the value of its elastic constants. As we discussed in chapter 2.1, close to phase transitions the elastic constants of lipid membranes have a maximum and the membrane is more compressible. As a result, one expects that even a small change in voltage would result in significant changes in the dimensions of the membrane, and therefore in big changes of its capacitance.

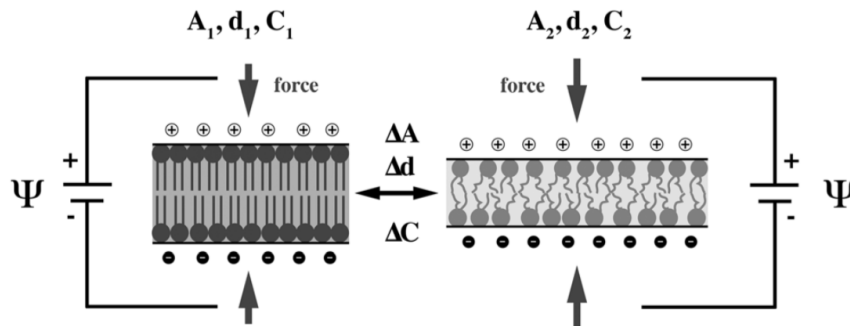


Figure 3.2: Electrostriction in a charged capacitor: a voltage  $\Psi$  across the membrane results in a force compressing it to a final state with larger area and smaller thickness. As a result, the value of the capacitance changes. Picture taken from [38]

**Spontaneous polarization** All the above considerations were made having in mind a perfectly symmetric membrane. In this case, as anticipated in chapter 1, the net electric dipoles in the two leaflets of the membrane are equal but have opposite direction, hence they cancel each other and result

in a zero polarization when there is no field applied, and the membrane is non polar.

Biological membranes, however, are highly asymmetric systems. The lipid composition of the two leaflets, for instance, is often very different and one usually finds more negatively charged lipids in the inner leaflet of the bilayer. Biological membranes contain also peripheral and transmembrane proteins which can carry both positive and negative charge, and they are also asymmetrically distributed across the membrane [14]. As a result of these compositional asymmetries, the membrane can have a net dipole moment in the absence of an applied field <sup>8</sup>. When a membrane with spontaneous polarization is surrounded by an electrolyte, the free charges in solution distribute as to cancel the bound polarization charges in the membrane. As a result, the membrane capacitor in equilibrium can be charged in the absence of an applied voltage. This is illustrated in Fig. (3.3) (left). In order to discharge the capacitor, a voltage  $\Psi = -\Psi_0$  needs to be applied (Fig. (3.3), right). We call  $\Psi_0$  the offset voltage or offset potential. Note that in the absence of voltage not only is the membrane charged, but also the electric field inside the membrane is zero, as a result of the complete bound charge cancellation from the free ions in solutions. In this respect, the case of a charged membrane and a polarized one are conceptually different and one has to be careful to account for both effects correctly in a theoretical treatment.

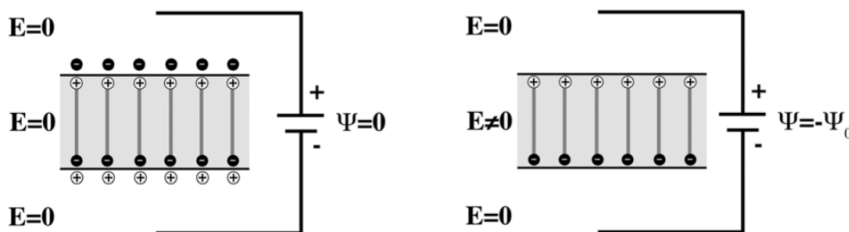


Figure 3.3: **Left:** a polarized membrane capacitor is charged in the absence of an applied voltage. The electric field is zero everywhere. **Right:** in order to discharge the capacitor, a voltage  $\Psi = -\Psi_0$  has to be applied. Figure from [38]

A chemical asymmetry of the two leaflets is not the only mechanism that can produce spontaneous polarization in the membrane. Another mechanism is, for example, curvature. In general, any deformation which alters the relative orientation of dipoles in the two monolayers, can induce spontaneous polarization. Curvature induced polarization is a concept that was first in-

<sup>8</sup>We call this dipole moment and the resulting polarization *spontaneous*, rather than permanent (as it is sometimes called in literature, *e.g.* for ferroelectric materials) because its value can vary in response to changes in the external parameters.

troduced by Meyer in 1969 in the context of liquid crystals [39], and applied to biological membranes by Petrov who named it *flexoelectricity* [40]. Curvature in the membrane induces different lateral pressure in the two monolayers, compressing one while expanding the other. The result is that the polarization (which is dipole moment per unit volume) will be different in the two leaflets and the membrane has a spontaneous polarization in the absence of an applied voltage (Fig. (3.4),b-c). Again, the curved membrane at equilibrium will be charged when surrounded by an electrolyte, and a voltage  $\Psi = -\Psi_0$  needs to be applied to discharge it. (Fig. (3.4),d).

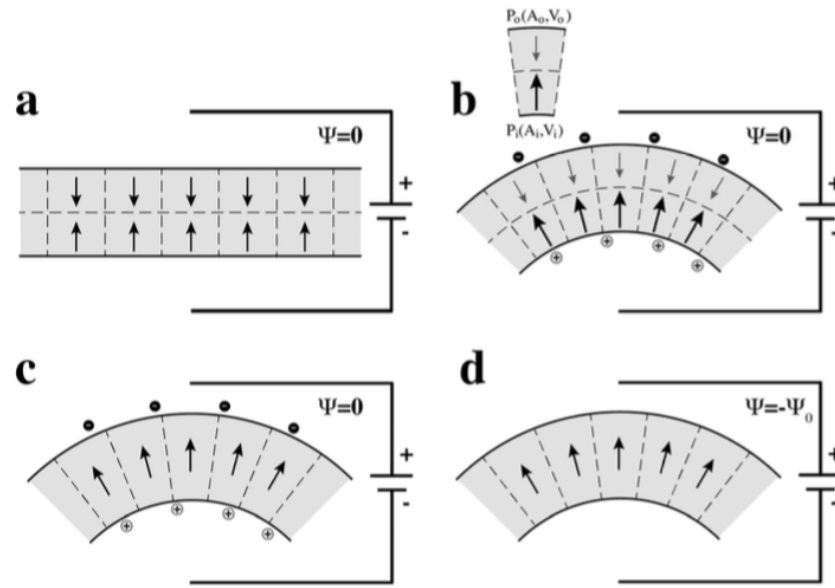


Figure 3.4: Illustration of curvature induced polarization. **a:** The polarization of a chemically symmetric membrane in the absence of an electric is zero when flat. **b:** Upon bending the relative volume of the two monolayers change and so does their polarization. The membrane in the absence of a field has a polarization different from zero (**c**). The membrane capacitor is then charged with  $\Psi = 0$ . **d:** In order to discharge the membrane, a voltage  $\Psi = -\Psi_0$  has to be applied. Figure from [38]

We see that flexoelectricity and chemical asymmetry have the same result and behaviour in terms of membrane polarization and thus we will not distinguish between the mechanisms in the theoretical treatment. Note, however, that in general the two phenomena are combined, since biologically membranes not only have asymmetric composition but are often found in convoluted curved shapes.

## 3.2 Thermodynamics of membranes in electric fields

In this section we will derive the thermodynamical tools with which one can solve the fundamental problem of thermodynamics for a a membrane in an electric field *i.e.* to predict the new state of equilibrium for the closed system made of a membrane in an electrolyte when some internal constraints are removed. We will follow the approach of chapter 2, adding an extra thermodynamical coordinate to describe the state of the system in the presence of electric fields. This corresponds to finding the fundamental equation for the entropy of the system and applying the extremum principle to study the equilibrium states of the system. We start by writing the internal energy of the system instead of the entropy, but we have seen already that the two formulations have identical thermodynamical content.

In the presence of an electric field an extra extensive variable is needed to fully characterize the thermodynamical state of the system, in addition to entropy ( $S$ ), volume ( $v$ ), and area ( $A$ ). Particular care must be taken when choosing the correct extensive variable and conjugated intensive ones so that they constitute a conjugated pair in the thermodynamical sense. Furthermore, when we consider the membrane capacitor, we expect mechanical changes to be observed in response to an applied field. In other words, the hydrophobic interior of the membrane separates the capacitor plates acting both as a dielectric and compressible material. This type of considerations were first discussed by Frank in 1955 when studying the thermodynamics of a fluid in an electric field [41]. He wrote the electrical work done on a fluid during any reversible and infinitesimal change as  $dW_{el} = Ed(vD)$ . This corresponds to having the electric displacement ( $D$ ) in a volume  $v$ , as extensive variable and the electric field ( $E$ ) as the conjugated intensive one. The differential form of the fundamental equation takes the form:

$$dU = TdS - pdv - \pi dA + Ed(vD), \quad (3.3)$$

In his thought experiment, Frank considered an homogeneous and isotropic fluid contained between the plates of a planar capacitor. In this geometry the electric displacement and electric field are both normal to the plate surface, hence vector notation can be dropped.

Eq. (3.3) is the fundamental equation of the system in the presence of a field. We now want to work out the last term in order to write it explicitly and make physical predictions. To do this we have to get the aid of electrostatics.

**Electric displacement in asymmetric membranes** The electric displacement,  $D$ , is defined as:

$$D \equiv \epsilon_0 E + P \quad (3.4)$$

where  $E$  is the electric field and  $P$  is the polarization (or polarization density).

When placed in an electric field a dielectric gets polarized, meaning that it will have a net dipole moment per unit volume, also called polarization. This can be induced by deformation or orientation, but in both cases the polarization is a linear function of the field for small field strengths<sup>9</sup>. In the case of an isotropic material the induced polarization has the same direction as the field and can be written as:

$$P_{ind} = \epsilon_0 \chi_{el} E$$

where  $\chi_{el}$  is the electric susceptibility, which in anisotropic materials is a tensor taking into account the different polarizability of the material in the different directions. The material will have a net dipole moment per unit volume as a consequence of the field. If the field is removed, the net polarization is also removed.

Let's now consider the case of an asymmetric membrane. No matter how the asymmetry has come about (if through curvature or asymmetric lipid distribution), the result will be the appearance of a net spontaneous polarization,  $P_0$ , in the absence of any applied field. If we now apply a field normal to the membrane, the total polarization can be written as:

$$\begin{aligned} P &= P_{ind} + P_0 \\ &= \epsilon_0 \chi_{el} E + P_0 \end{aligned} \tag{3.5}$$

We see that when the field is zero, the total polarization doesn't vanish. Moreover, the magnitude and direction of the spontaneous polarization is independent of the electric field. Depending on its direction relative to the applied field the total polarization can be increased or decreased by the presence of a field. The polarization density is a measure of the surface bound charges in a dielectric, according to Gauss Law,  $\nabla \cdot \mathbf{P} = -\rho_b$  ( $\rho_b$ , volume density of bound charges in the dielectric). According to its definition, it follows that the electric displacement is a measure of the free charges in our system. In the case of an asymmetric membrane, the electric displacement takes the form:

$$\begin{aligned} D &= \epsilon_0(1 + \chi_{el})E + P_0 \\ &= \epsilon E + P_0 \end{aligned} \tag{3.6}$$

Where  $\epsilon$  is the dielectric constant,  $\epsilon = \epsilon_0(1 + \chi_{el})$ . We see that in the absence of an applied field the electric displacement is different from zero. From its definition combined to Gauss Law, we have that  $D$  is a measure of the free charges in the system:

$$\nabla \cdot \mathbf{D} = \rho_f \quad \text{or, for planar geometry} \quad D = \frac{q}{A} \tag{3.7}$$

<sup>9</sup>small compared to the dielectric strength of the material, *i.e.* the maximum electric field that can be applied to a material without incurring in dielectric breakdown

### 3.2. Thermodynamics of membranes in electric fields

---

where  $\rho_f$  is the volume charge density of free charges. This means that in the presence of spontaneous polarization there is a net free charge on the plates of the capacitor. We call this charge  $q_0$ , offset charge:

$$D|_{E=0} = P_0 = \frac{q_0}{A} \quad (3.8)$$

The offset charge is equal to the bound polarization charge of the membrane, and therefore it is responsible for screening it and canceling the total field. As a result the membrane capacitor is charged but there is no net electric field, nor inside nor outside the membrane.

**Gibbs Free Energy with electric fields** We started this section by writing the fundamental equation for the internal energy with respect to the extensive variables of the system  $U(S, v, A, vD)$ . We notice, however, that in experiments on membranes, one usually has control over the intensive variables, namely temperature  $T$ , pressure  $p$ , lateral pressure  $\pi$  and electric field  $E$ . In order to get useful informations, the thermodynamical potential of choice is then the Gibbs Free Energy  $G(T, p, \pi, E)$ . The Legendre transforms guarantees that the thermodynamical content of the two formulation is equivalent. The differential of the Gibbs Free Energy in the presence of a field is given by:

$$dG = -SdT + vdp + Ad\pi - (vD)dE \quad (3.9)$$

The last term is the electrical contribution, which we will refer to as electrical free energy,  $G_{el}$ . Knowing the expression of the electric displacement in terms of the applied field for an asymmetric membrane, we can calculate the electrical free energy using Eq. (3.6):

$$G_{el} = - \int_0^E (vD)dE' = -\frac{\epsilon v}{2} E^2 - vP_0 E \quad (3.10)$$

where the volume of the lipid membrane was assumed to be constant. If we assume the membrane to be homogeneous and isotropic, the electric potential across it can be simply written in terms of the electric field,  $Ed = \Psi$ . This leads to:

$$G_{el} = -\frac{\epsilon}{2} \frac{A}{d} \Psi^2 - AP_0 \Psi, \quad (3.11)$$

The prefactor of the first term in the previous expression is equal to the membrane capacitance and we call it  $C_m$ . We further define the offset voltage as

$$\Psi_0 = \frac{P_0 d}{\epsilon} \quad (3.12)$$

The offset voltage is the voltage one would need to apply to the membrane capacitor in order to induce a charge equal to the offset charge,  $q_0$ . In other

words, it is the voltage at which one would have  $D = P_0$  in the absence of any spontaneous polarization. Finally, using this definition, we can re-write the electrical free energy in the following:

$$\begin{aligned} G_{el} &= -\frac{C_m}{2}(\Psi^2 + 2\Psi_0\Psi) \\ &= -\frac{C_m}{2}((\Psi + \Psi_0)^2 - \Psi_0^2), \end{aligned} \quad (3.13)$$

We stress that due to the presence of the screening charge  $q_0$ , in the presence of an electrolyte the actual voltage difference across the membrane due to the spontaneous polarization is zero. This is confirmed by the fact that in the absence of an applied field, the electrical free energy is zero, *i.e.* there is no contribution to the energy from the offset potential. This point will be clarified in the course of the chapter.<sup>10</sup>

### 3.2.1 Electrostriction

We have already anticipated that when a voltage is applied across the membrane capacitor, we expect electrostrictive forces to arise which tend to compress the membrane. We now want to quantify this effect. In the absence of spontaneous polarization the electrical free energy is  $G_{el} = -\frac{1}{2}C_m\Psi^2$ . For constant voltage and area, the electrostrictive force is given by:

$$\mathcal{F} = \frac{\partial G_{el}}{\partial d} = -\frac{1}{2} \left( \frac{\partial C_m}{\partial d} \right) \Psi^2 = \frac{1}{2} \frac{C_m \Psi^2}{d} \quad (3.14)$$

In the case of an asymmetric membrane displaying spontaneous polarization, one has

$$\mathcal{F} = \frac{\partial G_{el}}{\partial d} = \frac{1}{2} \frac{C_m}{d} (\Psi^2 + 2\Psi_0\Psi) \quad (3.15)$$

The electrostrictive force is therefore a quadratic function of the voltage and in the case of asymmetric membranes with spontaneous polarization, it displays an additional linear term proportional to the offset voltage. We see that when  $(\Psi^2 + 2\Psi_0\Psi) < 0$  the force is negative, so applying a voltage whose magnitude is included in the interval  $(0, -2\Psi_0)$  will decrease the value of the capacitance. Assuming that the changes in the thickness are very small ( $\Delta d \ll d$ ) and that the area stays constant, the change in thickness will produce a change in the capacitance equal to:

$$\Delta C_m = -\epsilon \frac{A}{d^2} \Delta d \quad (3.16)$$

---

<sup>10</sup>Note that using  $P_0$  or  $\Psi_0$  is not strictly equivalent, since they involve different assumptions on the geometry of the system. The spontaneous polarization is defined as dipole moment per unit volume. Since we consider the membrane volume to be constant,  $P_0$  is independent of the geometry of the system, unlike  $\Psi_0$  which depends on the membrane thickness. The particular choice of one or the other must follow the specific experimental conditions considered. Similar considerations apply to the choice of  $E$  or  $\Psi$ .

### 3.2. Thermodynamics of membranes in electric fields

The change in capacitance is therefore proportional to the change in thickness. We find that if the thickness is linearly proportional to the force, then the capacitance is also a quadratic function of the voltage with a voltage offset:

$$\Delta C_m \propto (\Psi^2 + 2\Psi_0\Psi) \quad (3.17)$$

Electrostriction has been studied by several authors in both synthetic and biological membranes [42, 43]. A quadratic dependence of the capacitance on the voltage was for instance found by Alvarez and Latorre in 1978 as shown in Fig. (3.5).

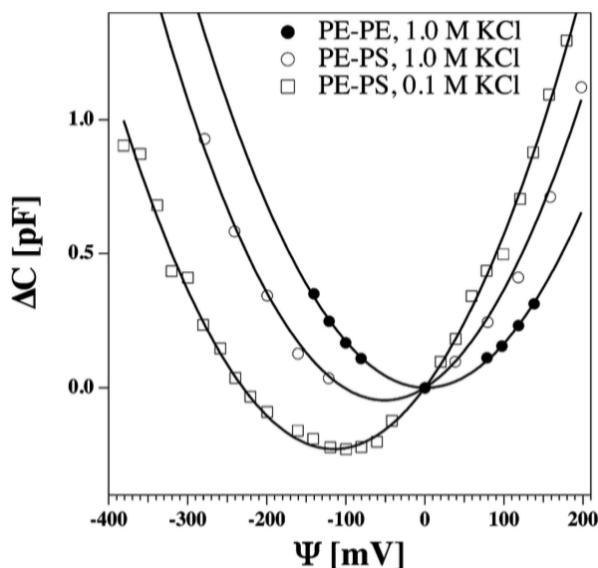


Figure 3.5: Quadratic voltage dependence of the membrane capacitance in a black lipid membrane. **Solid circles:** symmetric membrane made of zwitterionic PE in 1 M KCl, **Open circles:** asymmetric membrane made of PE and charged PS in 1M KCl, **Open squares:** same asymmetric membrane in 0.1 M KCl. The relative change in capacitance due to voltage in the range investigated is below 1%. Picture adapted from [42]

Interestingly, they studied membranes of different composition, symmetric and asymmetric, the latter with one monolayer made of zwitterionic phosphatidylethanolamine (PE) and the other made of the charged phosphatidylserine (PS). They found that in the case of asymmetric membranes the minimum of capacitance-voltage curve is shifted on the voltage axis. This is in line with our expectation of a chemically induced spontaneous polarization. They found a voltage offset of  $\Psi_0 = 47mV$ , which is dependent on the ionic strength. The membranes studied by Alvarez and Latorre had a capacitance of approximately 300 pF at zero voltage, compared to which

the change in capacitance shown in figure results very small. Their experiments, however, were carried out far from the phase transition, where the compressibility of the membrane is low.

### 3.2.2 Phase transition in the presence of an electric field

As discussed before (and shown in Fig. (3.5)), the effect of electrostriction and the correspondent change in capacitance with voltage are expected to be very small in the pure fluid and gel phase, due to the low compressibility of the membrane. However, close to the phase transition the effect is enhanced by the increased compressibility of the membrane, and significant changes in the membrane dimensions are expected to occur even for small changes in the voltage. Based on this, we now try to answer to the question of whether voltage could induce a phase transition from a gel to the fluid phase at constant temperature and to quantify the effect of voltage on the membrane dimension and capacitance. Following the same approach of chapter 2, we start by writing the difference in electric Gibbs Free energy between the fluid and the gel state in the presence of a voltage for an asymmetric membrane:<sup>11</sup>

$$\Delta G_{el} = G_{el}^{fluid} - G_{el}^{gel} = -\frac{\Delta C_m}{2} (\Psi^2 + 2\Psi_0\Psi), \quad (3.18)$$

where  $\Delta C_m = C_m^f - C_m^g$  is the difference between the capacitance in the fluid and in the gel state. In Eq. (3.18) we assumed that both the dielectric constant  $\epsilon$  and the offset voltage  $\Psi_0$  are the same in the fluid and gel state. The first assumption was confirmed in experiments on oleic acid (data not shown). The second one will be discussed later on in the chapter. The equilibrium constant between the fluid and the gel state is given by:

$$K(T, \Psi) = \exp\left(-n\frac{\Delta G(T, \Psi)}{RT}\right) \quad (3.19)$$

where the Gibbs Free energy between gel and fluid state as a function of both temperature and voltage is given by

$$\Delta G = (\Delta H_0 - T\Delta S_0) + \Delta G_{el} \quad (3.20)$$

One can then calculate the fluid fraction according to Eq. (2.13), using the equilibrium constant (Eq. (3.19)). We now have all the tools to derive the effect of voltage on the dimensions of the membrane. Fig. (3.6) shows the voltage dependence of the area for different temperatures for a DPPC membrane (values taken from [16]). The same is shown for the capacitance  $C_m(T, \Psi) = \epsilon A(T, \Psi)/d(T, \Psi)$ . In both cases a voltage offset of  $\Psi_0 = 70mV$  was chosen.

<sup>11</sup>the whole calculation can be made using 3.11.

### 3.2. Thermodynamics of membranes in electric fields

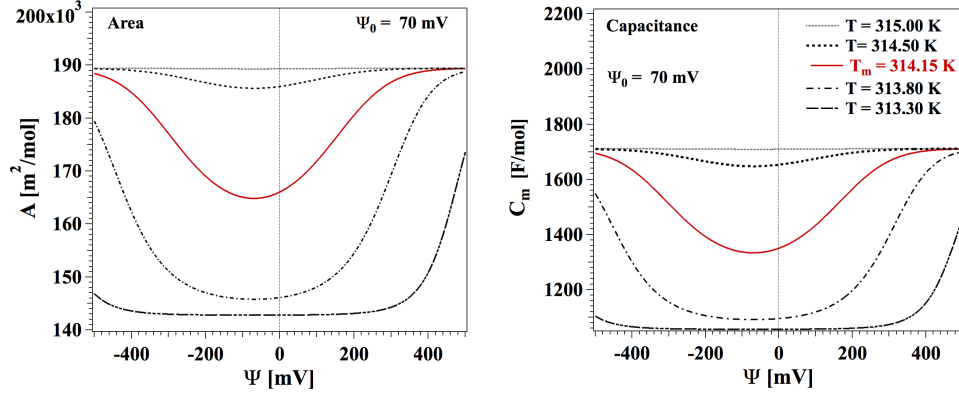


Figure 3.6: Membrane area (left) and capacitance (right) as a function of voltage for five different temperatures close to the melting temperature. The voltage offset was set to  $\Psi_0 = 70\text{mV}$ . Values from [16].

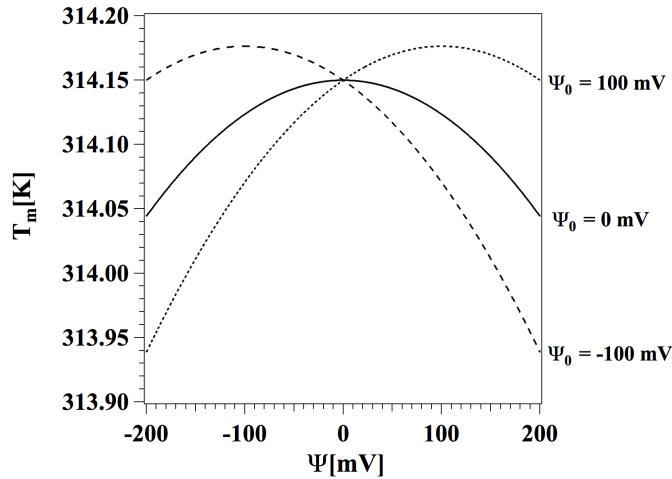


Figure 3.7: Voltage dependence of the melting temperature (Eq. (3.21)) in the case of no offset voltage (solid line) and for polarized membrane with two different voltage offsets  $\Psi_0 = 100\text{mV}$  and  $\Psi_0 = -100\text{mV}$ . The offset voltage in the fluid and gel phase is assumed to be equal.

At the melting temperature  $T_m$ , the Gibbs Free energy between the gel and the fluid state is zero. From Eq. (3.20) we have:

$$\begin{aligned}
 T_m &= T_{m,0} \left( 1 + \frac{\Delta G_{el}}{\Delta H_0} \right) \\
 &= T_{m,0} \left( 1 - \frac{\Delta C_m}{\Delta H_0} \left( \frac{\Psi^2}{2} + \Psi_0 \Psi \right) \right)
 \end{aligned} \tag{3.21}$$

Where  $T_{m,0}$  is the melting temperature in the absence of applied voltage. We see the result in Fig. (3.7). In the case of a symmetric membrane ( $\Psi_0 = 0$ ) the melting temperature is decreasing quadratically with voltage, thus positive and negative voltage have exactly the same effect on the melting temperature. This was already found by Heimburg [24]. When the membrane is asymmetric the effect of voltage on the melting temperature depends on the direction and the magnitude of the offset voltage, so that the same applied voltage can induce or inhibit a phase transition depending on the value of  $\Psi_0$ .

**Generalization for  $\Psi_{0,f} \neq \Psi_{0,g}$**  In the previous derivation we assumed the voltage offset to be constant in the transition. It is worth reminding that the voltage offset is given by  $\Psi_0 = P_0 d / \epsilon$ . This means that it is linked to the net dipole moment per unit area (dipole density). We know from monolayers experiments that the dipole moment in the two state is different [44], and we expect the same in bilayers. Even if we assume that the dipole moment stays constant, the area in the gel and fluid phase changes significantly, meaning that the voltage offset would change as a consequence of dipole dilution going from the gel to the fluid phase. In the general case, the offset will not be constant and we call  $\Psi_{0,f}$  and  $\Psi_{0,g}$  the offset in the fluid and in the gel phase, respectively. The electrical Gibbs free energy difference between the two states takes the form:<sup>12</sup>

$$\Delta G_{el} = -\frac{\Delta C_m}{2} ((\Psi^2 + \Psi_{0,g}\Psi) - C_m^f \Psi(\Psi_{0,f} - \Psi_{0,g})), \quad (3.22)$$

From this, one can again calculate the effect of voltage on melting temperature, membrane dimensions and capacitance.

### 3.2.3 Charge on the membrane capacitor

The total charge on the membrane capacitor in the presence of an applied field is, according to Eq. (3.7), given by:

$$q = A \cdot D = A(\epsilon E + P_0) = \epsilon \frac{A}{d} (\Psi + \Psi_0) = C_m (\Psi + \Psi_0) \quad (3.23)$$

We see that the charge is made of two contributions. The first is the familiar term  $C_m \Psi$  and the second can be written as  $AP_0 = q_0$  and it is the offset charge discussed before. The charge can change in response to changes in

<sup>12</sup>note that one could use 3.11 instead of 3.13. In that case, one could discuss whether  $P_0$  stays constant rather than  $\Psi_0$ . Since  $P_0$  is independent of the membrane geometry this corresponds to discussing whether net dipole moment of the membrane changes in the fluid and the gel phase.

voltage ( $\Psi$ ), area ( $A$ ), curvature ( $c$ )<sup>13</sup> and temperature ( $T$ ):

$$dq = \left( \frac{\partial q}{\partial \Psi} \right)_{A,c,T} d\Psi + \left( \frac{\partial q}{\partial A} \right)_{\Psi,c,T} dA + \left( \frac{\partial q}{\partial c} \right)_{\Psi,A,T} dc + \left( \frac{\partial q}{\partial T} \right)_{\Psi,A,c} dT \quad (3.24)$$

Eq. (3.24) assumes that voltage, area, curvature and temperature are all variables that can be changed independently in experiments. This is not the case in general. In this framework however, we can write the partial derivative explicitly using 3.23:

$$dq = \left[ (\Psi + \Psi_0) \left( \frac{\partial C_m}{\partial \Psi} \right)_{A,c,T} + C_m + C_m \left( \frac{\partial \Psi_0}{\partial \Psi} \right)_{A,c,T} \right] d\Psi + \left[ (\Psi + \Psi_0) \left( \frac{\partial C_m}{\partial A} \right)_{\Psi,c,T} + C_m \left( \frac{\partial \Psi_0}{\partial A} \right)_{\Psi,c,T} \right] dA + \left[ (\Psi + \Psi_0) \left( \frac{\partial C_m}{\partial c} \right)_{\Psi,A,T} + C_m \left( \frac{\partial \Psi_0}{\partial c} \right)_{\Psi,A,T} \right] dc + \left[ (\Psi + \Psi_0) \left( \frac{\partial C_m}{\partial T} \right)_{\Psi,A,c} + C_m \left( \frac{\partial \Psi_0}{\partial T} \right)_{\Psi,A,c} \right] dT \quad (3.25)$$

Equivalent relations can be obtained for different sets of free variables, for example by choosing  $\pi$  instead of  $A$ . Each term of Eq. (3.25) contains information on the coupling between electric (charge  $dq$ ) and mechanical and thermal variables. The first term expresses the nonlinearity of the membrane charge with respect to voltage, the second and third express the electromechanical couplings, namely the fact that the membrane is piezoelectric and flexoelectric, respectively, and the last defines the thermoelectric behaviour. In the following we analyse each term. We will discuss experimental situations where two variable (like, for example, temperature and area) are coupled and not independent.

**Capacitive susceptibility** The first term on the right hand side of Eqs. 3.25 describes the change in charge as a response to changes in the applied voltage. It is the capacitive susceptibility of the membrane  $\hat{C}_m = (\partial q / \partial \Psi)$ , already discussed by Heimburg [24]. In addition to the geometric membrane capacitance  $C_m$ , it includes changes in membrane dimensions and spontaneous polarization induced by the voltage. As the changes in area and dimension with voltage are maxima in the transition we expect the capacitive susceptibility to display a maximum in the transition. If we fix curvature

---

<sup>13</sup>we assume spherical geometry, hence  $c=2/R$ .

and temperature and let the area change with the voltage, the capacitive susceptibility has the form:

$$\hat{C}_m = C_m + (\Psi + \Psi_0) \left( \frac{\partial C_m}{\partial \Psi} \right)_{c,T} + C_m \left( \frac{\partial \Psi_0}{\partial \Psi} \right)_{c,T} \quad (3.26)$$

In the case where the voltage offset doesn't change with voltage or with changes in the dimensions of the membrane, we have:

$$\hat{C}_m = C_m + (\Psi + \Psi_0) \left( \frac{\partial C_m}{\partial \Psi} \right)_{c,T} \quad (3.27)$$

Finally, if the spontaneous polarization is zero for all voltages, we obtain the expression derived by Heimburg [24]:

$$\hat{C}_m = C_m + \Psi \left( \frac{\partial C_m}{\partial \Psi} \right)_{c,T} \quad (3.28)$$

**Piezoelectricity** The second term of 3.25 expresses the change in charge due to changes in area. The more general response of charge to changes in dimension is known as piezoelectricity. It means that the charge on a capacitor can change even when the voltage is kept constant. If in addition to the voltage, also curvature and temperature are kept constant it is given by:

$$dq = \left[ (\Psi + \Psi_0) \left( \frac{\partial C_m}{\partial A} \right)_{\Psi,c,T} + C_m \left( \frac{\partial \Psi_0}{\partial A} \right)_{\Psi,c,T} \right] dA \quad (3.29)$$

In the absence of an applied voltage,  $\Psi = 0$ , and for small changes in area, we get:

$$\Delta q \simeq \left[ \Psi_0 \left( \frac{\partial C_m}{\partial A} \right)_{\Psi,c,T} + C_m \left( \frac{\partial \Psi_0}{\partial A} \right)_{\Psi,c,T} \right] \Delta A \quad (3.30)$$

If the voltage offset is zero for an uncompressed or unstretched membrane,  $\Psi_0(\Delta A = 0) = 0$ , then the total charge on the membrane due to a change in area is given by:

$$q(\Delta A) \simeq C_m \left( \frac{\partial \Psi_0}{\partial A} \right)_{\Psi,c,T} \Delta A \quad \text{or} \quad \Psi_0(\Delta A) \simeq \left( \frac{\partial \Psi_0}{\partial A} \right)_{\Psi,c,T} \Delta A \quad (3.31)$$

**Inverse piezoelectricity** The inverse piezoelectric effect describes the change in membrane dimensions as a result of an applied field or a change in the charge on the capacitor. We start by writing the free energy density of compression ( $g_A$ ) for a membrane with an applied electric potential:

$$g_A = \frac{1}{2} \kappa_T^A \left( \frac{\Delta A}{A_0} \right)^2 - \frac{C_m}{A_0} \left( \frac{\Psi^2}{2} + \Psi_0 \Psi \right) \quad (3.32)$$

where the first term is the elastic and the second is the electric free energy density. At constant  $\Psi$  and  $\kappa_T^A$  the equilibrium value for the change in area  $\Delta A$  from the uncompressed value  $A_0$ , is the one that minimizes the free energy density with respect to the area:

$$\begin{aligned} \frac{\partial g_A}{\partial A} = & \kappa_T^A \frac{\Delta A}{A_0^2} + \frac{C_m}{A_0} \left( \frac{\partial \Psi_0}{\partial A} \right)_{\Psi, c, T} \Psi \\ & - \frac{1}{A_0} \left( \frac{\partial C_m}{\partial A} \right)_{\Psi, c, T} \left( \frac{\Psi^2}{2} + \Psi_0 \Psi \right) = 0 \end{aligned} \quad (3.33)$$

Which is given by

$$\Delta A(\Psi) = \frac{A_0}{\kappa_T^A} \left[ C_m \left( \frac{\partial \Psi_0}{\partial A} \right)_{\Psi, c, T} \Psi + \left( \frac{\partial C_m}{\partial A} \right)_{\Psi, c, T} \left( \frac{\Psi^2}{2} + \Psi_0 \Psi \right) \right] \quad (3.34)$$

Here the first term contains the changes of polarization with the area while the second is linked to the area dependence of the capacitance. The prefactor contains the area compressibility, hence the changes in area due to an applied voltage are expected to be maximum at the transition where the compressibility is maximum.

**Flexoelectricity** Flexoelectricity is curvature-induced polarization. The change in charge due to a change in the curvature is given by the third term of Eq. (3.25), derived in the assumption of constant voltage, area and temperature. In experiments, however, changes in curvature are coupled to changes in area, so that one can not control the area independently of the curvature. We therefore consider the area to be dependent on curvature and assume that  $\Psi$  and  $T$  are kept constant:

$$dq = \left[ (\Psi + \Psi_0) \left( \frac{\partial C_m}{\partial c} \right)_{\Psi, T} + C_m \left( \frac{\partial \Psi_0}{\partial c} \right)_{\Psi, T} \right] dc \quad (3.35)$$

In the simplified case where the capacitance is independent of the curvature and the offset voltage is a linear function of curvature (thus its partial derivative in Eq. (3.35) is constant), we can write the total charge on a curved membrane which displays flexoelectricity:

$$q(c) = C_m(\Psi + \Psi_0(0)) + C_m \left( \frac{\partial \Psi_0}{\partial c} \right)_{\Psi, T} \cdot c \quad (3.36)$$

where the first term on the right hand-side is equal to the charge on the flat capacitor ( $c=0$ ). In the case where no voltage is applied to the membrane and where the spontaneous polarization for the flat capacitor is zero (*i.e.*  $\Psi = 0$  and  $\Psi_0(0) = 0$ ), one gets:

$$q(c) = C_m \left( \frac{\partial \Psi_0}{\partial c} \right)_{\Psi, T} \cdot c \quad \text{or} \quad \Psi_0(c) = \left( \frac{\partial \Psi_0}{\partial c} \right)_{\Psi, T} \cdot c \quad (3.37)$$

which states that the offset polarization is proportional to curvature. This is a special case of Eq. (3.35) and equivalent to the formulation of Petrov [40]. It is valid in the absence of an applied voltage, for a membrane whose capacitance is independent of curvature, that has no spontaneous polarization in the absence of a curvature (so a chemically symmetric membrane), and whose spontaneous polarization is linearly dependent on curvature. In Petrov's formulation, the proportionality between curvature and polarization is quantified by the flexoelectric coefficient,  $f$ , which is given by  $f \equiv \epsilon \left( \frac{\partial \Psi_0}{\partial c} \right)_{\Psi, T}$ . He measured the flexoelectric coefficient and found it to be of the order  $10^{18} C$ , which corresponds to  $\left( \frac{\partial \Psi_0}{\partial c} \right)_{\Psi, T} \simeq 3 \cdot 10^{-8} [V/m]$ .

**Inverse flexoelectricity** As with the piezoelectric effect, also for flexoelectricity there is an inverse effect, which describes the effect by which curvature can be induced by an applied electric field. We follow the same approach as for piezoelectricity and start by writing the free energy density for a curved membrane in the presence of an applied field. Again, we assume that the capacitance does not depend on curvature.

$$g_c = \frac{1}{2} \kappa_B c^2 - \frac{C_m}{A} \left( \frac{\Psi^2}{2} + \Psi_0 \Psi \right) \quad (3.38)$$

where the first term is the elastic free energy of bending in the absence of a spontaneous curvature ( $\kappa_B$  is the bending modulus). The equilibrium condition for this system is given by:

$$\frac{\partial g_c}{\partial c} = \kappa_B c - \frac{C_m}{A} \left( \frac{\partial \Psi_0}{\partial c} \right)_{\Psi, T} \Psi = 0 \quad (3.39)$$

Which is satisfied for

$$c(\Psi) = \frac{C_m}{\kappa_B A} \left( \frac{\partial \Psi_0}{\partial c} \right)_{\Psi, T} \Psi \quad (3.40)$$

the last equation describes the effect by which the membrane bends as a response to an applied field, also called inverse flexoelectricity. As for the inverse piezoelectric effect and electrostriction, the magnitude of the mechanical response depends on the elastic properties (here, the bending elastic constant) of the membrane. It is therefore expected to be greatly enhanced in the transition. The inverse flexoelectric effect was first introduced and measured by Petrov [45]. In his formalism the voltage induced curvature takes the form:  $c(\Psi) = (f/d \cdot \kappa_B) \Psi$ .

**Thermoelectricity** The last term of Eq. (3.25) describes thermoelectricity, *i.e.* changes in charge induced by temperature. Let's consider a

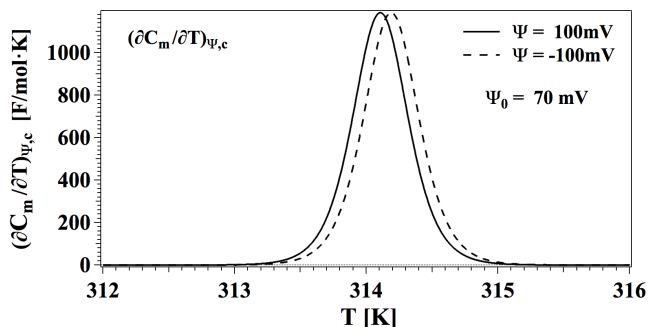


Figure 3.8: Partial derivative of the capacitance with respect to temperature at constant curvature and constant voltage assuming an offset voltage of  $\Psi_0 = 70\text{mV}$ . The value of the voltage was fixed to  $\Psi = 100\text{mV}$  (solid line) and  $\Psi = -100\text{mV}$  (dashed line). Values for DPPC membranes were taken from [16].

membrane of fixed curvature and at fixed voltage and allow the temperature to change. The area will not stay constant in general (and especially close to the transition) but will rather be a function of temperature. We will then have:

$$dq = \left[ (\Psi + \Psi_0) \left( \frac{\partial C_m}{\partial T} \right)_{\Psi,c} + C_m \left( \frac{\partial \Psi_0}{\partial T} \right)_{\Psi,c} \right] dT \quad (3.41)$$

This is also called Seebeck effect. The magnitude of the response depends on the temperature dependence of the capacitance and the offset voltage. We discussed the former and found that the changes in capacitance with temperature are expected to be large especially close to transition, so that the first coupling function will display a maximum in the transition. Fig. (3.8) shows the partial derivative of the membrane capacitance as a function of temperature for two different values of the offset voltage. The latter will also be largest at the transition in the case where fluid and gel state have a different polarization or due to the geometry changes. If we instead consider a membrane for which the offset voltage is not a function of temperature we have

$$dq = (\Psi + \Psi_0) \left( \frac{\partial C_m}{\partial T} \right)_{\Psi,c} dT \quad (3.42)$$

If we further assume that the spontaneous polarization is zero, one recovers the expression by Heimburg [24]. It is expected to have a maximum in the transition. This will be compared to experimental measurements on a lipid bilayer patch. The inverse effect is called Peltier effect, and it describes temperature changes by charging of the membrane.

### 3.3 Discussion

In this chapter we provided a thermodynamical framework to describe the effect of polarization on the properties of lipid membranes. This allowed us to write the free energy of a polarized membrane as a quadratic function in the voltage plus a linear term that depends on the spontaneous polarization of the membrane. In this framework, we could relate the polarization of the membrane to the charging of a capacitor. For instance, it allowed us to describe the charging of a membrane by means other than just an electric field. The lipid membrane capacitor can in fact be charged or discharged by changes in area, curvature and temperature, as well as voltage. Each of these mechanisms is strictly related to the presence of a spontaneous polarization and a transmembrane voltage. Biological membranes are polar structure that sustain voltage differences of hundreds of mV in physiological conditions, and changes in such voltages are at the basis of important biological functions for the cell, most notably the propagation of the nerve pulse [20]. Hence, it is essential to have a theory that correctly accounts for polarization and capacitive effects in the presence of electric fields.

In the presence of a spontaneous polarization, applying a voltage to the membrane capacitor can lead to the release of charges from its plates and in general the membrane will be charged in the absence of a voltage. As a result the electrical properties of the lipid bilayers will be affected differently by positive or negative voltages.

An example of this is the effect of electrostriction on the membrane capacitor. A quadratic dependence of the capacitance of the membrane on the voltage due to electrostriction has been observed in experiments by different authors in artificial [42, 46–48] and biological membranes [43]. We showed that in the presence of a spontaneous polarization the minimum value of the capacitance is at a voltage different from zero and equal to the offset voltage (Fig. (3.6), right). This is in agreement with the experimental results of Alvarez and Latorre on polar black lipid membranes, in which the polarization originated from chemical asymmetry of the two monolayers [42]. The magnitude of the capacitance change in experiments on lipid bilayers is very small and has led to the widely accepted assumption that the capacitance of the lipid portion of biological membrane is constant and independent of the applied voltage. We here showed that this is not the case close the transition, where the enhanced compressibility of the membrane makes it more susceptible to changes in voltage. Biological membranes display transitions close to body temperature, therefore capacitive effects are expected to be significant in physiological conditions. The present treatment of electrostriction is a generalization of the findings of Heimburg [24] to include membranes with a spontaneous polarization. Our findings suggest that the capacitive behaviour in response to a voltage change can vary in magnitude and direc-

tion depending on the value of  $P_0$ . An intrinsic polarization of the membrane in the absence of a field is also a feature that is usually not considered in the electrical models of the membrane, like the Hodgkin and Huxley model for the nerve pulse [20], despite the polar nature of biological membranes [14].

The electrostrictive forces on a symmetric and not polarized membrane tend to compress it to its thinnest state, namely the fluid state. We investigated the effect of voltage on the melting temperature of a DPPC bilayer (Fig. (3.7)) and found that it decreases quadratically with the applied voltage for symmetric membranes (in agreement with [24]). However, when assuming the presence of a spontaneous polarization, the linear term in the expression of the free energy becomes dominant for small voltages (*i.e.* for  $\Psi \ll \Psi_0$ ), which results in a linear increase in the melting temperature for positive or negative voltages, depending on the direction of the spontaneous polarization. This is so in either cases of fixed or state dependent voltage offset. A linear increase of the melting temperature was measured on Black Lipid Membranes made of DPPA by Antonov [26] in the only experimental study to our knowledge on the influence of voltage on the phase transition of membranes. Our findings suggests that the membranes investigated by Antonov and collaborators were polar. He detected the phase transition by measuring the membrane conductance at different voltages, using the observation that the membrane permeability is maximum at the transition. In the next chapter we will apply the present findings to study the effect of a spontaneous polarization on the conduction properties of the membrane, and in particular we will investigate its effect on the current-voltage relationship measured for lipid membrane patches.

We showed two mechanisms that can result in a spontaneous polarization in the membrane. The first involves a chemical or physical asymmetry between the two monolayers. A physical asymmetry could for example be achieved by having the two monolayers in different physical states. Chemical asymmetry is widely present and conserved in biological membranes and can involve an asymmetric distribution of charged and zwitterionic lipids on the two leaflets. The polarization of each leaflet can be affected by changes in the surrounding electrolyte in terms of salt concentration, pH, and type of ions (if monovalent or divalent). This can happen through a direct effect on the dipole potential (e.g. ion shielding, or binding to the membrane) or by affecting the state of the membrane [49]. Therefore, changes in those parameters or having an asymmetric electrolyte environment on the two sides of the membrane, can affect the value of the spontaneous polarization. In particular, ionic strength has been shown to affect the magnitude of the voltage offset, as shown in Fig. (3.5). In biological membranes, integral proteins or any adhesive molecule with large dipole moment can contribute to an asymmetric polarization. One would expect biological membranes to show larger

polarization than the one measured for pure lipid bilayers. Depending on the nature of the asymmetry, the system can display piezoelectric properties. The other mechanism that can produce a polarization in the membrane is flexoelectricity which acts by breaking the geometrical symmetry of the system through curvature. Flexoelectricity was widely studied in theory and experiments by Petrov who pioneered the field [13, 40, 50]. We here derived general relations for the flexoelectric and the inverse flexoelectric effect and showed that in some simple limiting cases, our derivations lead to the same results of Petrov.

All the findings of this chapter relate to equilibrium properties of the system. The changes in charge discussed here, however, involve changes in capacitance and polarization which are not expected to happen instantaneously but rather to follow the relaxation dynamics of the membranes. In the next chapter we will investigate the dynamical behaviour of the capacitive and polarization effects studied here and will compare it to common experiments performed on artificial and biological membranes. We note already at this stage, however, that in the simple case case of constant spontaneous polarization, temperature, and curvature, the expression for the capacitive current in the case of constant polarization according to Eq. (3.23) is given by:

$$I_c(t) = \frac{dq}{dt} = C_m \frac{d\Psi}{dt} + (\Psi + \Psi_0) \frac{dC_m}{dt} \quad (3.43)$$

Here the first term is a fast capacitive peak when the voltage change is instantaneous. The second term is usually completely disregarded in any model for the interpretation of electrical recordings on the basis of the presumed independence of the membrane capacitance on the applied voltage. We will see in the next chapter, that when including the polarization of the membrane, the second term can give rise to many interesting behaviours.

Due to the piezoelectric effect, a change in the area can lead to a charging of the membrane according to Eq. (3.29). On the other hand, because of the inverse piezoelectric effect a change in the applied membrane voltage can induce changes in the area. Furthermore, an electric voltage across the membrane can influence the physical state of the membrane, and this, in turn, can affect the electrical response of the membrane. These type of phenomena have been considered to be key players in the electromechanical mechanism for the nerve pulse propagation proposed by Heimburg and Jackson in 2005 [18]. In their model, the nerve pulse is considered to be a density wave propagating as a local phase change of the membrane from the fluid to the gel state. Depending on the magnitude of the inverse piezoelectric effect, a transmembrane voltage could induce area changes and therefore induce a density wave. The magnitude of the electromechanical couplings is dependent on the elastic constants of the membrane, and is therefore expected to

be maximum close to the transition.

Finally, we would like to remark that some of the effects derived here are not very pronounced in lipid bilayers, and their magnitude depends on the value of the polarization. The shift in melting temperature, for instance, is around 0.1K for an applied voltage of 200 mV when the voltage offset is zero while it is double when the voltage offset is around 100mV. Though the absolute magnitude is still very small, this suggests that in highly polar systems with large dipole moments, their effect could become significant. This could be the case for membrane associated proteins bearing large dipole moments.



## 4

# Nonlinear dynamic behaviour in common experiments

With the thermodynamical tools at hand, we have derived a number of interesting equilibrium properties which highlight the intercoupling between electrical, mechanical and thermal phenomena. They deal with static phenomena, such as the storage of charge in a capacitor. We will now extend the findings of chapter 3 to describe the dynamical behaviour of membranes, which includes the time dependence of the charge, *i.e.* currents. We do this with respect to experiments that are commonly performed on synthetic and biological membranes and which go under the name of electrophysiology.<sup>1</sup>

In a common electrophysiological experiment, the electrical properties of the membrane are probed by exposing it to an electrical perturbation (in the form of a time dependent voltage or current change) and the relevant information is extracted from the measured output. In the following we will exclusively refer to voltage clamp experiments, in which the perturbation is in the form of a voltage signal. In this respect, the membrane acts as a sort of black box standing between a known input (voltage) and the measured output (current). The relevant information is then extracted from the output by finding an electrical circuit which would show the same or similar response if exposed to the same perturbation. In circuit theory, however, there is no uniqueness of solution for this type of problem. Different circuit configurations can behave in the same way under particular conditions [51,52]. This is a well known fact in material science where techniques like impedance spectroscopy are flanked by complementary structural investigations (using for example, electron microscopy means). These structural information help in choosing the most appropriate circuit configuration for the specific system.

It is with a voltage clamp experiment, for instance, that Hodgkin and Huxley first proposed the equivalent circuit of the squid axon membrane, now

---

<sup>1</sup>The theoretical development of this chapter has been made in collaboration with Lars D. Mosgaard.

the textbook model for the electrical representation of the membrane [20]. In their model, the role of conduction through the membrane is appointed to voltage and time dependent resistors representing the different protein channels, while the lipid bilayer is pictured as a capacitor and hence it accounts for the energy storage in the membrane.

In this framework, the membrane capacitor is assumed to be constant in value. The traditional equivalent circuit of the lipid portion of the membrane is illustrated in Fig. (4.1), where the membrane capacitor is in parallel with a resistor of constant and infinite value, representing the impermeable nature of the lipid matrix. This model is in line with what was known at the time (1952) on the physical properties of the lipid bilayer, namely that they are impermeable barriers providing insulation to the cell. Detailed and direct structural information were not yet available (the first electron microscopy image of a bilayer came about six years after owing to Robertson [6]), yet the lipidic bimolecular structure of the lipid bilayer had been suggested and indirectly observed for more than twenty-five years prior to this [4]. In the following decades our understanding of the bilayer properties has greatly advanced.

In particular, we have shown in the previous chapter that the assumption of constant capacitance for the lipid membrane is not met under physiological conditions, *i.e.*, for voltage magnitudes of hundreds of mV and close to the chain melting transition. Furthermore, lipid membranes show finite permeability to ions in the form of lipid ion channels [53], so also the assumption of constant resistance is questionable. In other words, the complementary information we now have on the physical properties of the lipid bilayer doesn't match with the electrical equivalent that is still the circuit of choice for the interpretation of electrophysiological data. In the following, we aim at updating that model in the light of the findings of the last chapter. We will start by considering the voltage and time dependence of the circuit elements of 4.1, and will then predict the response of the membrane to two types of voltage perturbation commonly performed in experiments: voltage jumps and sinusoidal perturbation (in the context of impedance spectroscopy). Finally, we will compare our results to experimental findings on biological membranes.

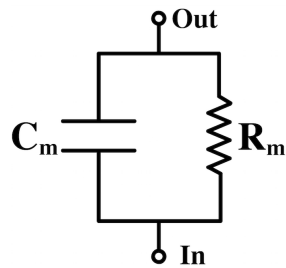


Figure 4.1: Lipid bilayers are modeled as RC circuit.  $C_m$  is the capacitance of the membrane.  $R_m$  is the infinite resistance. They are commonly assumed to be constant.

## 4.1 Nonlinearities

### 4.1.1 Conduction through the membrane

Permeability of lipid bilayers for water [54], small molecules [55] and ions [56–58] has been observed since the early 70s. It was found to be largest at the lipid phase transition [56, 57] and to be proportional to the heat capacity [55, 59]. Ion permeability through the lipid membrane has been shown to occur in the form of quantized steps in the membrane current [60, 61], resembling those observed in the presence of protein channels. In particular, they share similar amplitude and life time as well as the same distinctive patterns (e.g. quantized current steps, burst, flickering, multi-step conductances and spikes) [62]. Hence, they are often referred to as lipid channels (or lipid ion channels).

As for protein channels, the quantized nature of the channel events observed in lipid bilayers suggests the transient formation of pores of fixed conductance (*i.e.* geometry) as the underlying conduction mechanism. According to the approach of Nagle and Scott [57], the work required for the formation of a pore is proportional to the area compressibility of the membrane, therefore the likelihood of finding an open pore is expected to be small in the pure fluid or gel phase, where the membrane compressibility is low [16]. As we showed in chapter 2, however, close to the lipid melting area and volume compressibilities are proportional to the heat capacity and as the fluctuations in their correspondent extensive variables, they are at a maximum at the transition [16]. This means that the work needed to create a pore is minimum at the lipid melting, where the formation of pores can occur spontaneously as a result of the enhanced area fluctuations.

This scenario has been confirmed in the last four decades by several studies observing an increase in membrane permeability and the appearance of channel-like events in the membrane current at the phase transition [55, 56, 59, 61, 63]. In particular, Andersen and collaborators observed transient permeation events by locally melting Giant Unilamellar Vesicles using fluorescence microscopy, providing direct evidence of the interplay between the membrane permeability and its physical state [64]. As a result of this interplay, any change in the intensive variables that affects the lipid melting is expected to affect the likelihood of pore formation and hence the membrane conduction, effectively blocking or gating lipid ion channels depending on whether they inhibit or induce phase transition. This has indeed been observed with respect to changes in temperature [61], lateral tension, pH [58], concentration of divalent ions (*calcium*), presence of anesthetics, and, of special relevance for the present treatment, voltage [65].

We have described in chapter 3 how a constant voltage across the membrane can affect the state of the membrane due to electrostriction. From a phenomenological point of view, in the presence of voltage the membrane is

compressed and its thickness decreases, hence the likelihood of pore formation increases<sup>2</sup>. Following the approach of Blicher [65], we can write the free energy of pore formation in the presence of voltage:

$$\Delta G_p = \Delta G_{p,0} + \alpha(\Psi^2 + 2\Psi_0\Psi) \quad (4.1)$$

where  $\Delta G_{p,0}$  is the free energy difference between an open and a closed pore in the absence of voltage and  $\alpha$  is a coupling coefficient between voltage and pore formation. They both depend on the state of the membrane, as a consequence of the proportionality between conduction and the heat capacity. If we assume that a pore can be found only in two states (open and closed), we can then write the equilibrium constant,  $K$ , between a closed and an open pore and the probability to find an open pore as:

$$K = \exp\left(-\frac{\Delta G_p}{kT}\right) \quad \text{and} \quad P_{open} = \frac{K}{1 + K} \quad (4.2)$$

One of the distinctive features of ion channels (in the presence and absence of proteins) is the quantized nature of their current traces, which means that a single open channel has a constant conductance,  $\gamma_p$ , as confirmed in experiments [65]. The total current through a single channel can then be written as:

$$I_m = \gamma_p P_{open} \Psi \quad (4.3)$$

A similar expression was used by Blicher and Heimburg in [65], to describe the outward rectified current-voltage relationship measured on a protein-free membrane reconstituted at the tip of a glass pipette shown in Fig. (4.2) (left). Outward (or inward) rectification describes the preferential direction of ionic currents out (or into) the cell, due to an asymmetric conductance profile for positive and negative voltage. It is a phenomenon commonly observed in protein channels and explained in terms of asymmetries in the energy barrier for gating inside the protein, by a transition state model (the Eyring model) [66, 67]. Interestingly, the simple model outlined above was shown to better fit experimental data from both synthetic and biological membrane, as shown in Fig. (4.2) for a lipid bilayer and two TRP channels in HEK cells [68].

---

<sup>2</sup>Note that this is true for any voltage in the absence of spontaneous polarization. In a polarized membrane, however, there can be a voltage range in which the effect is opposite, hence applying voltage would discharge the capacitor, increase the thickness and decrease the likelihood of pore formation.

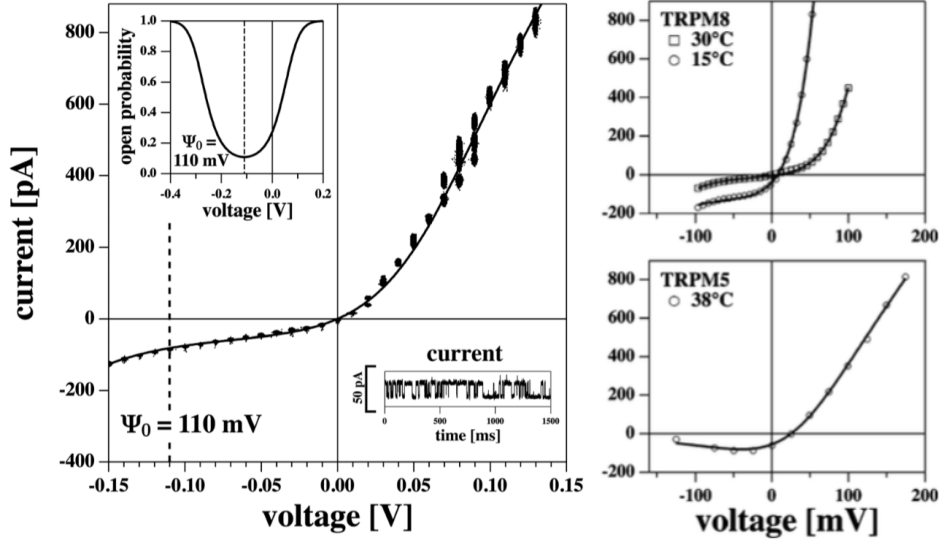


Figure 4.2: **Left:** Current-voltage relationship of a synthetic lipid membrane made of DMCP:DLPC=10:1. The solid line is a fit to Eq. (4.3), with an offset voltage of  $\Psi_0 = 110$  mV. Left inset: Open probability as a function of voltage. It has a minimum at a voltage  $\Psi = -\Psi_0$ . Right Inset: Opening and closing of a lipid channel as a function of time at a voltage  $\Psi = 50$  mV. **Right:** Current-voltage relations of a TRPM8 channel in HEK cells at two different temperatures (top, adapted from [66]) and of a TRPM5 channel in HEK cell (bottom, adapted from [67]). Solid lines are fit to Eq. (4.3) [68].

The nonlinear asymmetric I-V curve measured for a lipid bilayer (Fig. (4.2) (left)) is well fitted by assuming a voltage offset of  $\Psi_0 = 110$  mV. According to the capacitor model (Eq. (4.1) -(4.3)) one would expect that a completely symmetric membrane shows a nonlinear yet symmetric I-V profile. This means that the membrane studied by Blicher and Heimburg was polar, despite the identical lipid composition of the two monolayers.

As discussed in chapter 3, curvature of the membrane can account for the presence of spontaneous polarization and hence of a nonzero voltage offset. A flexoelectric origin of the offset voltage was indeed discussed by the authors who related it to the applied suction on the glass pipette during membrane formation (see chapter 5). They suggested that the measured voltage offset could be explained by the membrane having a radius of curvature which is compatible with the geometry of the glass pipette. In the experimental part of this thesis we will further investigate the appearance of asymmetric, outward rectified current-voltage relationships in chemically symmetric lipid membranes. It seems clear at this stage, that the conductance of the lipid bilayer cannot be a priori assumed to be constant. Not only can it be a nonlinear function of voltage (as shown here), but it is expected to be a

function of the state of the membrane [59].

#### 4.1.2 Charge on the membrane capacitor

We saw in section 3.2.3 that, at equilibrium, the charge on the membrane capacitor is given by:

$$q = C_m(\Psi + \Psi_0) = C_m\Psi + AP_0, \quad (4.4)$$

where the capacitance, the membrane area and the spontaneous polarization can all dependent on the applied voltage and on the state of the membrane. We now want to work out the change in charge on the membrane capacitor when the voltage is changed from an initial value which can be different from zero, as it's usually the case in voltage clamp experiments. We call the initial value of the voltage  $\Psi_h$ , holding voltage. The charge on the capacitor at the holding voltage is given by:

$$q(\Psi_h) = C_{m,h}\Psi_h + A_hP_{0,h} \quad (4.5)$$

where  $C_{m,h}$ ,  $A_h$ ,  $P_{0,h}$  are the membrane capacitance, area and spontaneous polarization at the holding voltage. Note that they can all be functions of temperature, especially close to the transition, even though we won't write the dependence explicitly in the following. The change in charge due to the change in voltage  $\Delta\Psi = \Psi - \Psi_h$ , at equilibrium, is then given by:

$$\begin{aligned} \Delta q &= q(\Psi) - q(\Psi_h) = [C_m(\Psi)\Psi + A(\Psi)P_0(\Psi)] - [C_{m,h}\Psi_h + A_hP_{0,h}] \\ &= C_m(\Psi)\Psi - C_{m,h}\Psi_h + \Delta(AP_0)(\Psi) \end{aligned} \quad (4.6)$$

which can be written in a more convenient way using  $C_m(\Psi) = C_{m,h} + \Delta C_m(\Psi)$ ,

$$\Delta q(\Psi) = C_{m,h}\Delta\Psi + \Delta C_m(\Psi)\Psi + \Delta(AP_0)(\Psi) \quad (4.7)$$

Here, the first term is the linear part of the charge, the second is the change in charge due to the nonlinear dependence of the capacitance on voltage (see Fig. (3.6)) and the last term describes the change in offset charge due to a voltage induced change in area and/or spontaneous polarization. The linear part of Eq. (4.7) represents the response of the membrane if no electro-mechanical couplings were present. One sees that in the linear case, for a positive change in voltage there is an uptake of charges on the capacitor, while decreasing the voltage with respect to the holding value results in a release of charges. This is in line with our intuition. However, in the presence of electrostrictive and polarization effects, the situation gets more complicated and whether charges are released or absorbed on the capacitor depends not only on the sign of  $\Delta\Psi$  but also on the value of the holding voltage and the spontaneous polarization. To clarify this, we plotted the nonlinear part of Eq. (4.7) as a function of the voltage step we call it  $\Delta q_{nl} \equiv \Delta q - C_{m,h}\Delta\Psi$ , see

Fig. (4.3)), for different holding voltages (left) and for different values of the polarization (right). In the absence of spontaneous polarization (left panel of Fig. (4.3)), the nonlinear change in charge is determined by the change in capacitance,  $\Delta C_m(\Psi)$ . Therefore, when the holding voltage is zero (solid line, Fig. (4.3)(left)), the change in charge is a nonlinear function of the voltage step, and its sign follows the direction of the voltage jump (positive for positive step and negative for negative step). This is a consequence of the capacitance having a minimum at  $\Psi = 0$  ( *i.e.*  $\Delta C_m$  is always positive when  $\Psi_0 = 0$  and the direction of the charge change is determined by the sign of the final voltage). We see in Fig. (4.3)(left, dotted line) that when the holding voltage is  $\Psi_h = -100mV$ , a decrease in voltage ( $\Delta\Psi < 0$ ) always results in release of charge from the capacitor. When the voltage is increased from the holding voltage, however, there is a voltage range in which charges are released from the capacitor plates. This anomaly is a consequence of the fact that the membrane capacitance is not in a minimum at the holding voltage. We saw in Fig. (3.5) that a spontaneous polarization results in a shift of the capacitance-voltage curve on the voltage axis. This means that the capacitance has a minimum at a voltage different from zero. We therefore expect similar anomalies in the direction of the charge change when the holding voltage is zero but the spontaneous polarization is not. This is illustrated Fig. (4.3)(right), for three different values of the spontaneous polarization (assuming constant polarization in the gel and in the fluid phase).

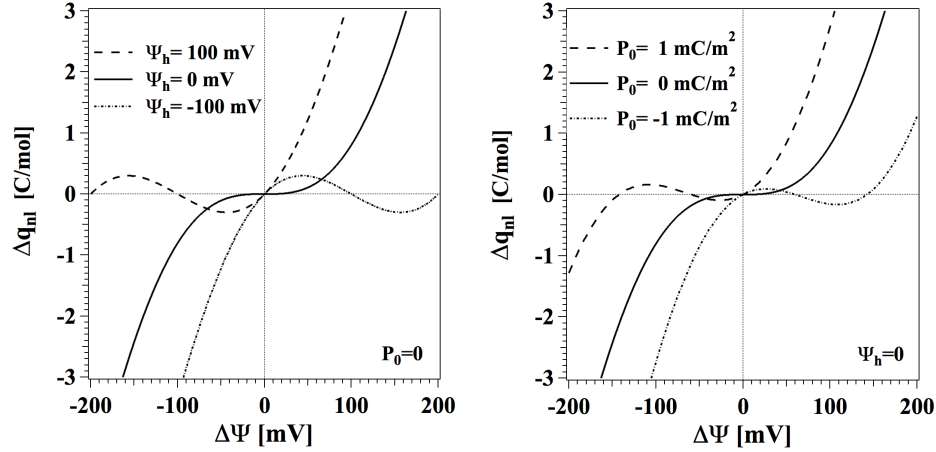


Figure 4.3: Nonlinear part of the change in charge  $\Delta q_{nl} \equiv \Delta q - C_{m,h} \Delta\Psi$  from Eq. (4.7) as a function of the the amplitude of the voltage change. **Left:** In the case of no spontaneous polarization, for three different values of the holding voltage. **Right:** When the holding voltage is zero, for three different values of the spontaneous polarization. Values of the parameter are for a DPPC [16], at a temperature of  $T=214.5K$ .  $C_m(T, \Psi) = \epsilon A(T, \Psi)/d(T, \Psi)$ , as derived in chapter 3.

The above considerations were made at constant temperature. However, the response of charge to changes in voltage is expected to be greatly affected by the melting transition.

## 4.2 Voltage jumps

One common type of voltage-clamp experiment consists in an instantaneous change in the voltage from a holding voltage  $\Psi_h$  to an end voltage,  $\Psi_e$ , also called voltage jump.

In the following we calculate the dynamic response to voltage jumps due to the nonlinearity of the capacitance and conductance. We assume that the voltage jump is performed at  $t = 0$  and that any change in the applied voltage is instantaneous.

### 4.2.1 Ionic currents

We now want to calculate the ionic (or resistive) current response of the membrane to voltage jumps due to the voltage dependence of the membrane conductance. We have already discussed how the conduction through the membrane is affected by the state of the membrane and the voltage applied. We will assume that the voltage dependence of the membrane conductance is well approximated by nonlinearity of the current-voltage relationships like the one shown in Fig. (4.2). In particular, we write the conductance after a voltage jump from a holding value of  $\Psi_h$  in the following way:

$$g_m(\Psi) = g_{m,h} + \Delta g_m(\Psi) \quad (4.8)$$

where  $g_{m,h} = g_m(\Psi_h)$  is the conductance of the membrane at the holding voltage and  $\Delta g_m(\Psi) = g_m(\Psi) - g_m(\Psi_h)$  is the change in conductance after the voltage jump.

As discussed earlier, conduction through the lipid bilayer is proportional to the heat capacity and hence it follows the magnitude of the membrane fluctuations. We therefore expect changes in conductance not to happen instantaneously, but rather to follow the relaxation dynamics of the membrane. We assume that the relaxation behaviour of the membrane is well described by a single exponential function (as proposed in [69]) and treat the dynamics of the membrane conductance as a relaxation between two equilibrium states. We then write the ionic current through the lipid membrane after a voltage jump as follows:

$$I_\Omega(t) = (g_{m,h} + \Delta g_m(1 - e^{-\frac{t}{\tau}}))\Psi_e \quad (4.9)$$

where  $\Delta g_m = g_{m,e} - g_{m,h}$  and  $\tau$  is the relaxation time of the lipid membranes. It has been shown in theory [69] and experiments [31, 69] that it is proportional to the heat capacity of the membrane. It is therefore largest

at the transition, which means that the fluctuations in the extensive variables are largest and slowest at the lipid melting. It has been found that the magnitude of the relaxation time spans several orders of magnitude, from milliseconds to seconds [70] up to a minute [69] in the transition.

The resistive current is plotted in Fig. (4.4) for two voltage steps from a holding voltage of  $\Psi_h=0\text{mV}$ , a positive step of  $\Delta\Psi=100\text{ mV}$  and a negative one of  $\Delta\Psi=-100\text{ mV}$ .

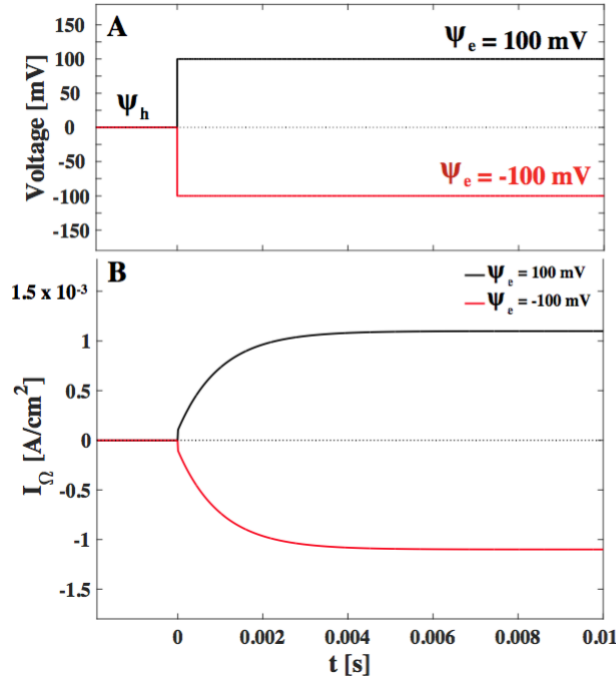


Figure 4.4: **A:** Voltage jumps at  $t=0$  from a holding voltage of  $\Psi_h=0\text{ mV}$  to an end voltage of  $\Psi_e=100\text{mV}$  (black line) and  $\Psi_e=-100\text{mV}$  (red line). **B:** Ionic current response of the membrane according to Eq. (4.9). Values of the parameter were:  $g_{m,h}=1\text{ mS/cm}^2$ ,  $\Delta g_m=10\text{ mS/cm}^2$  [20, 51] and  $\tau=1\text{ ms}$ . Figure adapted from [71].

### 4.2.2 Capacitive current

Using Eq. (4.7) we are able to calculate the equilibrium change in charge on the membrane after a voltage change  $\Delta\Psi = \Psi_e - \Psi_h$ . The nonlinear part of the change in charge depends on how the capacitance, the area and the spontaneous polarization of the membrane change with voltage. As for the membrane conductance we expect these changes follow the relaxation dynamics of the membrane. Assuming again a single exponential relaxation for the membrane equilibration, we can write the time dependence of the

change in charge after a voltage jump can then be written like this:

$$\Delta q(t) = C_{m,h}\Delta\Psi + (\Delta C_m\Psi_e + \Delta(AP_0))\left(1 - e^{-\frac{t}{\tau}}\right) \quad (4.10)$$

We can now calculate the capacitive current due to the voltage jump, by differentiating Eq. (4.10) with respect to time. In the assumption of instantaneous voltage change, the linear term in Eq. (4.10) results in a capacitive spike which is much faster than any other time scale involved. We remove it by considering only  $t > 0$  and that in experiments it is canceled with compensatory circuits. The capacitive current is then given by:

$$I_c(t) = \frac{d}{dt}\Delta q(t) = (\Delta C_m\Psi_e + \Delta(AP_0))\frac{e^{-\frac{t}{\tau}}}{\tau} \quad (4.11)$$

The capacitive current is plotted in Fig. (4.5) in units of [A/mol]<sup>3</sup>. The holding voltage was set to  $\Psi_h = -100mV$ , and current response is shown for two voltage steps, both positive,  $\Delta\Psi = 40mV$  and  $\Delta\Psi = 160mV$  corresponding to an end voltage of  $\Psi_e = -60mV$  and  $\Psi_e = +60mV$ , respectively.

Panel **B** shows the capacitive response when no spontaneous polarization is present. As expected from inspection of Fig. (4.3) depending on the magnitude of the step we observe currents following or not the direction of the voltage. Panel **C** shows the current response to the same voltage steps in the case where the membrane has spontaneous polarization only in the fluid phase. One can expect capacitive currents of up to  $20 \mu A/cm^2$  in response to a voltage step, the actual values depending strongly on the proximity of the phase transition. At the melting transition the capacitive current can reach values around  $60\mu A/cm^2$ . We also note that from Eq. (4.11) that the the amplitude of the current is inversely proportional to the characteristic relaxation time. We then expect capacitive current originating from the non-linearity of the membrane to be significant when compared to response of electrophysiological recordings. Interestingly, they are remarkably similar to gating currents, which will be discussed in section 4.4.

Once the current through the nonlinear capacitor and the nonlinear resistor of Fig. (4.1) have been calculated, one can write the total membrane current as the sum of the two:

$$I_m(t) = (g_{m,h} + \Delta g_m(1 - e^{-\frac{t}{\tau}}))\Psi_e + (\Delta C_m\Psi_e + \Delta(AP_0))\frac{e^{-\frac{t}{\tau}}}{\tau} \quad (4.12)$$

---

<sup>3</sup>mol refers to mole of lipid. Therefore  $1 \text{ A/mol} \simeq 2/3 \text{ nA/cm}^2$ , assuming an area per mole of lipid of  $A \simeq 1.5 \cdot 10^5 m^2/mol$  [16]

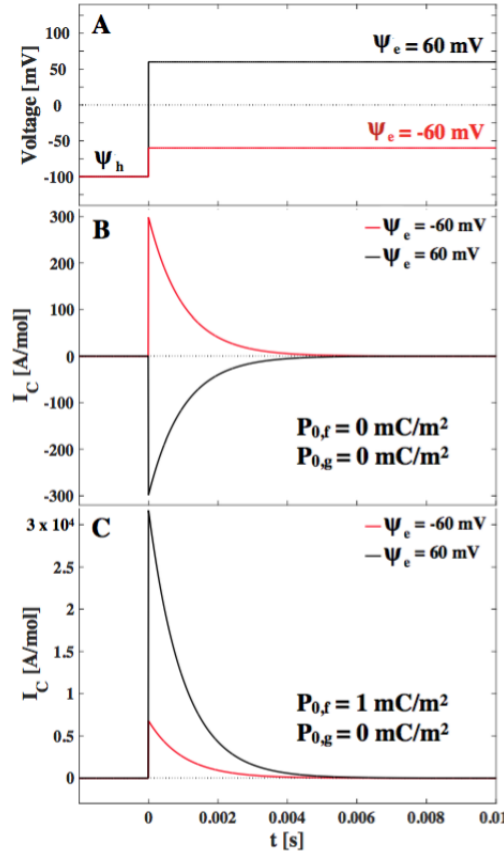


Figure 4.5: Capacitive current. (A): Voltage jumps at time  $t = 0$  from a holding voltage of  $\Psi_h = -100$  mV To an end voltage of  $\Psi_e = -60$  mV ( $\Delta\Psi = 40$  mV, red) and  $\Psi_e = 60$  mV ( $\Delta\Psi = 160$  mV, black). (B): Current response in the case of no polarization. (C): Capacitive response for a polar membrane with spontaneous polarization  $P_{0,f} = 1$  mC/m<sup>2</sup> in the fluid phase and no polarization in the gel phase. Values used are from DPPC [16].  $T = 324.5$  K and  $\tau = 1$  ms.

### 4.3 Impedance spectroscopy

Another common type of experiments used to probe the electrical properties of biological membranes is impedance spectroscopy. Impedance spectroscopy consists in measuring the impedance of a system as a function of frequency (the so called impedance spectrum). This is achieved by applying a low amplitude sinusoidal perturbation and measuring the amplitude and the phase of the current response for different frequencies of the applied voltage. The membrane impedance,  $Z$ , is then calculated as the ratio between the complex

voltage and current:

$$Z(\omega) \equiv \frac{\Psi(\omega)}{I(\omega)} \quad (4.13)$$

where  $\omega$  is the frequency of the sinusoidal perturbation.

The working hypothesis of impedance spectroscopy is that the system under investigation behaves linearly with voltage<sup>4</sup>. We will in the following restrict ourselves to low amplitude voltage perturbations, for which the membrane can be assumed to respond linearly. In that limit we can linearize the the equilibrium change in charge and the change in conduction by Taylor expanding them with respect to voltage. The dynamics of the response can then be derived using linear response theory.

The linear response of a system to a change in the applied voltage is given by

$$\alpha(t) = \int_{-\infty}^t \Gamma(t-t') \dot{\Psi} dt' \quad (4.14)$$

where  $\alpha$  is the response function,  $\dot{\Psi} = d\Psi/dt'$  is the rate of change of voltage and  $\Gamma = (\partial\alpha/\partial\Psi)(t)$  is the linear transfer function<sup>5</sup> that relates the change in voltage to the response. If the system under investigation is a simple time dependent capacitor, the response function is the change in charge and the transfer function is the capacitance. In the case of a simple time dependent resistor, the response function is the ionic current and the transfer function is the conductance. One then has:

$$\Delta q(t) = \int_{-\infty}^t \hat{C}(t-t') \dot{\Psi} dt' \quad \text{and} \quad \Delta I_{\Omega}(t) = \int_{-\infty}^t \hat{g}(t-t') \dot{\Psi} dt' \quad (4.15)$$

Note that for time and voltage independent conductance and capacitance (*i.e.*  $\hat{C} = C_m$  and  $\hat{g} = g_m$ ), one obtains the formalism expected from linear electronics.

### 4.3.1 Linearized equilibrium response

The voltage dependence of the transfer functions (discussed in section 4.1) implies that the response is not linear with respect to the perturbation, which is the working hypothesis of linear response theory. To overcome this, we consider only small voltage perturbations, for which the membrane can be assumed to respond linearly. The equilibrium change in ionic current after a small change of voltage from a holding voltage  $\Psi_h$  can be written as the

---

<sup>4</sup> Therefore the amplitude of the applied perturbation has to be low compared to the voltage at which the system deviates from linearity.

<sup>5</sup> which is a function of time and not of voltage

first order Taylor expansion around the holding voltage:

$$\begin{aligned} \Delta I_\Omega &\simeq \left( \frac{\partial I_\Omega}{\partial \Psi} \right)_{\Psi_h} \Delta \Psi = \left( \frac{\partial (g_m \Psi)}{\partial \Psi} \right)_{\Psi_h} \Delta \Psi = \\ &\left( g_{m,h} + \left( \frac{\partial g_m}{\partial \Psi} \right)_{\Psi_h} \Psi_h \right) \Delta \Psi \equiv \underbrace{(g_0 + \Delta g_0)}_{\hat{g}} \Delta \Psi \end{aligned} \quad (4.16)$$

where  $g_0 = g_{m,h}$ . In the same way, the equilibrium change in charge can be obtained by expanding  $q(\Psi)$  (Eq. (4.5)):

$$\begin{aligned} \Delta q &\simeq \left( \frac{\partial q}{\partial \Psi} \right)_{\Psi_h} \Delta \Psi = \left( \frac{\partial (C_m \Psi + AP_0)}{\partial \Psi} \right)_{\Psi_h} \Delta \Psi = \\ &\left( C_{m,h} + \left( \frac{\partial C_m}{\partial \Psi} \right)_{\Psi_h} \Psi_h + \left( \frac{\partial AP_0}{\partial \Psi} \right)_{\Psi_h} \right) \Delta \Psi \equiv \underbrace{(C_0 + \Delta C_0)}_{\hat{C}} \Delta \Psi \end{aligned} \quad (4.17)$$

where  $C_0 = C_{m,h}$ . Note that  $g_0$ ,  $\Delta g_0$ ,  $C_0$  and  $\Delta C_0$  they all depend on the holding voltage and the state of the membrane.

**Time dependence of the transfer function** We now introduce the time dependence of both transfer functions  $\hat{g}$  and  $\hat{C}$  based on the considerations that after a voltage change the membrane needs to relax into a new equilibrium state with a characteristic time constant. Assuming again single exponential relaxation for the equilibration dynamics of the membrane we have:

$$\begin{aligned} \hat{g}(t-t') &\simeq g_0 + \Delta g_0 (1 - e^{-\frac{t-t'}{\tau}}) \\ \hat{C}(t-t') &\simeq C_0 + \Delta C_0 (1 - e^{-\frac{t-t'}{\tau}}) \end{aligned} \quad (4.18)$$

Substituting these expressions in Eq. (4.15)

$$\begin{aligned} \Delta I_\Omega(t) &= g_0 \Delta \Psi(t) + \Delta g_0 \int_{-\infty}^t (1 - e^{-\frac{(t-t')}{\tau}}) \dot{\Psi}(t') dt' \\ \Delta I_C(t) &= C_0 \frac{d\Delta \Psi(t)}{dt} + \Delta C_0 \frac{d}{dt} \int_{-\infty}^t (1 - e^{-\frac{(t-t')}{\tau}}) \dot{\Psi}(t') dt' \end{aligned} \quad (4.19)$$

**Impedance spectrum** We now have all the tools to calculate the impedance of the membrane. The expression for the ionic and capacitive currents in the frequency domain can be obtained by Fourier transforming Eq. (4.19) and using that the applied voltage is sinusoidal:

$$\begin{aligned} \Delta I_\Omega(\omega) &= \left( g_0 + \Delta g_0 \frac{1}{1 + i\omega\tau} \right) \Psi(\omega) \\ \Delta I_C(\omega) &= \left( i\omega C_0 + \Delta C_0 \frac{i\omega}{1 + i\omega\tau} \right) \Psi(\omega) \end{aligned} \quad (4.20)$$

where  $V(\omega)$  is the Fourier transform of the applied voltage. The impedance of the membrane capacitor and conductance is then given by:

$$\begin{aligned} Z_{\Omega}(\omega) &= \left( g_0 + \Delta g_0 \frac{1}{1 + i\omega\tau} \right)^{-1} \\ Z_C(\omega) &= \left( i\omega C_0 + \Delta C_0 \frac{i\omega}{1 + i\omega\tau} \right)^{-1} \end{aligned} \quad (4.21)$$

Note that for constant conductance ( $\Delta g_0 = 0$ ) and constant capacitance ( $\Delta C_0 = 0$ ), one obtains the classical impedance of a resistor and a capacitor (the blue semicircle in Fig. (4.1) ).

We can now calculate the impedance of the membrane having the circuit configuration of Fig. (4.1) in mind <sup>6</sup>. We therefore have:

$$\begin{aligned} Z(\omega) &= \left( \frac{1}{Z_{\Omega}(\omega)} + \frac{1}{Z_C(\omega)} \right)^{-1} \\ &= \left( g_0 + \Delta g_0 \frac{1}{1 + i\omega\tau} + i\omega C_0 + \Delta C_0 \frac{i\omega}{1 + i\omega\tau} \right)^{-1} \end{aligned} \quad (4.22)$$

The impedance spectrum of the membrane is plotted in figure for different sets of parameters on a Nyquist plot. As it's clear from panel **A**, the time dependence of the conductance changes has the strongest effect on the impedance spectrum of the membrane, and it's responsible for the spiraling in the Nyquist plot that is commonly associated with inductance. This will be discussed in section 4.4.

## 4.4 Discussion

In the present chapter we derived the response of lipid bilayers to voltage perturbations commonly used in experiments. In such experiments, the lipid portion of the membrane is often considered to be equivalent to a parallel RC circuit, like the one in Fig. (4.1). Any behaviour in the measured current that deviates from that of a standard RC circuit, is commonly ascribed to other components of the membrane, most notably transmembrane protein channels. We have here included the voltage and time dependence of the lipid membrane capacitor and conductance, and showed that they both results in electrical response of the membrane, that not only deviates from that of a constant RC circuit, but that interestingly resemble the response of biological membranes. . Here we discuss some of the similarities.

---

<sup>6</sup>The impedance of a parallel combination of electric components is the inverse of the sum of the inverses of the components impedances

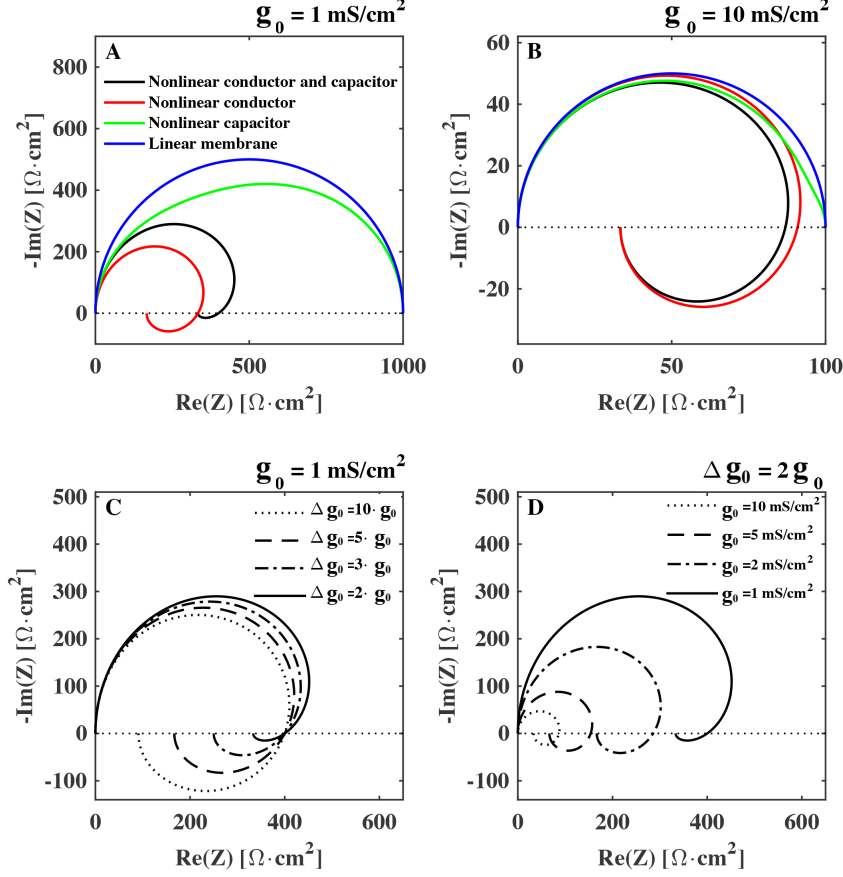


Figure 4.6: Calculated Nyquist plot of the impedance of a membrane (Eq. (4.22) for different choices of parameters. **A-B**, blue: linear membrane,  $\Delta C_0 = \Delta g_0 = 0$ , green: nonlinear capacitor ( $\Delta C_0 = 0.5 \cdot C_0$  and  $\Delta g_0 = 0$ ), red: nonlinear conductance ( $\Delta C_0 = 0$  and  $\Delta g_0 = 2 \cdot g_0$ ) black: nonlinear membrane ( $\Delta C_0 = 0.5 \cdot C_0$  and  $\Delta g_0 = 2 \cdot g_0$ ). Membrane capacitance is  $C_0 = 1 \mu F/cm^2$ . Membrane background conductance:  $g_0 = 1 mS/cm^2$  [20,72] (**A**) and  $g_0 = 10 mS/cm^2$  (**B**). **C**: different values of  $\Delta g_0$ . **D**: different values of membrane conductance,  $g_0$ .  $\tau = 1 ms$ .

#### 4.4.1 Lipid channels and rectification

Since the invention of the patch clamp technique by Neher and Sackmann [73], the quantized nature of current recordings on membrane patches has been taken as evidence of the existence of protein channels in the membrane, which by opening and closing in response to external stimuli, allow and

selectively control the passage of ions through the otherwise impermeable membrane. This conclusion relied on the assumption that the lipid bilayer is an inert and impermeable insulator. A substantial amount of evidence in the last four decades has proved that this is not true close to the lipid phase transition. Lipid bilayers show conduction events which are indistinguishable from the ones measured in the presence of proteins. Lipid channels are thought to be pores in the lipid membrane that can spontaneously form due to the enhanced fluctuations at the lipid transition. Since voltage can change the state of the membrane (as we showed in chapter 3), they are expected to depend on voltage. This has been indeed observed in experiments [65]. In the same work the authors measured an outward rectified current-voltage relation for a lipid bilayer. Rectification is another distinct feature usually ascribed to protein channels.

Here showed that by using a simple model for electrostriction which includes the possibility that the membrane has a spontaneous polarization in the absence of voltage, we can predict an asymmetric nonlinear dependence of the membrane current on the voltage which is in perfect agreement with the experimental data on artificial bilayers and protein containing membranes. Our derivation is very similar to that made by Blicher and Heimburg [65]. We speculated on the role of membrane curvature as possible origin of polarization in the lipid bilayer. This will be further discussed in the experimental part of this Thesis.

#### 4.4.2 Gating Currents

In their model for the nerve pulse propagation along the giant squid axon [20], Hodgkin and Huxley first proposed a voltage gating mechanism behind the functioning of protein ion channels. This was suggested by the steep voltage dependence of the nerve permeability for potassium and sodium ions. They concluded that changes in ionic permeability must be related to the movement of polar components in the membrane bearing large charge or dipole moment. Such *voltage sensors* were later suggested to lie in the charged portion of the proteins which, by moving under the effect of an electric field, effectively opens or closes the channels.

Gating currents (currents related to the movement of the charged "gate" of proteins) were directly measured for the first time by Armstrong and Bezanilla only 20 years after their prediction by Hodgkin and Huxley [74]. By lowering the ionic current through the membrane of a squid axon, small displacement currents could be detected showing a maximum amplitude of  $30 \mu\text{A}/\text{cm}^2$  and temporal width of about 1 ms [75]. In their model, Hodgkin and Huxley considered the capacitance of the membrane to be constant and independent of the applied voltage, therefore the potential role of the lipid bilayer in the measured gating current was not considered.

We have shown in chapter 3 that this is however not the case, especially

close to the melting transition. Voltage can change the state of the membrane and this can result in nonlinear changes in the membrane capacitance. We have here shown that the resulting capacitive current can display very different behaviours depending on the state of the membrane and the value of the spontaneous polarization (see 4.5). The changes include the maximum amplitude of the current, its temporal width and the direction of the current with respect to the applied voltage. The time scale of the electrostrictive capacitive current calculated here is set by the relaxation time of the membrane, and is therefore separable from the capacitive spike due to the linear part of the capacitance. We found that in proximity of the transition and in the absence of spontaneous polarization, the maximum amplitude of the capacitive current is on the order of  $20 \mu\text{A}/\text{cm}^2$ , and therefore comparable to the magnitude of gating currents. We, however, expect it to be larger in the transition and to be affected by the presence of spontaneous polarization.

Interestingly, several authors in the 70's discussed the possibility that gating currents could originate from the voltage dependence of the membrane capacitance as described here [35, 75, 76]. In his thorough analysis, Almers examined the potential role of the lipid bilayer in the mechanism behind the measured displacement currents and discarded the hypothesis only on the grounds of the small magnitude expected, based on the experimental findings on electrostriction in lipid bilayers available at the time [35]. Non-linear increase of the capacitance with voltage had indeed been observed, but mainly on solvent-containing lipid bilayers and ascribed to the movement of solvent in the membrane [36, 46, 47, 77]. It was therefore thought to be negligible for solvent-free membranes. Almost simultaneously (and using indirect measurements of the membrane compressibility), Blatt found that capacitive currents due to electrostriction were of the same order of magnitude as the gating currents but in the opposite direction [76]. We see that the current response follows or not the direction of the voltage step depending on the value of the holding voltage and the spontaneous polarization. We predict that gating currents and capacitive currents may have the same direction.

We conclude by stressing that with the knowledge we have on the electromechanical properties of pure lipid bilayers close the phase transition, it is not possible to *a priori* exclude a role of the lipid bilayer in the origin of gating currents. Further experiments and more in depth investigation is needed.

### 4.4.3 Membrane Inductance

Limiting ourselves to small voltage perturbations we derived the membrane response to sinusoidal perturbation and calculated the electrical impedance of the membrane. We considered only linear changes<sup>7</sup> in charge and in ionic

---

<sup>7</sup>Note that linear changes have been derived by linearizing the nonlinear membrane response. We will in the following refer to them as nonlinear changes or nonlinearities.

current with the voltage, and included the time dependence of such changes as a relaxation between equilibrium states which follows the dynamics of the membrane. This allowed us to simulate the impedance spectrum of the membrane for a set of different parameters (Fig. (4.6)). The blue curve in panel **A** of Fig. (4.6) is the impedance spectrum of the membrane when both  $\Delta g_0$  and  $\Delta C_0$  are zero, *i.e.* when capacitance and conductance are constant and the membrane is linear. In this case only can the membrane be represented by the circuit of Fig. (4.1), and in this ideal case the impedance spectrum is a semicircle in the Nyquist plot as expected for an RC circuit.

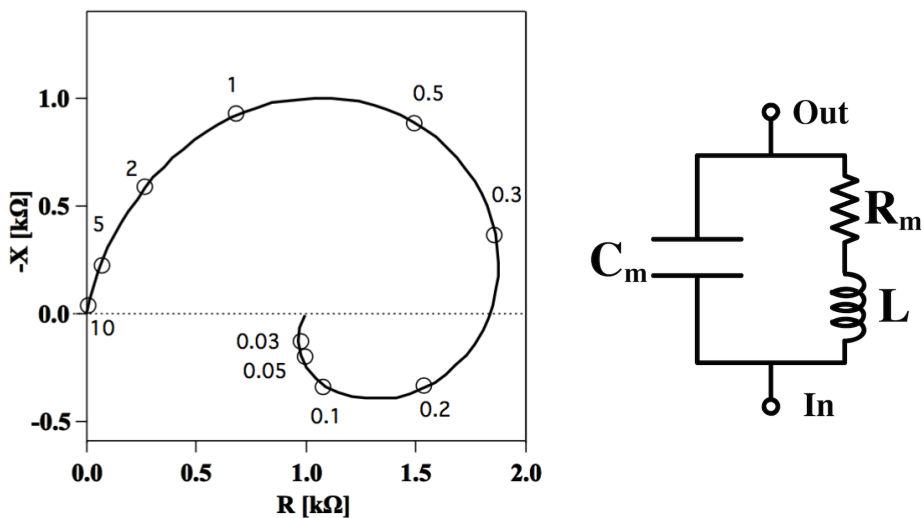


Figure 4.7: **Left:** Impedance spectrum of the squid giant axon measured by Cole and Baker in a frequency range between 10 KHz and 30 Hz [51]. The membrane shows inductive behaviour for frequencies below 200 Hz. Figure adapted from [71]. **Right:** Tentative equivalent circuit for the impedance spectrum measured by Cole and Baker. They could fit the experimental data by assuming an inductance of  $0.2 \text{ H cm}^2$ .

While the nonlinearity of the membrane capacitance has a subtle effect on the impedance spectrum, and mainly accountable for by considering a lossy capacitor in parallel with the membrane capacitor, the nonlinear membrane conduction has a more noticeable impact<sup>8</sup>. In particular it results in a positive reactance at low frequencies with a distinctive spiraling shape.

<sup>8</sup>Note that a lossy capacitor (a series combination of a resistor and a capacitor) is always added to model dielectric dispersion in any real dielectric. It originates from the observation that in real dielectrics, the phase angle between voltage and current is less than the ideal  $90^\circ$  [78]. As a result, the impedance spectrum of a real dielectric is a suppressed semicircle in the Nyquist Plot (the centre of the semicircle lies below the real axis). It is explained by the finite reorientation time of dipoles in the dielectric, due to friction (hence the resistor in series). Interestingly, in biological membrane the appearance of lossy capacitor behaviour in the impedance spectrum is linked to gating currents. Here

Interestingly, very similar impedance spectra were measured for the membrane of the squid giant axon by Cole and collaborators in the 40's. As shown in the left panel of Fig. (4.7), the measured impedance shows a positive reactance for frequencies below 200 Hz [51]. A positive reactance in linear circuit theory is characteristic of an inductance. Cole found that the equivalent circuit of Fig. (4.7) (right) could explain the experimental data, assuming an inductance of  $0.2 \text{ H}\cdot\text{cm}^2$ . However, lacking any structural evidence of an inductive element in the membrane, he was reluctant in suggesting any specific equivalent circuit and finally proposed the one Fig. (4.7) (right) stating that the choice would be just "*dictated by utility, convenience, and personal belief*" [51].

As noted by Cole, an inductive behaviour is not necessarily nor uniquely explained by the ability of a system to store magnetic energy. Any system for which the voltage difference is proportional to the rate of change of current will show the electrical properties of an inductance [72]. This could be any process in which the conductance changes with time. Without any complementary structural information of the system, this is the only information that can be extracted from impedance data like those of Fig. (4.7). On a similar note, Mauro showed that a resistor changing its value from a low conducting state to a high conducting state with a finite relaxation time would show an inductive spiraling in the impedance spectrum [79]. This is the case for the outward rectified membrane considered in our derivation.

Interestingly, among the processes which could account for the spectrum of Fig. (4.7), Cole discussed several which involve couplings between electrical properties and thermal or mechanical ones, e.g. thermoelectricity and piezoelectricity [72]. He discarded them based on their expected small magnitude. We showed here, however, that lipid bilayers display electromechanical, as well as thermoelectric properties, whose magnitude becomes significant close to the phase transition. This was not known at the time, but cannot be neglected when interpreting electrical data.

Finally, we showed that the inductive behaviour of the membrane impedance can be accounted for by the voltage induced changes in the lipid bilayer. We therefore expect the effect to be maximum at the transition where the permeability is enhanced and the membrane is more susceptible to changes in voltage. Since the lipid melting occurs a few degrees below physiological temperature, the nonlinear changes of capacitance and conductance must be considered when interpreting electrical data.

The physiological relevance of the dependencies introduced here is confirmed by the finding of the previous chapter. We want to stress again that the the membrane fluctuations and the electromechanical couplings which

---

we showed that it can originate from the finite relaxation time of voltage induced changes in capacitance and polarization.

#### *4. Nonlinear dynamic behaviour in common experiments*

---

are responsible for the nonlinearities discussed here, are all maxima at the phase transition. The proximity of the the lipid melting to the body temperature in biological membranes, is a strong indications that they all potentially play a role in physiological conditions

Part III

Experiments



# 5

## Materials and Methods

### 5.1 Materials

**Lipids:** 1,2-dimyristoyl-*sn*-glycero-3-phosphocholine (DMPC), 1,2-dilauroyl-*sn*-glycero-3-phosphocholine (DLPC), 1-palmitoyl-2-oleoyl-*sn*-glycero-3-phosphocholine (POPC), 1-palmitoyl-2-oleoyl-*sn*-glycero-3-phosphoethanolamine (POPE), and cholesterol were all purchased from Avanti Polar Lipids (Alabaster/AL, US), stored in a freezer at  $-18\text{ }^{\circ}\text{C}$  and used without further purification.

Electrolyte solutions were made from KCl (Fluka, Switzerland) and NaCl (VWR, US). The 150mM NaCl and 150mM KCl solutions used in the BLM setup were buffered with 2 mM HEPES and 1 mM EDTA (both from Sigma-Aldrich, Germany), pH was adjusted to 7.4. In experiments with the patch clamp setup the electrolyte solution was made of 150mM KCl, 150mM NaCl and buffered with 50 mM TRIS (Sigma Aldrich, Germany) to a final pH of 7.6.

All the water used in experiments was purified with a Direct-Q<sup>®</sup> Water Purification System (Merck Millipore, Germany) and had a resistivity  $>18.1\text{ M}\Omega\text{-cm}$ . Electrolyte solutions were filtered through a sterile  $0.2\text{ }\mu\text{m}$  filter (Minisart<sup>®</sup> Sartorius Stedim Biotech, Germany) to get rid of dust particles or impurities (this is particularly critical when working with small glass pipettes).

#### 5.1.1 Sample preparation

Stock solutions of each lipid were prepared by dissolving the lipid powder in chloroform to a final concentration of 10mM. When not used, stock solutions were stored in the freezer. The different mixtures used throughout the experiments were obtained by mixing the stock solutions in the desired molar ratio. After mixing, the samples were aliquoted and dried under a gentle stream of air and then placed under vacuum for minimum 2-3 hours.

The dried samples were then resuspended in an organic solvent to different concentrations depending on the methods used, as explained in the following:

**Calorimetry** All the lipid mixtures used in the permeability experiments were first placed in a DSC calorimeter to investigate their thermodynamical properties, namely their heat capacity profile in the melting transition. Samples were prepared by adding the electrolyte solution to the dried lipid aliquot to a final concentration of 10 mM. The sample was then shaken in an ultrasonic cleaner until the solution was uniformly milky, which is typical for a dispersion of multilamellar vesicles (MLV). Both the MLV and the reference solution (the buffered electrolyte) were degassed for about 10 minutes before being inserted in the calorimeter.

**Patch pipette setup** A 10:1 (mol:mol) mixture of DMPC and DLPC was used with the patch pipette setup. The dried aliquots were resuspended in a 4:1 (vol:vol) mixture of hexane and ethanol to a final concentration of 2 mM [80].

**BLM setup** (Black Lipid Membrane setup) Lipid samples used for experiments with the horizontal BLM setup were dissolved in decane to a final concentration of 10 mg/mL. The mixture used with this setup consisted of POPE:POPC=8:2 (mol:mol) for capacitance measurements and a mixture of DMPC:DLPC:chol= 77.3:7.7:15 (mol:mol:mol) for current measurements.

## 5.2 Methods

### 5.2.1 Calorimetry

Differential Scanning Calorimetry (DSC) measures the heat capacity difference between two cells as a function of temperature. A DSC calorimeter is made of two cells of tantalum contained in an adiabatic box. A schematic illustration of the instrument is shown in Fig. (5.1). In a typical experiment one cell (the sample cell) is filled with a solution of the molecule investigated (in our case, MLVs in buffer) and the other (the reference cell) with only the buffer. The temperature of the cells is changed at a fixed rate (set by the user) with two Peltier elements whose electric power is adjusted so that the temperature difference between the cells is zero. The calorimeter measures the difference in the electric power between the two cells as a function of temperature. In an endothermic process like the melting of lipids from the gel to the fluid phase, the sample requires more heating power than the reference in order to increase its temperature by the same amount. Therefore melting processes are characterised by a peak in the power difference between the cells.

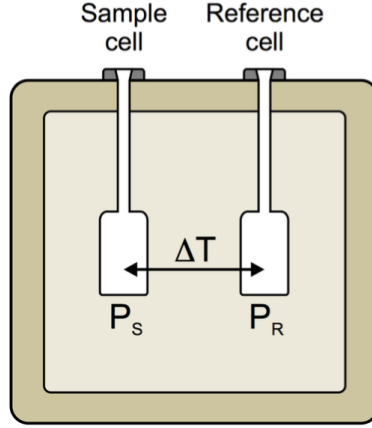


Figure 5.1: Illustration of the cells inside a calorimeter. Picture from [2].

The excess heat absorbed (or released),  $\Delta Q$  can be calculated from the power  $\Delta P$ , by integrating it over time  $t$ :

$$\Delta Q = \int_t^{t+\Delta t} \Delta P(t') dt' \simeq \Delta P \cdot \Delta t$$

Since the pressure in the cells is kept constant during the whole process, the molar heat capacity at constant pressure can be easily derived using Eq. (2.11):

$$\Delta c_p = \left( \frac{dQ}{dT} \right)_P \simeq \left( \frac{\Delta Q}{dT} \right)_P = \frac{\Delta P}{\Delta T / \Delta t}$$

where  $\Delta T / \Delta t$  is the scan rate. By dividing the raw signal of the calorimeter by the scan rate one obtains the excess heat capacity as a function of temperature. From the heat capacity profile, the melting enthalpy and entropy can be obtained by simple integration according to:

$$\Delta H_0 = \int_{T_g}^{T_f} \Delta c_p dT$$

$$\Delta S_0 = \int_{T_g}^{T_f} \frac{\Delta c_p}{T} dT = \frac{\Delta H_0}{T_m}$$

Throughout this thesis we used VP-DSC, produced by MicroCal (USA).

### 5.2.2 Patch Clamp Setup

The dried mixture of 10:1=DMPC:DLPC (mol:mol) was resuspended in a highly volatile solvent made of 4:1=hexane:ethanol (vol:vol) to a final concentration of 2mM. Synthetic lipid membranes were formed on the tip of a patch-clamp glass pipette using the droplet method introduced by Hanke [80, 81]

and illustrated in Fig. (5.2), in which a droplet of the lipid solution is placed on the outer surface of a vertically standing glass pipette filled with the electrolyte solution (A-C). The tip of the pipette is in contact with the surface of a beaker containing the same electrolyte solution as the pipette, and as the droplet flows down the glass surface, it seals the pipette tip with a spontaneously formed bilayer (D). The solvent is allowed to diffuse out of the bilayer for about 30s before starting the experiments.

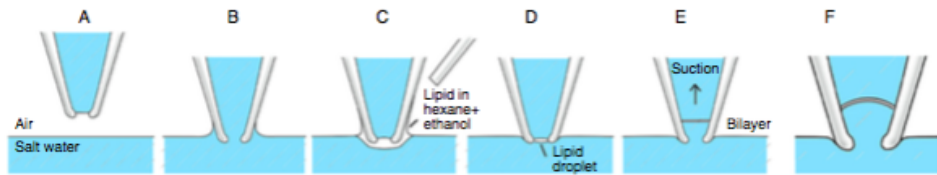


Figure 5.2: Schematic illustration of the bilayer formation. Picture from [81].

Glass pipettes were pulled from 1.5 mm/0.84 mm (OD/ID) borosilicate glass capillaries (World Precision Instruments, USA) with a vertical PC-10 puller (Narishige Group, Japan) following the two-step procedure explained in [62]. They were then fire polished using a Narishige MF-900 Microforge, which created pipette openings of about 10  $\mu\text{m}$ .

Fig. (5.3) shows the configuration of the patch clamp setup used in the experiments. Electrical recordings were made with an Axopatch 200B patch clamp amplifier (Molecular Devices, USA). Ag/AgCl electrodes were used inside the pipette and as ground reference in the bath solution, and mounted on a cooled capacitor feedback integrating headstage amplifier (CV 203 BU, Molecular Devices, USA). Current traces were recorded with Clampex 9.2 (Molecular Devices, USA) in the Whole Cell (headstage gain  $\beta=1$ ) in voltage clamp mode and the sampling frequency was 10 kHz. The position of the pipette with respect to the bath surface was finely adjusted and monitored with a micromanipulator (model SM1, Luigs and Neumann, Germany) onto which the headstage was mounted.

### 5.3 BLM setup

The DMPC:DLPC:chol=77.3:7.7:15 (mol:mol:mol) used for the IV measurement and the POPE:POPC=8:2 (mol:mol) mixture used for the capacitance measurements on the Black Lipid Membrane setup were both dissolved in decane to a final concentration of 10 mg/mL. Planar lipid bilayers were formed on a circular aperture in a 25  $\mu\text{m}$  thick Teflon film using a slightly modified version of the painting method introduced by Mueller et al. [82]. The original method consists in painting a small volume of the lipid solution on the hole of a Teflon film separating two chambers filled with an electrolyte

### 5.3. BLM setup

---

solution. The membrane is then allowed to thin out for a few minutes until a bilayer is formed which is in equilibrium with a surrounding annulus made of the bulk lipid solution (the so called Plateau-Gibbs border), as shown in Fig. (6.5). More details on the different methods for bilayer formation can be found [81].

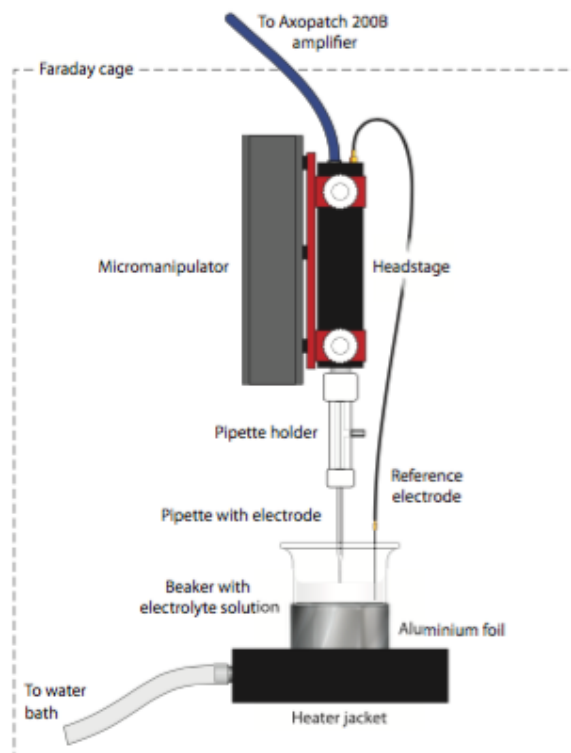


Figure 5.3: Schematic illustration of the patch clamp setup. Picture from [9].

Here we used commercially available horizontal bilayer slides (Ionovation GmbH, Germany) made of two microchambers (filled with approx  $150 \mu\text{L}$  of the same electrolyte solution) separated by an horizontal Teflon film. The upper and lower chambers are connected only through the  $120\mu\text{m}$  aperture in the film and each has an access port for the electrical connections and for buffer perfusion. Once a small droplet ( $\simeq 0.2 \mu\text{L}$ ) of lipid solution is placed in the upper chamber close to aperture, a bilayer is formed automatically by a perfusion system (Ionovation Explorer, Ionovation GmbH, Germany). The membrane formation was monitored with capacitance measurements and was automatically repeated until the membrane capacitance was stably above a minimum threshold value of  $40 \text{ pF}$ .

Current measurements were recorded using an EPC 10 USB patch clamp amplifier with an integrated AD/DA converter board (HEKA Elektronik,

Germany), controlled with the Patchmaster software (HEKA Elektronik, Germany), which was also used for data acquisition and analysis. Ag/AgCl electrodes inserted in an electrode holder filled with 3M KCl electrolyte were connected to the electrode ports of the two slide chambers through an agar bridge and mounted to the headstage of the patch clamp amplifier. The bilayer slide together with the headstage of the amplifier were contained in a metal lid which worked as a Faraday cage. Data traces were recorded with Patchmaster using the Whole Cell voltage clamp mode and sampled at 10 kHz.

The bilayer slides are made of an electrically insulating yet heat conducting material which allowed for temperature control through heat transfer from the heating frame of a temperature control unit (Thermomaster, Ionovation GmbH, Germany). The unit is connected to a water bath (Haake K10/DC30, Thermo Fisher Scientific, USA) and the temperature was regulated by adjusting the volume of water circulating in the heating frame with a peristaltic pump. The temperature was monitored through a sensor immersed in the upper chamber.

The bilayer slide was placed on the workstage of an inverted microscope (IX70, Olympus, Japan) which allowed for optical monitoring of the bilayer formation.

# 6

## Results

### 6.1 Temperature dependence of the membrane capacitance

We have discussed in chapter 3 that lipid membranes can be modeled as a planar capacitor when dealing with the electrical properties of membranes. The value of the membrane capacitance depends on the geometry of the membrane and hence it is state dependent. This means that everything that can induce a fluid to gel transition will affect the value of the capacitance. As a result, we expect the membrane capacitance to be affected by e.g. changes in voltage, lateral pressure and temperature. In chapter 3 we estimated a relative change of the capacitance of DPPC membranes of about 50% between the fluid and the gel state, due to the changes in area and thickness. Here we show experimental results on the temperature dependence of the capacitance of a black lipid membrane made of a mixture of POPE:POPC=8:2.

Since the largest change in capacitance is expected to occur around the lipid melting transition, we first used DSC calorimetry to determine the heat capacity profile of multilamellar vesicles made from the same mixture following the method described in chapter 5. The two lipids differ only by the headgroup, ethanolamine and choline, so both are zwitterionic. Fig. (6.1) (left) shows the heat capacity profile measured during heating (red curve) and cooling (blue curve). The melting temperature, determined as the temperature at which half of the lipids are melted, is 21.4°C for the heating scan and 20.6°C for the cooling one. The difference in the melting temperature and in the melting profiles is due to hysteresis. The melting enthalpy, calculated as the integral of the excess heat capacity, is shown in Fig. (6.1) (right).

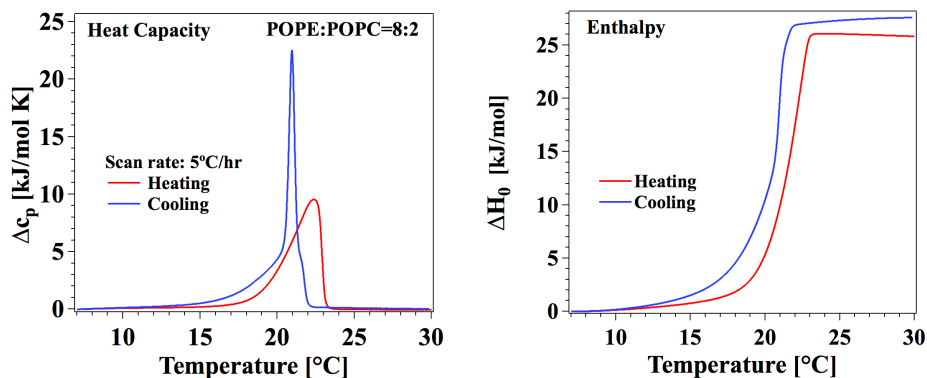


Figure 6.1: **Left:** Excess heat capacity profile of POPE:POPC=8:2 measured with DSC at a scan rate of 5°C/hr. Heating scan (red), cooling scan (blue). The electrolyte solution was made of 150mM KCl, pH 7.4. **Right:** Melting enthalpy, as calculated by integration of the heat capacity profile. Heating scan (red), cooling scan (blue).

Lipid bilayers were formed on a Ionovation Explorer, using the method described in 5, at a temperature above the phase transition. After bilayer formation, the system was left equilibrating for about 15 minutes, while monitoring the capacitance until it reached a steady value. Starting from a temperature of about 33°C, the system was cooled to a temperature below the melting transition and then heated up again to above the melting transition. This was made continuously and in cycles, while simultaneously measuring the membrane capacitance. Fig. (6.2) shows three of such cycles. The capacitance was determined from the current response of the membrane to a triangular voltage stimulus ramping between 50mV and -50mV at a rate of  $dV/dt=0.67$  V/s. The current response of a black lipid membrane to voltage perturbations is the sum of a resistive and a capacitive contribution,  $I_m = I_r + I_C$ . Assuming that the system behaves linearly for low voltages (in our case, lower than  $\pm 50$  mV), the capacitive current can be obtained by subtracting the current response to the positive ramp from the response to the negative ramp. The capacitance is then calculated as:

$$C = \frac{I_c}{dV/dt} \quad (6.1)$$

We want to stress that this method for calculating the capacitance is only valid under the assumption of constant resistance and capacitance. We will discuss the validity of this assumption in the voltage range used here in section 6.3

As shown in Fig. (6.2), the capacitance changes consistently upon melting, and as expected its value is larger in the fluid phase compared to the gel

### 6.1. Temperature dependence of the membrane capacitance

phase. The relative change is of the order of 90%, and is roughly proportional to the melting enthalpy shown in Fig. (6.1) (right). The temperature range over which the largest capacitance changes happen is quite different for the heating and the cooling scan, probably due to hysteresis, and it is roughly 5°C higher than the melting regime measured with DSC Fig. (6.1). This mismatch is probably a consequence of the fact that black lipid membranes, unlike the vesicles used for calorimetry, contain decane which is known to affect the lipid phase transition [83]. The presence of the solvent annulus is likely to influence the absolute value of the capacitance (it acts as an additional capacitor in parallel to the membrane capacitor), and also the magnitude of the capacitance change, as it will be discussed in section 6.3.

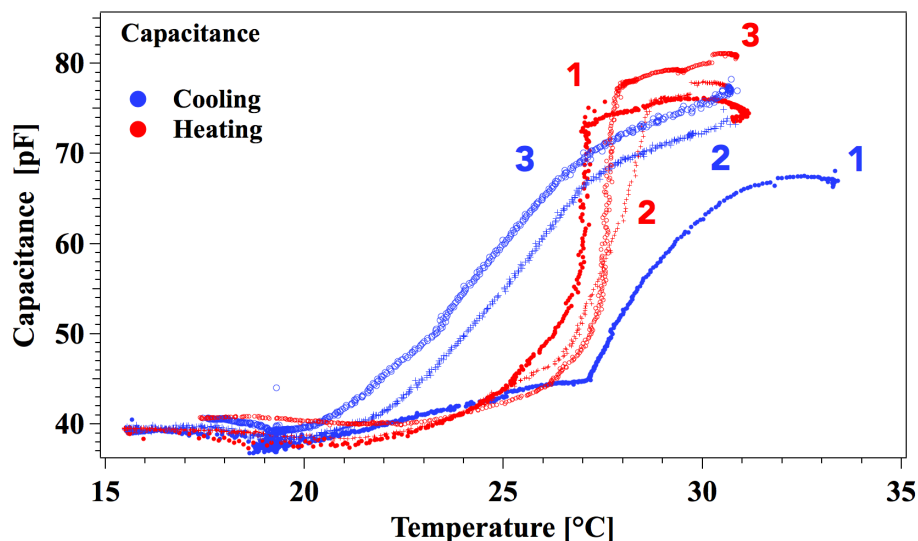


Figure 6.2: Membrane capacitance as a function of temperature for a BLM made of POPE:POPC=8:2. The bath solution on both sides was made of 150mM KCl, pH 7.4. Cooling and heating scans are indicated with blue and red markers, respectively. The numbers mark the order of the scans, which were made in cycles, as follows: Cooling scan 1 → heating scan 1 → cooling scan 2 → heating scan 2 → cooling scan 3 → heating scan 3.

We see that despite the hysteresis between cooling and heating curves, each of the two groups of curves share the same features, in terms of shape and magnitude, with the exception of the first cooling curve. This can be explained by the membrane not being fully in equilibrium with the solvent at the beginning of the measurement (see 6.3). Each curve was measured over a time of 30-40 minutes<sup>1</sup>. It is then likely that the bilayer was fully

<sup>1</sup>The heating and cooling rate was controlled manually and therefore could not be kept exactly constant and equal for all the scans.

equilibrated after the first scan, as suggested by the reproducibility of the successive curves. In particular, the curves almost collapse into one for low temperature, both heating and cooling ones. At higher temperature there is a large variability in the value of the capacitance. That is probably due to the limits in the accessible temperature range of the Thermomaster. It was in fact not possible to efficiently heat the system to higher temperatures without exceeding the limits set by the manufacturer on the maximum temperature of the water bath. As it is suggested by the nonzero slope of the cooling curves 2 and 3 at their highest temperature, it seems that the start of the cooling scan is inside the melting regime (unlike curve 1 which starts at higher temperature). It then seems plausible to assume that with a higher accessible temperature range, the variability in the capacitance value at high temperatures could be reduced.

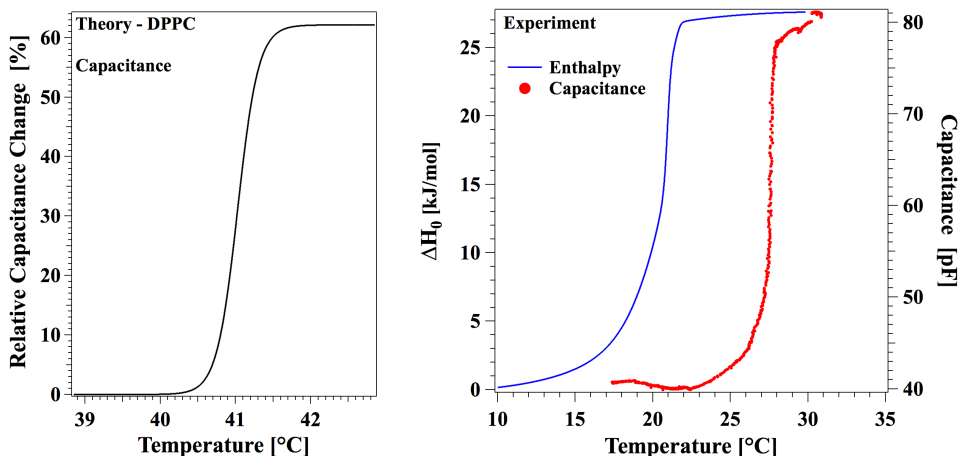


Figure 6.3: **Left:** Relative change in the capacitance of a DPPC membrane,  $(C_m(T) - C_g)/C_g$ , as expected from the theory. **Right:** Melting enthalpy (cooling scan, blue curve) and capacitance (third heating scan, red markers) as a function of temperature. The two curves have similar shapes and resemble the theoretical prediction for DPPC.

Previous studies have measured the change in the capacitance upon melting of black lipid membranes of different composition [77, 84, 85], and found changes in the same directions as the ones measured here. Here we measured the capacitance while continuously heating and cooling the system, which allows for thorough inspection of the transition regime. In particular, one can see how the capacitance changes are proportional to the enthalpy changes. Fig. (6.3) shows the temperature dependence of the relative change in capacitance as expected from the theory for a DPPC membrane and a comparison between the measured capacitance change from Fig. (6.2) and the enthalpy curve.

### 6.1. Temperature dependence of the membrane capacitance

Finally, we have discussed the thermoelectric effect in chapter 3, by which the membrane capacitor can be charged or discharged by changes in temperature (Eq. (3.41)). In the absence of spontaneous polarization it is given by:

$$dq = \Psi \left( \frac{\partial C_m}{\partial T} \right)_{\Psi, c} dT \quad (6.2)$$

The partial derivative of the capacitance with respect to temperature as predicted from the theory is plotted in Fig. (6.4) (left). It can be qualitatively compared to Fig. (6.4) (right) which shows the derivative of the capacitance with respect to the temperature as calculated from the experimental curve of Fig. (6.3)(right, red). Both have a maximum in the transition and the latter can be almost superimposed to the heat capacity.

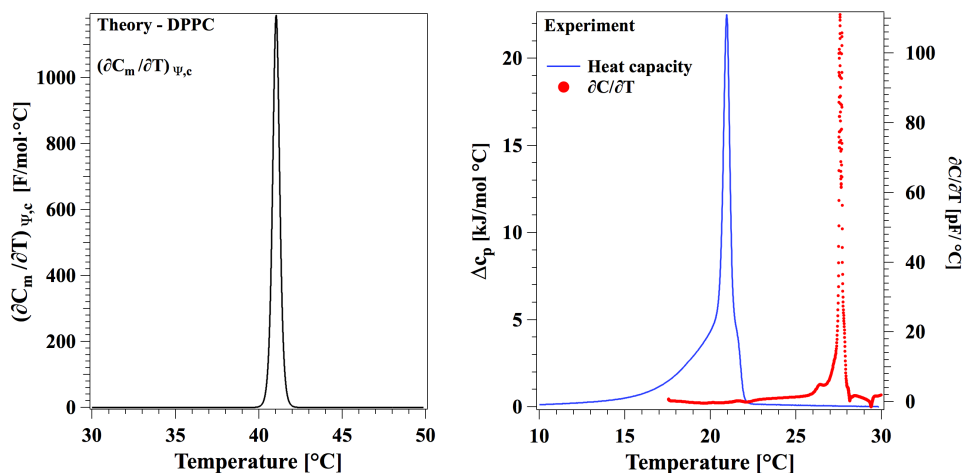


Figure 6.4: **Left:** The partial derivative of the membrane capacitance with respect to temperature at fixed voltage and curvature for a DPPC membrane (see chapter 3), shows a maximum at the transition temperature ( $T_m = 41^\circ\text{C}$ ).  $\Psi = 0$ ,  $\Psi_0 = 0$  **Right:** Measured heat capacity (cooling scan, blue curve) and the derivative of the measured capacitance of Fig. (6.3) (red markers). Both functions have a maximum at a temperature where the changes in the correspondent extensive variables are largest.

To conclude this section, the capacitance of the black lipid membrane shows an increase of about 90% from the gel to the fluid phase. The change is likely to be due to a combination of the melting of the lipid bilayer and consequent change in the membrane geometry, and membrane thinning due to the movement of the solvent into the annulus. As already discussed by [84], we suggest that melting is the dominating effect and that the solvent squeezing out is a side effect prompted by the transition and linked to the decreased pressure across the bilayer due to the increased thickness (see section

6.3). The shape of the capacitance change and its derivative qualitatively correlate with the enthalpy and the heat capacity measured with DSC and they are in perfect qualitative agreement with the theoretical predictions of chapter 3.

## 6.2 Lipid ion channels and rectification

Motivated by the theoretical analysis of chapter 4 on the occurrence of rectification in the I-V curve of lipid bilayers, we investigated it further in experiments using two different setup: a BLM setup and a patch clamp setup. According to our analysis and to the results of Blicher [65], outward rectified current voltage relationship can be observed in pure lipid bilayers reconstituted on the tip of glass pipette and can be fully described by a simple capacitor model which takes into account the nonlinearity of the membrane capacitance and the presence of a spontaneous polarization in the membrane. The former effect (and the resulting increase in likelihood of pore formation) is responsible for the nonlinearity of the I-V curve whereas the latter gives rise to the distinctive asymmetric current response to positive and negative voltages that goes under the name of rectification.

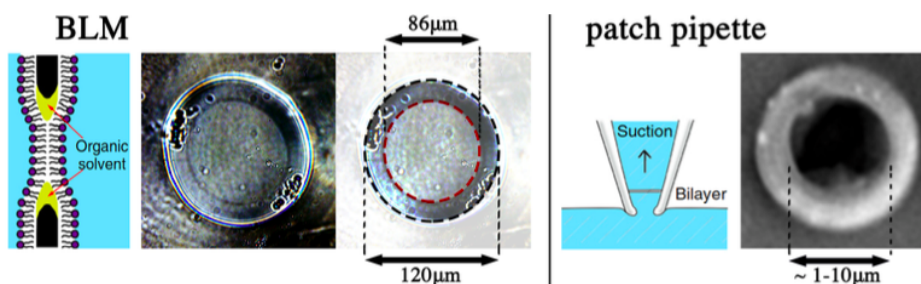


Figure 6.5: **Left:** Schematic drawing of the section of a black lipid membrane (left). Image of a BLM (centre), with highlighted hole aperture and bilayer perimeter (right). **Right:** Illustration of the final step of bilayer formation on a patch pipette (left). Image of the pipette tip (right).

Rectification can be described by introducing a voltage offset in the expression of the free energy of pore formation. In bilayers with symmetric composition, like the ones used by Blicher [65], a voltage offset could, for instance, be explained on the basis of a curvature induced polarization of the membrane, as discussed in chapter 3. In patch pipette experiments little suction is applied to facilitate membrane formation. This, combined to the small diameter of the pipette tip (between 1-10  $\mu\text{m}$ ), was suggested as a possible origin of the voltage offset of about 100 mV observed. If that is the case, one would expect a much lower offset in larger membrane patches like

those used in BLM experiments (see Fig. (6.5)).

With an aperture diameter of about 100  $\mu\text{m}$ , one would expect offset voltages between 10 and 100 times lower than those on glass pipettes. Previous permeability studies on BLM seem to confirm this prediction, showing symmetric nonlinear I-V curves [55].

We here show a comparative study of I-V currents in black lipid membranes and patch pipettes.

### 6.2.1 BLM

Black lipid membranes of DMPC:DLPC:Chol=77.3:7.7:15 were formed using the methods described in chapter 5. We measured the current response of the membrane as a function of voltage at constant temperature. Voltage was applied in alternated steps of  $\pm 10\text{mV}$  amplitude and 10s duration from a holding voltage of 0V.

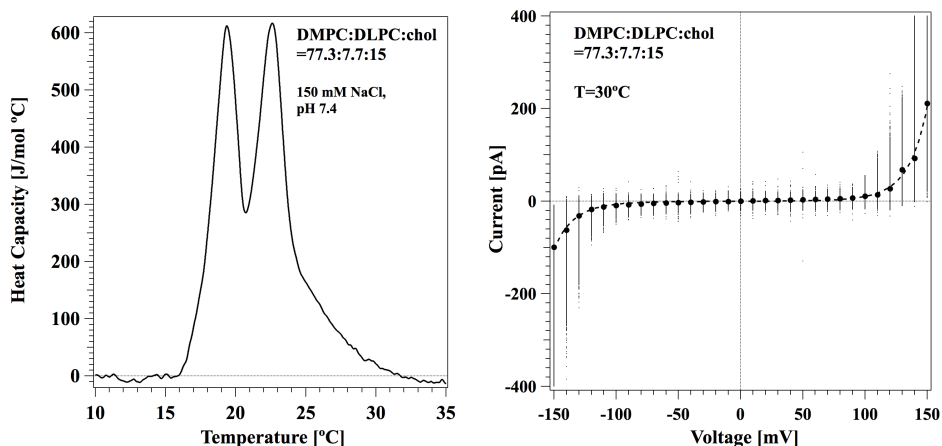


Figure 6.6: **Left:** Heat capacity profile of DMPC:DLPC:chol=77.4:7.7:15, measured at  $5^\circ\text{C}/\text{hr}$ . It shows two maxima at  $19.4^\circ\text{C}$  and  $22.6^\circ\text{C}$ . Buffer solution is made of 150mM NaCl, pH 7.4. **Right:** I-V curve for a bilayer at  $30^\circ$  between -150 mV and +150 mV. The membrane broke at 160 mV. Every data point of the current trace is plotted for each voltage. Black circles are the average of each 10s long current trace. The dashed line is a fit to Eq. (4.3). It gives a value of the offset voltage of  $\Psi_0 = 6\text{mV}$

Fig. (6.6) (right) shows a representative current-voltage relationship measured at  $30^\circ\text{C}$ . This corresponds to the upper end of the melting transition, as shown in the heat capacity profile measured with DSC calorimetry, Fig. (6.6) (left)<sup>2</sup>. The dashed line is a fit to Eq. (4.3). Fig. (6.6) (right) shows how the

<sup>2</sup>Note that the buffer used for DSC measurements is made of NaCl, whereas the one for the experiments with the BLM is made of KCl. This is not expected to have major effects, since the salt concentration is the same in the two experiments and the lipids used

ionic current through the membrane patch changes as a nonlinear but overall fairly symmetric function of voltage. The best fit gives a value of the offset voltage of about 6mV. For voltages below  $\pm 100$ mV the current response is linear and the bilayer has a conductance of about 80pS.

The steep increase in current observed at higher voltages (higher than  $\pm 100$  mV) corresponds to the appearance of current fluctuations in the current trace. An example is shown in Fig. (6.7) (left), for a different bilayer, at 32°.

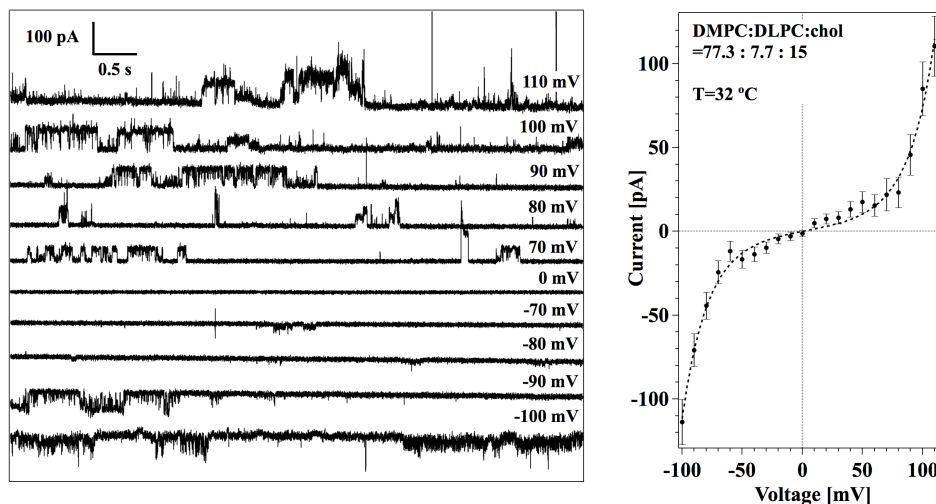


Figure 6.7: **Left:** Current traces for some values of the applied voltage. The traces were digitally filtered at 1 kHz **Right:** I-V curve for a bilayer at 32°C in a voltage interval between -100 mV and + 110 mV. Black circles are the average of the 10 s trace, and error bars are the standard deviation for each trace. The dashed line is a fit to Eq. (4.3). The resulting offset voltage is  $\Psi_0 = (-6.0 \pm 0.8)$ mV.

Current fluctuations appear in the nonlinear regime in the form of well defined quantized step, burst or increase in the noise. The onset of current nonlinearity in this membrane occurs at lower voltage ( $\pm 50$  mV) than the previous one, as shown in the I-V curve ( Fig. 6.7 - right), but the overall behaviour seems unchanged. Together, the nonlinearity of the I-V and the appearance of current fluctuations in the nonlinear regime are in line with the electrostrictive capacitor model for membrane breakdown and pore formation outlined in chapter 4 and proposed by Blicher and collaborators [65]. In this framework, the symmetric response of the membrane to positive and negative voltages results in a small value of the voltage offset<sup>3</sup>, on the order of 6 mV

are uncharged.

<sup>3</sup>small compared to the voltage at which the membrane starts to deviate from the linear behaviour.

for both membranes showed.

In several instances, the onset of current fluctuations was observed in conjunction with the membrane (*i.e.* bilayer + annulus) expanding outside the rim of the teflon aperture, as observed by optical microscopy. The phenomenon resembles the bulging of planar bilayers into cupola-shaped membranes observed and described by Antonov and collaborators in response to excess hydrostatic pressure [86] (a schematic drawing is shown in Fig. (6.11)d). Similar instabilities were reported by other authors for lecithin films in the presence of hexadecane as a solvent [87] or, on longer time scales, in the presence of decane [88]. In our case the hydrostatic pressure was not directly controlled but it is assumed to be constant during the experiment. It is, however, not guaranteed to be equal on the two sides of the membrane, hence the slow expansion and bulging could be interpreted as a long-time response of the system to eventual pressure differences at the time of membrane formation (see section 6.3). We didn't investigate the origin and the mechanism of this phenomenon further but we limited ourselves to the observation that its occurrence is somehow linked to the increase in current fluctuations (in the form of quantized steps, burst or just increased noise). Though some bilayers show nonlinearities in the absence of this anomaly (like the one in Fig. (6.7)), they do show current fluctuations in most of the cases in which the membrane is observed to "expand" out of the rim of the hole.

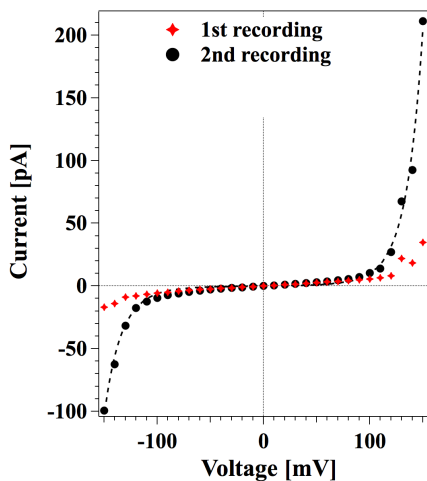


Figure 6.8: Two consecutive recordings of the same bilayer of DMPC:DLPC:chol =77.3:7.7:15 in the presence of the bulging anomaly. Red marker: first recording. Black marker: second recording.  $T=30^\circ$ .

To rule out that this mechanical instability can alone produce the non-linearity observed in experiments, *i.e.* that the conductance increase is more time dependent rather than voltage dependent, we measured subsequent I-V curves for the same membrane showing the slow expansion<sup>4</sup>. They are shown

<sup>4</sup>This turned out to be a difficult task, because once the membrane bulges out of the hole rim, it expands fast until it breaks.

in Fig. (6.8). Current fluctuations and nonlinearity of the I-V showed up in the first measurement at around 100 mV, when the bilayer had reached the rim of the aperture. The membrane kept expanding slowly during the second measurement and eventually broke at 160 mV. As it can be seen in the I-V curve of the second recording and in the current traces (not shown), for low voltages the current is a linear function of the voltage even in the presence of membrane bulging. However, the magnitude of the nonlinearity is larger in the second measurement. This suggests that the membrane current has indeed a nonlinear dependence of the voltage, but also that the magnitude of the effect is greatly influenced by the bulging of the membrane.

Finally, we stress that an expanding or bulging membrane is not an ideal system for a proper electrical characterization of the lipid bilayer. The obvious reason is that a time dependent change in the geometry of the system is an indication that the system is not in mechanical equilibrium. In the light of the electromechanical couplings discussed in chapter 3, changes in area and curvature can affect the equilibrium charge on the membrane capacitance and the dynamic electrical response to voltage perturbation, making it hard to correctly interpret the current data.

### 6.2.2 Patch pipette

Lipid bilayers made of DMPC:DLPC=10:1 were reconstituted on the tip of glass pipettes mounted on a patch clamp setup as described in chapter 5. Different voltages were applied to the membrane using a step protocol similar to the one used for the BLM setup and the response current was recorded. The voltage jumped from a holding voltage of 0 V to a final voltage which, starting from the highest in the explored range, decreased at every iteration by a constant step. In general, membranes formed on the patch pipettes were more resistant to voltage than those in BLM and therefore we could explore a wider voltage range, between -200mV and 200mV. As described in chapter 5, the pipette tip touches the surface of the electrolyte bath when the membrane is formed. We then changed the position of the tip relative to the bath surface and recorded the I-V curves of bilayers at different depths. A change in the tip position corresponds to a change in hydrostatic pressure which is proportional to its distance from the air-water interface. The melting profile of the mixture used is shown in Fig. (6.9) (left). It has a fairly cooperative transition with a single peak at 22.2°C. The temperature during the experiment was 24°C, which again is at the upper end of the melting transition. Fig. (6.9) (right) shows two I-V curves measured on the same bilayer at the surface (open circles) and at a depth of 8 mm (black circles), corresponding to a pressure difference of about 82 Pa. In the absence of pressure, the current response of the membrane is linear with the voltage. The I-V curve becomes asymmetric and nonlinear when the tip is at a depth of 8mm. A fit to Eq. (4.3) (dashed line in Fig. (6.9)) gives a

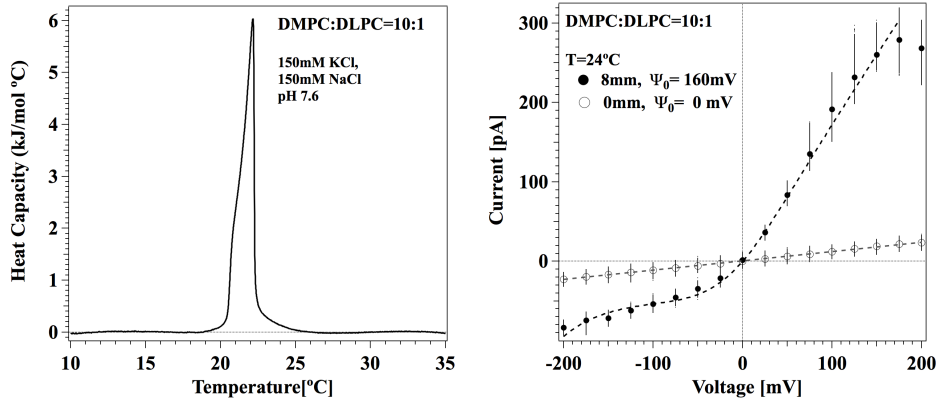


Figure 6.9: **Left:** Heat capacity profile for DMPC:DLPC=10:1 at 5°C/hr, showing a peak at 22.2°C. Buffer solution was 150mM NaCl, 150mM KCl, pH 7.6. **Right:** Two I-V curves for the same bilayer at 24°C in a voltage interval between -200 mV and +200 mV. All current points are plotted vs the voltage. Open circles are the average values of current when the pipette tip was at the surface. The dashed line is a linear fit ( $\Psi_0 = 0$ ). Solid circles are the average values of the current measured with the tip at a depth of 8mm. The dashed line is a fit to Eq. (4.3), which gives a voltage offset of  $\Psi_0 = 160\text{mV}$ .

value of the offset voltage of 160 mV. The distinctive profile of the nonlinear I-V shown here is commonly referred to as "outward rectified" due to the higher conductance for positive voltages than for negative ones<sup>5</sup>. It is very similar to the one measured by [65]. Similar curves are often observed in experiments on different protein channels (like the TRP channels, shown in Fig. (??)). They are usually interpreted on the basis of a transition state model (Eyring model) which assumes an energy barrier for the passage of ions whose position in the membrane (whether in the centre or not) determines the symmetric or asymmetric nature of the current response. Interestingly, the capacitor model of chapter 4 is able to fit experimental data for both the TRP channels and pure lipid bilayers. In the latter case, the capacitor model was shown to better explain the current response than the Eyring model (which agrees with the data only in a limited voltage range, as shown in [62]).

Although the nonlinear curve in Fig. (6.9) (right) is representative of the asymmetric behaviour of this - and other - membranes, its occurrence was often transient. This means that different recordings measured at the same depth for the same membrane could show current responses resembling both

<sup>5</sup>sign convention wants the current going out of the cell to be positive. An outward rectified channel is therefore a channel that preferentially allows current to flow out of the cells and opposes higher electrical resistance to currents flowing inside the cell.

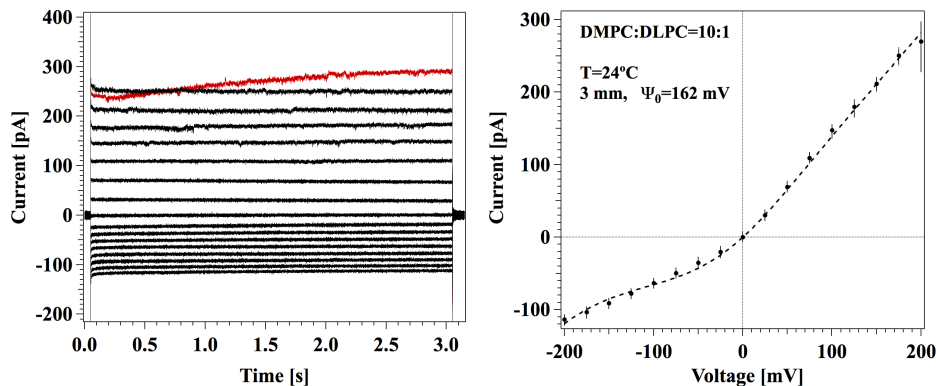


Figure 6.10: **Left:** Raw current traces in response to the voltage steps. **Right:** I-V curve for at  $24^\circ$  in a voltage interval between  $-200$  mV and  $+200$  mV. Black circles are the average of the traces on the left. The dashed line is a fit to Eq. (4.3). Fit parameters are  $\Psi_0 = (162.41 \pm 0.06)$  mV,  $\gamma_p = (1.4108 \pm 0.0009)$  nS,  $\Delta G_0 = (9.210 \pm 0.012)$  kJ/mol and  $\alpha = (453.8 \pm 0.6)$  kJ/mol V<sup>2</sup>

curves of Fig. (6.9) (right). One reason for this could be the flow of material inside the pipette and consequent release of pressure. Note that pressure was not directly controlled nor monitored, so from this stand the results shown here should not be overinterpreted to quantify the effect of pressure (or curvature) on the membrane asymmetry. What they do unequivocally show, however, is that compositionally symmetric bilayers formed on the tip of glass pipette can show outward rectification. Changing the depth of the tip in the aqueous buffer increases the likelihood of this occurrence.

While in some instances the increase in conductance was linked to the appearance of current fluctuations, as for the BLM, in most of the cases the nonlinearity was due to a voltage dependence of the baseline conductance, as shown in Fig. (6.10)(left). The red current trace at high positive voltage (200mV) shows an increased current relaxation time. This behaviour was observed in several recordings.

## 6.3 Discussion

### 6.3.1 Capacitance measurements

We measured the capacitance of a black lipid membrane of POPE:POPC=8:2 as a function of temperature in the phase transition regime. The capacitance of the membrane was found to be larger in the fluid phase than in the gel phase and fairly constant far from the transition, as expected from the theory and in agreement with previous studies by Antonov and collaborators on hydrogenated egg lecithin (HEL) [84].

We found that the temperature dependence of the capacitance at the transition is roughly proportional to the melting enthalpy as measured with DSC calorimetry (Fig. (6.3),right). This is also expected from the theory, under the assumption that the BLM can be modeled as a planar capacitor, due to the proportionality relation between changes in enthalpy and changes in thickness and area [16] (see chapter 2). As a result, the derivative of the capacitance with respect to the temperature was found to be qualitatively similar to the heat capacity profile (Fig. (6.1)), and hence to have a peak at the transition. The temperature derivative of the measured capacitance was further found to resemble the partial derivative of the capacitance with respect to temperature at constant curvature and voltage discussed in chapter 3 in the context of the thermoelectric effect. We note that, while the curvature could be considered as constant in our experiment, the same doesn't apply to the voltage across the membrane, which, as in any measurement aimed at giving information on the capacitance, was not fixed during the measurement. In particular, it was changing between -50mV and 50mV. If the membrane capacitance is constant with respect to voltage in that range, then the temperature derivative of the capacitance of (6.1, right) can effectively be considered as taken at constant voltage. That the membrane behaves linearly in that voltage range was also the assumption under which we could use Eq. (6.1) to measure the capacitance in the first place. This assumption is confirmed by measurements of the current voltage relationship in BLM which showed no significant voltage offset and linear behaviour for voltages below 50 mV.

The temperature range in which the changes in the capacitance are largest is about 6.6°C higher than the melting range measured with DSC calorimetry (measured as peak-to-peak distance in Fig. (6.1), right). This shift in the melting temperature is probably due to the presence of solvent in the black lipid membrane, as opposed to the vesicles used for DSC which are solvent free. Decane is mostly present in the annulus surrounding the bilayer but also in the bilayer region, in the form of microlenses spanning the bilayer thickness or as a separate phase in the bilayer midplane [83, 89, 90]. The capacitance of BLM was found to depend on the type of alkane used as solvent, mainly due to the dependence of the membrane thickness on the length of the alkane [87, 91]. In other words, longer alkanes like hexadecane were found to mix almost ideally in the bilayer along the lipid chains (hence not affecting the thickness significantly), whereas the shorter ones like hexane or decane were found between the acyl chains of lipids, therefore resulting in a larger thickness of the bilayer in the presence of short alkanes. This would mean that the absolute magnitude of the capacitance measured here is lower than that of solvent free membranes of the same mixture. McIntosh and collaborators studied the effect of different n-alkanes on the melting temperature of DPPC bilayers. They found that shorter alkanes ( $n < 12$ ) lower the transition

temperature (of about 4°C for decane) while longer ones tend to increase it. In DMPC bilayers the effect of decane is not as pronounced as for DPPC and goes in the opposite direction [83]. There seems to be a change in the way the alkane interacts with the lipid when the alkane chain length is more than four carbons smaller than that of the lipid. POPC and POPE used here have a mixed tail made of palmitic (16 carbons long) and oleic acid (18 carbons long). They are both more than four carbons longer than decane. Therefore, one would expect the melting temperature to be lowered in the presence of solvent, in contrast to our observation. It is unclear at this stage why the capacitance changes observed here happen at a higher temperature than that expected from calorimetric measurements. Further investigations are therefore essential to draw final conclusions. We stress at this point that the black lipid membrane is a highly heterogeneous system. Although we are mostly interested in the bilayer portion of the membrane, it is the annulus that controls the equilibrium of the system. Being significantly more massive than the bilayer, the chemical potential of the components of the bilayer is determined and constraint by the chemical potential of the annulus, at equilibrium [92]. The annulus, however, can exhibit a complex phase behaviour and it can be expected that the overall phase behaviour of the BLM differs from that of lipid suspension used in calorimetry, even when alkanes are present.

In addition to the the melting temperature and the absolute value of the capacitance of the BLM, the relative magnitude of the capacitance change is also likely to be influenced by the presence of the solvent. As pointed out by Stephen White in his insightful book chapter on the physical nature of planar bilayer membranes, [92] the black lipid membrane does not form spontaneously on the film aperture because it *"is inherently not an equilibrium system - work must be done to create it. There is always a lower free energy state for the system, which is the bulk solution with no black film; that is, the films tend toward the broken state."* He then continues by analyzing the aspects of the complex equilibrium which makes it possible for membranes to exist for many hours. In particular, the formation process (the thinning of the bilayer from the bulk forming solution) is the result of three driving forces. First, the curved interface formed by the bulk solution in order to adjust to the rim of the aperture creates a pressure difference according to Laplace law (lower in the membrane than in the water phase) which triggers the movement of solvent molecules from the bilayer area to the annulus (also called Plateau-Gibbs border suction). Thereafter, when the bilayer thickness is on the order of few hundreds Å, the London-Van der Waals attraction between the aqueous phases on the two sides of the membrane exert a hydrostatic pressure which tends to further thin the bilayer. The thinning continues until steric repulsion between the lipid acyl chains inhibit further thinning. The London-Van der Waals pressure is inversely proportional to the distance between the aqueous phases (*i.e.* the

membrane thickness). In agreement with the analysis of Antonov and collaborators [84], we suggest that the change in capacitance is primarily produced by melting of lipid bilayer. The thickness increase from the fluid to the gel phase results in a decrease in the Van der Waals pressure which, in turn, triggers the movement of solvent in the bilayer area that further thickens the membrane. The combined action of these effects could account for the 90% change in the capacitance observed here. Finally, knowledge of the average area per mol of lipid, or alternatively, simultaneous measurement of membrane area, would allow for a theoretical estimation of the magnitude of the effect and quantitative comparison with the experiment.

We reported here the one measurement of consistent and reproducible capacitance changes over the melting transition, made of three entire cycles. Other attempts failed for either the rupture of the membrane during the measurement or for the high variability of the capacitance changes in subsequent scans. We took the almost complete restoration of the capacitance value far from the transition as indication that the bilayer was fully equilibrated before the experiment and therefore discarded the measurements giving erratic values of capacitance at the same temperature in consecutive scans. This behaviour was observed even though measurements were usually started at least 15 minutes after membrane formation to allow for bilayer thinning and always after the capacitance readings were stable for minutes. An attempt of explanation can be made again with the aid of the studies made by White in the 70s who studied the time dependence of the membrane capacitance after formation and found a time constant of about 15 minutes, with capacitance changing slightly its value even after one hour [48]. This is the time it takes to the membrane to thin, so to the solvent molecules to diffuse out of the bilayer. He also found, that in the presence of a constant voltage bias prior to measurement, the thinning process could be efficiently speeded up [89]. This would explain the first scan in Fig. (6.2) differing from the following ones on the basis of not perfect equilibration of the bilayer. It also suggests that equilibration of the system is essential for the reproducibility.

Hysteresis between heating and cooling scans is in line with that measured by DSC and probably linked to the differences in the heating rate for the different scans. Keeping the heating and cooling scan constant on a time scale of about 40 min was a challenging operation and the resulting scan rate varies between 10 and 30 degrees per hour. At this rate, hysteresis has to be expected due to the not complete equilibration of the system. At the high limit of these range the system cannot be assumed to be in thermal equilibrium and hysteresis plays a role.

To conclude, the measurement confirms the theoretical predictions and points at a common origin for enthalpy and capacitance changes. Due mainly

to the presence of solvent, however, the results are mainly of qualitative nature. One way of separating the capacitance contribution of the solvent annulus from that of the bilayer is by applying sinusoidal perturbations, since solvent molecules and lipids have different characteristic frequency. Note that sinusoidal perturbations would also be well suited for measurements of voltage dependence capacitance, where the nonlinear behaviour would show up in the second harmonics of the response [47, 93].

### 6.3.2 Lipid Ion channels and rectification

We here showed that lipid bilayers reconstituted with different techniques show nonlinear current-voltage relationships and current fluctuations that are voltage dependent. It is a general observation in experiments that nonlinear I-V curves measured on BLM are symmetric with respect to voltage whereas those measured on patch pipettes are asymmetric displaying outward rectification (see 6.6(right) compared to 6.9(right)). Both types of curves can be fitted by the membrane capacitor model outlined in chapter 4, which gives a larger value of the offset voltage in the case of the patch pipette compared to the BLM. This indicates that the bilayers on the tip of glass pipettes have a spontaneous polarization whereas those on the BLM setup have not (or have it much smaller). In chapter 3 we discussed two possible mechanisms for membrane polarization, namely chemical (and physical) asymmetry between the two monolayers and geometrical asymmetry (flexoelectricity). The former can be discarded on the grounds that both monolayers are made of the same mixture in both setups. The most evident difference in the two systems is the size of the membrane patch. While the pipette tips have a diameter of about 10  $\mu\text{m}$ , the aperture in the teflon film has a diameter which is about 10 times larger than that. We would then expect that if flexoelectricity plays a role in the membrane polarization, then it should result in different magnitudes of polarization and offset voltage, as observed in the experiments.. This is illustrated in Fig. (6.11).

On the left of Fig. (6.11) different scenarios are shown for the black lipid membrane setup. In the case of a planar membrane (a), no curvature is present and no polarization is expected ( $\Psi_0 = 0$ ). The maximum curvature in this setup can be obtained when the radius of curvature of the membrane is equal to the radius of the aperture (c). All the other scenarios would lead to a smaller curvature. In particular, case (d) is an illustration of the bulging phenomenon described earlier. If the the outer edge of the membrane disconnects from the rim of the hole and the membrane becomes larger, the resulting curvature would be decreased further. This could happen if there is enough lipid reservoir surrounding the aperture. In the case of a membrane with a diameter of 80  $\mu\text{m}$ , the maximum radius of curvature is 40 $\mu\text{m}$ . Taking Petrov's expression for the flexocoefficient,  $f = \Psi_0\epsilon/2c$ , the maximum curvature and an offset voltage of  $\Psi_0 \simeq 6$  mV, one gets a value for

$f$  of about  $3 \cdot 10^{-18} C$  for the mixture DMPC:DLPC:chol=77.3:7.7:15.

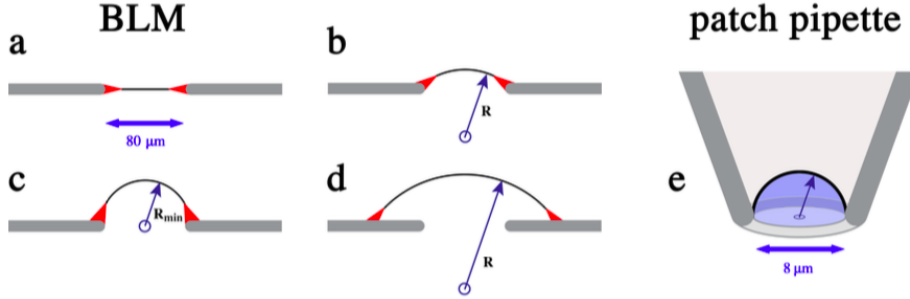


Figure 6.11: **Left:** Illustration of four different possible configurations for a bilayer on a horizontal BLM setup. Red areas represent the solvent annulus. (a): planar bilayer ( $c=0$ ). (b) Curved bilayer. (c) Maximum possible curvature for this hole geometry. (d) Bulging membrane. If the membrane disconnects from the hole the resulting curvature is lower than the other scenarios. **Right:** Curved bilayer on the tip of a glass pipette. Due to the small diameter compared to the hole of the BLM setup, the curvature can reach higher values.

The case of a patch pipette is illustrated on the right of Fig. (6.11) (right). Because of the smaller tip diameter one can expect larger curvatures. Again, the maximum curvature is for a radius of curvature equal to the radius of the tip,  $4 \mu\text{m}$  in the case illustrated here. If we take a voltage offset of  $\Psi_0 = 160 \text{mV}$ , this would give a flexocoefficient of  $f = 8.5 \cdot 10^{-18} C$  for the mixture DMPC:DLPC=10:1.

Note that both numbers are lower estimates, since we considered the maximum possible curvature for each setup. Interestingly, they are very close to the values of the flexocoefficient reported in literature for different membrane composition. Todorov, Petrov and collaborators found  $f = 4.0 \cdot 10^{-18} C$  for bovine brain PS [94],  $f = 2.6 \cdot 10^{-18} C$  for bacterial PE [50] and  $f = 1.8 \cdot 10^{-18} C$  for egg PC [95]. Their measurements of the flexoelectric coefficient involve direct measurement of the membrane curvature. Here, we indirectly estimated the order of magnitude of the curvatures involved. The agreement of our estimation with the literature values for the value of  $f$ , however, points in the direction of a curvature mechanism behind the electrical asymmetries measured. Simultaneous curvature and current measurements could allow for correct and conclusive interpretation of the the electrical asymmetries in lipid bilayers.



## Conclusions

We have here provided a unified thermodynamical framework which describes the electrical, electro-mechanical and thermo-electrical behaviours in the membrane. The biologically relevant case of asymmetric membranes - with respect to geometry and composition - has been included in our description by considering their spontaneous polarization in the absence of a field. In our unified language, spontaneous polarization, electrostriction, flexoelectricity, piezoelectricity and thermoelectricity can all be related to the charging of a capacitor, and may then all be referred to as polarization effects. In the case of flexoelectricity, for example, our results agree with the original development of Petrov in the special case of a membrane which is fully symmetric in the planar state, whose voltage offset is a linear function of curvature, at constant temperature and in the absence of an applied voltage, showing the generality of our treatment. Similar considerations apply to the capacitive susceptibility proposed by Heimburg [24]. Therefore it is a general theory which contains all the different couplings as special cases.

One of the strengths of our approach is that it allowed us to make a number of predictions on the behaviour of membranes in electric fields that can be tested in experiments. Within our framework, for instance, we predicted the effect of the state of the membrane on the membrane capacitance. Our prediction was qualitatively confirmed by our experiments on black lipid membranes. Further experiments using sinusoidal perturbations and simultaneous measurement of the membrane area are suggested. We further predicted how an applied voltage would, in turn, influence the state of the membrane depending on the spontaneous polarization. On the same line, we expect the capacitance to change with voltage. Our theoretical results indicate that these two quantities are affected by the membrane asymmetry, which should be included in the parameter space and controlled in experiments for a correct interpretation of the data. Both experiments could give valuable information, especially in the context of the models for the nerve

pulse propagation.

With the findings of chapter 3 we were able to finally update the traditional equivalent circuit of the lipid portion of the membrane in order to include the time and voltage dependence that is expected for the membrane capacitance and conductance close to the melting transition. We used the new updated circuit to explain and fit existing data and to simulate the response of the lipid membrane to common voltage perturbations. In all of these application we found striking similarities between the response expected from - or measured for - pure lipid bilayers close to the phase transition and biological membranes. Outward and inward rectified I-V curves, gating currents, appearance of quantized step in the membrane, are all phenomena that are considered distinctive of protein channels. We measured or predicted them also for lipid bilayers. This indicates that attention should be employed when interpreting electrical data from biological membranes. It also indicates a more active role of the bilayer in the membrane than what assumed until now. Our hope is that it will encourage the development of new experimental approaches in the electrical investigation of the membrane.

Finally, we want to stress that our proposed equivalent circuit is not based on empirical inspection of the electrical response of the membrane, but it is suggested from our understanding of the structure and the physical properties of the lipid bilayer. In this sense, it is completely general. From this comes the predictive power of our formulation. In this lies its beauty and strength.

# Bibliography

- [1] T. Hianik. Structure and physical properties of biomembranes and model membranes. *Acta Physica Slovaca*, 56:678–806, 2006.
- [2] Thomas Heimburg. *Thermal biophysics of membranes*. Wiley-VCH, first edition, 2007.
- [3] William Hewson. On the figure and composition of the red particles of the blood, commonly called the red globules. *Phil. Trans.*, 63:303–323, 1773.
- [4] E. Gorter and F. Grendel. On bimolecular layers of lipoids on the chromocytes of the blood. *The Journal of Experimental Medicine*, 41(4):439–443, 1925.
- [5] J. F. Danielli and H. Davson. A contribution to the theory of permeability of thin films. *Journal of cellular and comparative physiology*, 5(4):495–508, 1935.
- [6] JD Robertson. The ultrastructure of cell membranes and their derivatives. *Biochemical Society symposium*, 16:3–43, 1959.
- [7] S J Singer and G L L Nicolson. The Fluid Mosaic Model of the Structure of Cell Membranes. *Science*, 175(4023):720–731, 1972.
- [8] O.G. Mouritsen and M. Bloom. Mattress model of lipid-protein interactions in membranes. *Biophysical Journal*, 46(2):141 – 153, 1984.
- [9] Andreas Blicher. *Electrical aspects of lipid membranes*. PhD thesis, Niels Bohr Institute, Copenhagen University, 2011.
- [10] Kai Simons and Elina Ikonen. Functional rafts in cell membranes. *Nature*, 387(6633):569–572, jun 1997.
- [11] Rodney Cotterill. *Biophysics. An introduction*. Wiley-VCH, second edition, 2002.
- [12] EF DeLong and AA Yayanos. Adaptation of the membrane lipids of a deep-sea bacterium to changes in hydrostatic pressure. *Science*, 228(4703):1101–1103, 1985.

- 
- [13] Alexander G Petrov. Flexoelectricity of model and living membranes. *Biochimica et Biophysica Acta*, 1561(1):1–25, 2002.
- [14] JE Rothman and J Lenard. Membrane asymmetry. *Science*, 195(4280):743–753, 1977.
- [15] J. Hjort Ipsen, G. Karlström, O.G. Mourtisen, H. Wennerström, and M.J. Zuckermann. Phase equilibria in the phosphatidylcholine-cholesterol system. *Biochimica et Biophysica Acta (BBA) - Biomembranes*, 905(1):162 – 172, 1987.
- [16] Thomas Heimburg. Mechanical aspects of membrane thermodynamics. Estimation of the mechanical properties of lipid membranes close to the chain melting transition from calorimetry. *Biochimica et Biophysica Acta (BBA) - Biomembranes*, 1415(1):147–162, 1998.
- [17] John F Nagle. Theory of the main lipid bilayer phase transition. *Annual Review of Physical Chemistry*, 31:157–195, 1980.
- [18] Thomas Heimburg and Andrew D. Jackson. On soliton propagation in biomembranes and nerves. *Proceedings of the National Academy of Sciences of the United States of America*, 102(28), 2005.
- [19] K. S. Cole. ELECTRIC IMPEDANCE OF THE SQUID GIANT AXON DURING ACTIVITY. *The Journal of General Physiology*, 22(5):649–670, may 1939.
- [20] A L Hodgkin and A F Huxley. A quantitative description of membrane current and its application to conduction and excitation in nerve. *The Journal of physiology*, 117(4):500–44, aug 1952.
- [21] B. C. Abbott, A. V. Hill, and J. V. Howarth. The positive and negative heat production associated with a nerve impulse. *Proceedings of the Royal Society of London B: Biological Sciences*, 148(931):149–187, 1958.
- [22] K. Iwasa and I. Tasaki. Mechanical changes in squid giant axons associated with production of action potentials. *Biochemical and Biophysical Research Communications*, 95(3):1328 – 1331, 1980.
- [23] A Gonzalez-Perez, L D Mosgaard, R Budvytyte, E Villagran-Vargas, A D Jackson, and T Heimburg. Solitary electromechanical pulses in lobster neurons. *Biophysical Chemistry*, 216:51–59, sep 2016.
- [24] Thomas Heimburg. The capacitance and electromechanical coupling of lipid membranes close to transitions: the effect of electrostriction. *Biophysical journal*, 103(5):918–29, 2012.
- [25] Herbert B. Callen. *Thermodynamics and an introduction to thermostatistics*. Wiley-VCH, second edition, 1985.

- [26] V.F. Antonov, E.Yu. Smirnova, and E.V. Shevchenko. Electric field increases the phase transition temperature in the bilayer membrane of phosphatidic acid. *Chemistry and Physics of Lipids*, 52(3–4):251 – 257, 1990.
- [27] Hermann Träuble and Hansjörg Eibl. Electrostatic Effects on Lipid Phase Transitions: Membrane Structure and Ionic Environment. *Proceedings of the National Academy of Sciences of the United States of America*, 71(1):214–219, jan 1974.
- [28] Rainer A Böckmann, Agnieszka Hac, Thomas Heimburg, and Helmut Grubmüller. Effect of Sodium Chloride on a Lipid Bilayer. *Biophysical Journal*, 85(3):1647–1655, sep 2003.
- [29] V.P. Ivanova, I.M. Makarov, T.E. Schäffer, and T. Heimburg. Analyzing heat capacity profiles of peptide-containing membranes: Cluster formation of gramicidin a. *Biophysical Journal*, 84(4):2427 – 2439, 2003.
- [30] Kaare Graesboell, Henrike Sasse-Middelhoff, and Thomas Heimburg. The thermodynamics of general and local anesthesia. *Biophysical Journal*, 106(10):2143 – 2156, 2014.
- [31] Heiko M. Seeger, Marie L. Gudmundsson, and Thomas Heimburg. How anesthetics, neurotransmitters, and antibiotics influence the relaxation processes in lipid membranes. *The Journal of Physical Chemistry B*, 111(49):13858–13866, 2007. PMID: 18020440.
- [32] Richard F. Greene and Herbert B. Callen. On the formalism of thermodynamic fluctuation theory. *Phys. Rev.*, 83:1231–1235, Sep 1951.
- [33] Holger Ebel, Peter Grabitz, and Thomas Heimburg. Enthalpy and volume changes in lipid membranes. i. the proportionality of heat and volume changes in the lipid melting transition and its implication for the elastic constants. *The Journal of Physical Chemistry B*, 105(30):7353–7360, 2001.
- [34] T Hanai, D A Haydon, and J Taylor. Polar group orientation and the electrical properties of lecithin bimolecular leaflets. *Journal of Theoretical Biology*, 9(2):278–296, 1965.
- [35] Wolfhard Almers. Gating currents and charge movements in excitable membranes. *Rex. Physiol. Biochem. Pharmacol.*, 82:96–190, 1978.
- [36] R Benz, O Fröhlich, P Läger, and M Montal. Electrical capacity of black lipid films and of lipid bilayers made from monolayers. *Biochimica et Biophysica Acta (BBA) - Biomembranes*, 394(3):323–334, 1975.

- 
- [37] S McLaughlin. The electrostatic properties of membranes. *Annual Review of Biophysics and Biophysical Chemistry*, 18(1):113–136, 1989. PMID: 2660821.
- [38] Lars D. Mosgaard, Karis A. Zecchi, and Thomas Heimburg. Mechano-capacitive properties of polarized membranes. *Soft Matter*, 11:7899–7910, 2015.
- [39] Robert B Meyer. Piezoelectric Effects in Liquid Crystals. *Phys. Rev. Lett.*, 22(18):918–921, 1969.
- [40] AlexanderG. Petrov. Flexoelectric model for active transport. In JuliaG. Vassileva-Popova, editor, *Physical and Chemical Bases of Biological Information Transfer*, pages 111–125. Springer US, 1975.
- [41] Henry S. Frank. Thermodynamics of a Fluid Substance in the Electrostatic Field. *The Journal of Chemical Physics*, 23(11):2023, dec 1955.
- [42] O Alvarez and R Latorre. Voltage-dependent capacitance in lipid bilayers made from monolayers. *Biophysical Journal*, 21(1):1–17, 1978.
- [43] Brenda Farrell, Cythnia Do Shope, and William E. Brownell. Voltage-dependent capacitance of human embryonic kidney cells. *Phys. Rev. E*, 73(4):041930, 2006.
- [44] Heinz Beitinger, Viola Vogel, Dietmar Möbius, and Hinrich Rahmann. Surface potentials and electric dipole moments of ganglioside and phospholipid monolayers: contribution of the polar headgroup at the water/lipid interface. *Biochimica et Biophysica Acta (BBA) - Biomembranes*, 984(3):293 – 300, 1989.
- [45] Alexander G Petrov. *The Lyotropic State of Matter: Molecular Physics and Living Matter Physics*. CRC PressI Llc, 1999.
- [46] A.V. Babakov, L.N. Ermishkin, and E.A. Liberman. Influence of electric field on the capacity of phospholipid membranes. *Nature*, 210(5039):953–955, 1966. cited By (since 1996)13.
- [47] Darold Wobschall. Voltage dependence of bilayer membrane capacitance. *Journal of Colloid and Interface Science*, 40(3):417 – 423, 1972.
- [48] Stephen H. White. A study of lipid bilayer membrane stability using precise measurements of specific capacitance. *Biophysical Journal*, 10(12):1127 – 1148, 1970.
- [49] H. Trauble and H. Eibl. Electrostatic effects on lipid phase transitions: Membrane structure and ionic environment. *Proceedings of the National Academy of Sciences*, 71(1):214–219, 1976.

- [50] A.G. Petrov and V.S. Sokolov. Curvature-electric effect in black lipid membranes. *European Biophysics Journal*, 13(3):139–155, 1986.
- [51] Kenneth S Cole and Richard F Baker. Longitudinal impedance of the squid giant axon. *The Journal of General Physiology*, 24(6):771–788, jul 1941.
- [52] K S Cole. Electric Impedance of Suspensions of Spheres. *The Journal of general physiology*, 12(1):29–36, sep 1928.
- [53] T. Heimburg. Lipid ion channels. *Biophysical Chemistry*, 150(1–3):2 – 22, 2010. <ce:title>Special Issue: Membrane Interacting Peptides - Towards the Understanding of Biological Membranes</ce:title>.
- [54] M. Jansen and A. Blume. A comparative study of diffusive and osmotic water permeation across bilayers composed of phospholipids with different head groups and fatty acyl chains. *Biophysical Journal*, 68(3):997 – 1008, 1995.
- [55] Andreas Blicher, Katarzyna Wodzinska, Matthias Fidorra, Mathias Winterhalter, and Thomas Heimburg. The temperature dependence of lipid membrane permeability, its quantized nature, and the influence of anesthetics. *Biophysical journal*, 96(11):4581–91, jun 2009.
- [56] D. Papahadjopoulos, K. Jacobson, S. Nir, and I. Isac. Phase transitions in phospholipid vesicles. fluorescence polarization and permeability measurements concerning the effect of temperature and cholesterol. *Biochimica et Biophysica Acta (BBA) - Biomembranes*, 311(3):330 – 348, 1973.
- [57] J.F. Nagle and H.L. Scott. Lateral compressibility of lipid mono- and bilayers. theory of membrane permeability. *Biochimica et Biophysica Acta (BBA) - Biomembranes*, 513(2):236 – 243, 1978.
- [58] Konrad Kaufmann and Israel Silman. The induction by protons of ion channels through lipid bilayer membranes. *Biophysical Chemistry*, 18(2):89 – 99, 1983.
- [59] B. Wunderlich, C. Leirer, A.-L. Idzko, U.F. Keyser, A. Wixforth, V.M. Myles, T. Heimburg, and M.F. Schneider. Phase-state dependent current fluctuations in pure lipid membranes. *Biophysical Journal*, 96(11):4592 – 4597, 2009.
- [60] Masao Yafuso, StephenJ. Kennedy, and AlanR. Freeman. Spontaneous conductance changes, multilevel conductance states and negative differential resistance in oxidized cholesterol black lipid membranes. *The Journal of Membrane Biology*, 17(1):201–212, 1974.

- 
- [61] V. F. Antonov, V. V. Petrov, Molnar A. A., D. A. Predvoditelev, and A. S. Ivanov. The appearance of single-ion channels in unmodified lipid bilayer membranes at the phase transition temperature. *Nature*, 283:585–586, 1980.
- [62] Katrine R Laub, Katja Witschas, Andreas Blicher, Søren B Madsen, Andreas Lückhoff, and Thomas Heimburg. Comparing ion conductance recordings of synthetic lipid bilayers with cell membranes containing TRP channels. *Biochimica et Biophysica Acta (BBA) - Biomembranes*, 1818(5):1123–1134, may 2012.
- [63] Mads C. Sabra, Kent Jørgensen, and Ole G. Mouritsen. Lindane suppresses the lipid-bilayer permeability in the main transition region. *Biochimica et Biophysica Acta (BBA) - Biomembranes*, 1282(1):85 – 92, 1996.
- [64] Thomas Andersen, Anders Kyrsting, and Poul M. Bendix. Local and transient permeation events are associated with local melting of giant liposomes. *Soft Matter*, 10:4268–4274, 2014.
- [65] Andreas Blicher and Thomas Heimburg. Voltage-Gated Lipid Ion Channels. *PLoS one*, 8(6):e65707, 2013.
- [66] Thomas Voets, Guy Droogmans, Ulrich Wissenbach, Annelies Janssens, Veit Flockerzi, and Bernd Nilius. The principle of temperature-dependent gating in cold- and heat-sensitive TRP channels. *Nature*, 430(7001):748–754, aug 2004.
- [67] Karel Talavera, Keiko Yasumatsu, Thomas Voets, Guy Droogmans, Noriatsu Shigemura, Yuzo Ninomiya, Robert F Margolskee, and Bernd Nilius. Heat activation of TRPM5 underlies thermal sensitivity of sweet taste. *Nature*, 438(7070):1022–1025, dec 2005.
- [68] Lars D. Mosgaard and Thomas Heimburg. Lipid ion channels and the role of proteins. *Accounts of Chemical Research*, 46(12):2966–2976, 2013. PMID: 23902303.
- [69] Peter Grabitz, Vesselka P. Ivanova, and Thomas Heimburg. Relaxation kinetics of lipid membranes and its relation to the heat capacity. *Biophysical Journal*, 82(1):299 – 309, 2002.
- [70] Martin Schiewek and Alfred Blume. Pressure jump relaxation investigations of lipid membranes using ftir spectroscopy. *European Biophysics Journal*, 38(2):219, 2008.
- [71] Thomas Heimburg Lars D. Mosgaard, Karis A. Zecchi and Rima Budvytyte. The effect of the nonlinearity of the response of lipid membranes to

- voltage perturbations on the interpretation of their electrical properties. a new theoretical description. *Membranes*, 5:495–512, 2015.
- [72] K S Cole. Rectification And Inductance In The Squid Giant Axon. *The Journal of general physiology*, 25(1):29–51, sep 1941.
- [73] E Neher and B Sakmann. Single-channel currents recorded from membrane of denervated frog muscle fibres. *Nature*, 250(5554):799–802, 1976.
- [74] Clay M. Armstrong and Francisco Bezanilla. Currents Related to Movement of the Gating Particles of the Sodium Channels. *Nature*, 242(5398):459–461, apr 1973.
- [75] R D Keynes and E Rojas. Kinetics and steady-state properties of the charged system controlling sodium conductance in the squid giant axon. *The Journal of physiology*, 239(2):393–434, jun 1974.
- [76] F.J. Blatt. Gating currents: the role of nonlinear capacitative currents of electrostrictive origin. *Biophysical Journal*, 18(1):43 – 52, 1977.
- [77] Stephen H. White. Temperature-dependent structural changes in planar bilayer membranes: Solvent “freeze-out”. *Biochimica et Biophysica Acta (BBA) - Biomembranes*, 356(1):8 – 16, 1974.
- [78] Kenneth S. Cole and Robert H. Cole. Dispersion and Absorption in Dielectrics I. Alternating Current Characteristics. *The Journal of Chemical Physics*, 9(4):341, dec 1941.
- [79] Alexander Mauro. Anomalous Impedance, A Phenomenological Property of Time-Variant Resistance: An Analytic Review. *Biophysical Journal*, 1(4):353–372, mar 1961.
- [80] W. Hanke, C. Methfessel, U. Wilmsen, and G. Boheim. Ion channel reconstitution into lipid bilayer membranes on glass patch pipettes. *Bioelectrochemistry and Bioenergetics*, 12(3–4):329 – 339, 1984.
- [81] Thomas Gutschmann, Thomas Heimburg, Ulrich Keyser, Kozhinjampara R Mahendran, and Mathias Winterhalter. Protein reconstitution into freestanding planar lipid membranes for electrophysiological characterization. *Nat. Protocols*, 10(1):188–198, jan 2015.
- [82] Paul Mueller, Donald O. Rudin, H. TI TIEN, and WILLIAM C. WESCOTT. Reconstitution of Cell Membrane Structure in vitro and its Transformation into an Excitable System. *Nature*, 194(4832):979–980, jun 1962.
- [83] T.J. McIntosh, S.A. Simon, and R.C. MacDonald. The organization of n-alkanes in lipid bilayers. *Biochimica et Biophysica Acta (BBA) - Biomembranes*, 597(3):445 – 463, 1980.

- 
- [84] Valerij F. Antonov, Andrej A. Anosov, Vladimir P. Norik, Evgenija A. Korepanova, and Elena Y. Smirnova. Electrical capacitance of lipid bilayer membranes of hydrogenated egg lecithin at the temperature phase transition. *European Biophysics Journal*, 32(1):55–59, 2003.
- [85] S. H. White. Phase transition in planar bilayer membranes. *Biophysical Journal*, 15(2):95–117, 1975.
- [86] V.F. Antonov, E.V. Shevchenko, E.Yu. Smirnova, E.V. Yakovenko, and A.V. Frolov. Stable cupola-shaped bilayer lipid membranes with mobile Plateau-Gibbs border: expansion-shrinkage of membrane due to thermal transitions. *Chemistry and Physics of Lipids*, 61(3):219–224, may 1992.
- [87] R. Fettiplace, D. M. Andrews, and D. A. Haydon. The thickness, composition and structure of some lipid bilayers and natural membranes. *The Journal of Membrane Biology*, 5(3):277–296, 1971.
- [88] T Hanai, D A Haydon, and J Taylor. An Investigation by Electrical Methods of Lecithin-in-Hydrocarbon Films in Aqueous Solutions. *Proceedings of the Royal Society A Mathematical Physical and Engineering Sciences*, 281(1386):377–391, 1964.
- [89] Stephen H. White. How Electric Fields Modify Alkane Solubility in Lipid Bilayers. *Science*, 207(4435), 1980.
- [90] Stephen H White. Studies of the physical chemistry of planar bilayer membranes using high-precision measurements of specific capacitance. *Annals of the New York Academy of Sciences*, 303:243–265, 1977.
- [91] D.A. Haydon, B.M. Hendry, S.R. Levinson, and J. Requena. Anaesthesia by the n-alkanes. a comparative study of nerve impulse blockage and the properties of black lipid bilayer membranes. *Biochimica et Biophysica Acta (BBA) - Biomembranes*, 470(1):17 – 34, 1977.
- [92] Stephen H. White. *The Physical Nature of Planar Bilayer Membranes*, pages 3–35. Springer US, Boston, MA, 1986.
- [93] Wolf Carius. Voltage dependence of bilayer membrane capacitance. *Journal of Colloid and Interface Science*, 57(2):301 – 307, 1976.
- [94] A. T. Todorov, A. G. Petrov, and J. H. Fendler. First observation of the converse flexoelectric effect in bilayer lipid membranes. *The Journal of Physical Chemistry*, 98(12):3076–3079, 1994.
- [95] A. Todorov, A. Petrov, Michael O. Brandt, and Janos H. Fendler. Electrical and real-time stroboscopic interferometric measurements of bilayer lipid membrane flexoelectricity. *Langmuir*, 7(12):3127–3137, 1991.